Assessing visualized response phenomena of grapevine root-stocks exposed to lime and drought stress

Swantje Schulitz

Master's thesis to obtain the degree of
European Master of Science in Viticulture and Enology

Advisor: Prof. Dr. Astrid Forneck

Advisor: Prof. Dr. Carlos Lopes

Jury:

President:

Joaquim Miguel Rangel da Cunha Costa (PhD), Assistant Professor at Instituto Superior de Agronomia, Universidade de Lisboa.

Members:

Astrid Forneck (PhD), Full Professor at Universität für Bodenkultur Wien;

Pilar Baeza Trujillo (PhD), Associated Professor at IUniversidad Politecnica de Madrid;

Amaia Miren Nogales Garcia (PhD), Assistant Researcher at Instituto Superior de Agronomia, Universidade de Lisboa.

2021

Acknowledgement

For the professional supervision and the target-oriented and always friendly support, that this work has received, it appears appropriate to acknowledge an expression of gratitude by this point.

In this regard, it is due first of all to Prof. Astrid Forneck (BOKU, Tulln) and Prof. Carlos M.A. Lopes (ISA, Lisbon) for their flexible encouragement of independent decision-making, scientific adventurousness and the support of a European interdisciplinarity and inter-instituionality.

Very special and heartfelt thanks, of course, go to Dr. Michaela Griesser (BOKU, Tulln), who was not only steering and guiding to all work phases, of which there were many, but also patiently and motivating rendered form and feasibility to the actual project. Much obliged, indeed.

In addition to especially Roswitha Prinz-Mammerler, who deserves particular thanks for the many practical support in the laboratory and at the microscope, a warm thank you also goes to Federica de Berardinis for her ever-ingenious backing in preparation questions and procedures.

The author also owes a great deal of learning to the professional chats with Sarhan Khalil, PhD, who instructed many subject areas with friendly guidance.

Thanks are also to be given to all the staff at the BOKU site in Tulln, whose aimable cooperativeness at all times ensured an excellent working atmosphere and made efficient activity possible - representative of many more, Dr. Christoph Schüller and Franz Zehetbauer should be mentioned here; in addition, and most emphasizedly, Dr. Monika Debreczeny from the Core Facility Multiscale Imaging, BOKU Vienna, must be mentioned with the very best appreciation.

For the informal and straightforward leads and explanations to special questions, the present work is furthermore obliged to Dr. Tino Kreszies, Dr. Peter Kitin and Prof. Gregory Gambetta.

The author hopes to have made good use of all this support. Thanks again.

Abstract

Iron-deficiency induced chlorosis and drought stress are major constraints in viticulture influencing grape yield and quality. Notably when occurring simultaneously, these stresses can have intense negative effects on plant physiology and plant nutrition. Grapevine rootstocks have the capacity to adapt to different abiotic stresses by morphological, biochemical or gene expression changes, but the mechanisms in detail are not well studied.

It can be assumed, that root differentiation has a functional key role in rootstocks adaptation to abiotic stresses. Therefore, the current study aims to characterize the Casparian strip formation and the suberization of endodermis and exodermis to conclude on the plasticity in nutrient and water uptake of grapevine rootstocks. In in-vitro approaches Fercal and 3309 C were subjected to iron free growth conditions and osmolyte induced drought stress as well as the combined stress. Furthermore, rootstock cuttings were grown in rhizoboxes to evaluate the root system architecture.

For the intra-treatment comparison, significant differences in root pattern distribution and length parameters were found. For the rootstocks compared, intensified main root length growth seemed not to be a mitigative strategy. In contrast, Fercal had significantly fewer and shorter lateral roots than 3309 C. This implies, Fercal is more efficient per unit root surface. i.e. by increasing the area of the root hair zone.

A systematic lignification and suberization can incrementally be observed with increasing stress intensity. For 3309 C, the rhizobox experiments also showed intra-treatment effects. For iron deficiency, foraging seemed to be the main strategy.

The results confirmed a high variability between rootstocks supposing specific adaptations strategies to no-iron and drought stress conditions on the root system development as well as on the root molecular differentiation process. The established in-vitro based method could provide a tool to test different environment versus genotype interactions of grapevine rootstocks.

Keywords: Casparian strips, suberin, root system architecture, abiotic stress, phenetics

Resumo

A clorose férrica induzida pela carência de ferro e o stress da seca são grandes constrangimentos na viticultura que influenciam a qualidade das uvas. Notavelmente, quando ocorrem simultaneamente, estas tensões podem ter efeitos negativos na nutrição das plantas. As raízes têm a capacidade de se adaptar às tensões abióticas por alterações morfológicas, bioquímicas ou transcriptómicas, mas os mecanismos não são bem estudados. Assumimos, que a diferenciação das raízes tem um papel fundamental funcional na adaptação dos porta-enxertos às tensões. Este estudo visa caracterizar a formação da faixa Casparian e a suberização da endoderme para concluir sobre a plasticidade na absorção de nutrientes e água dos porta-enxertos. Fercal e 3309 C foram cultivados em cultura in-vitro sujeitos a condições de crescimento sem ferro e ao stress da seca induzido pela osmólita, bem como ao stress combinado. Além disso, foram cultivadas estacas de porta-enxertos em rizoboxes para avaliar a arquitectura do sistema radicular.

Para a comparação intra-tratamento, foram encontradas diferenças significativas na distribuição do padrão radicular e nos parâmetros de comprimento. Para os porta-enxertos comparados, a intensificação do crescimento do comprimento da raiz principal parecia não ser uma estratégia mitigadora. Fercal tinha significativamente menos e mais curtas raízes laterais do que 3309 C. Isto implica que Fercal é mais eficiente por unidade de superfície da raiz, ou seja, por aumentar a zona do pelo da raiz.

Uma lenhificação e suberização sistemáticas podem ser observadas de forma crescente com uma intensidade de stress crescente. As experiências de rhizobox também mostraram efeitos intra-tratamento. Para a deficiência de ferro, a forragem parecia ser a estratégia principal.

Confirmámos uma elevada variabilidade entre os porta-enxertos, supondo estratégias específicas de adaptação às condições de stress sem ferro e de seca no desenvolvimento radicular, bem como no processo de diferenciação molecular radicular. O método in-vitro estabelecido poderia fornecer uma ferramenta para testar diferentes ambientes versus interações genotípicas dos porta-enxertos.

Palavras-chave: faixa Casparian, suberina, arquitetura do sistema radicular, stress abiótico, fenética

Resumo alargado

Os solos suficientemente drenantes e moderadamente alcalinos, tais como os formados por envelhecimento químico do gesso ou rocha dolomítica, são considerados favoráveis à viticultura, pelo menos devido à sua boa retenção de temperatura e ao amortecimento das tendências de acidificação. Na Europa, encontram-se exemplos na Thermenregion na Áustria, na Borgonha, na região alemã da Francónia ou em alguns climas do sul de França, entre muitos outros em todo o mundo.

Para se adaptar a condições específicas, tais como espessura do solo superficial, teor de argila, regime de precipitação anual, contaminação por filoxera e nematodes e regulação dos objetivos de rendimento, os porta-enxertos são selecionados de acordo com as suas capacidades de moderação. Nesta função, os porta-enxertos de videira são uma zona de trânsito hiper-dinâmico em que toda a reciprocidade entre os outros contribuintes para a organização holobiontica total das realidades vitivinícolas é organizada. As inter-relações bi-genómicas entre o enxerto, ou seja, em particular também o rendimento económico sustentável e a qualidade da colheita, e as condições abaixo do solo, são, numa medida decisiva, orquestradas pelo transcriptoma do ADN do porta-enxerto.

Num contexto de maior intensidade de seca e secagem, eventos climáticos extremos e ciclos de crescimento acelerado, bem como erosão, degradação do solo e salinização devido às alterações climáticas, a saúde vegetal está a tornar-se cada vez mais importante. Especialmente em solos de calcário, uma vez que a clorose férrica induzida pelo ferro é um importante fator limitante para o rendimento sólido e equilibrado das culturas. No entanto, fatores proeminentes, mas específicos na formulação de respostas de stress das raízes das plantas à seca e valores elevados de calcário ativo são a adaptação da arquitetura, a suberização ou lenhificação das paredes celulares exo- e endodérmicas e a manipulação de domínio cruzado da rizosfera pela exsudação metabólica em condições redox e micro-edáficas mais favoráveis às plantas. A formação de faixas Casparianas e lamelas semelhantes de lenhina-suberina em paredes celulares tangenciais, radiais e transversais é de primordial importância na adaptação funcional osmoregulatória da arquitetura hidráulica e, portanto, da absorção e retenção de nutrientes.

Impregnando as paredes celulares com uma camada de proteção hidrofóbica, a barreira endodérmica aumenta a sua estabilidade a fenómenos de degradação e aumenta a seletividade da difusão em secções radiculares jovens. Para além da transferência de massa controlada, a regulação da via também ajusta a condutividade, a resistividade e a pressão negativa às condições em mudança. De forma análoga, mas mais indesejada, a formação de faixas Casparianas na exoderme contribui para a adaptação da resistência ao fluxo de água radial e presumivelmente para a plasticidade total da raiz em condições rizosféricas desfavoráveis.

No entanto, a medida em que isto ocorre e como exatamente os representantes do género *vitis* dirigem a captação de água e iões para assegurar a homeostasia através da lenhificação e suberização requer mais investigação que, naturalmente, se aplica ainda mais à interdinâmica da simultaneidade do stress. Uma vez que a logística do ferro e o stress induzido pela cal, por um lado, e as estratégias de mitigação do stress provocado pela seca, por outro, poderiam tornar possíveis as inter-relações observáveis, numa primeira fase, a experiência subjacente a este trabalho irá expor três raízes de cruzamentos discriminatórios a diferentes gradientes de stress relacionados com o ferro, durante um

período de tempo predefinido, numa abordagem controlada in vitro, a fim de visualizar a dinâmica da formação e diferenciação da faixa Casparian com técnicas de microscópio adaptadas. Uma segunda etapa aproveita as representações radiculares visualizadas, captadas a partir de rizoboxes, proporcionando condições seminaturais de crescimento.

Embora a deficiência de ferro mediada por ambientes de raízes alcalinas e fenómenos de seca determinem o desenvolvimento de diferentes abordagens no que diz respeito a reações de defesa e manobras morfológicas estratégicas, respetivamente, as videiras não raramente têm de suportar ambas as condições malignas ao mesmo tempo. Neste contexto, a diferenciação do padrão de enraizamento e as propriedades de lenhificação ou suberização são melhorias da resiliência do processamento de variedades bastante tolerantes à cal, tão evidentemente como de os representantes serem bastante insuscetíveis à seca, no entanto, curiosamente, muitas vezes de formas aparentemente opostas no que diz respeito aos reforços das camadas de barreira.

Dicot representativas Estratégia I respostas como a libertação intensificada de H^+ para a rizosfera juntamente com a produção intensificada de quelato férrico redutase (FCR) e o aumento do efluente do exsudado radicular são mecanismos para os quais a formação de faixas Casparianas e outro reforço da parede celular seria desfavorável como formação de barreira especialmente nas camadas dérmicas laterais finas da raiz interferem com as medidas de rizodeposição mediando a absorção de ferro. Por este motivo, o comportamento morfo-adaptativo da ponta da raiz é particularmente importante e requer observação micro-segmentar, uma vez que os metabolitos parecem difundir-se principalmente osmoticamente através de apoplastos de tecidos indiferenciados da ponta da raiz, enquanto que, ao contrário, a formação de camadas protetivas é estendida para a zona de alongamento sob tensão abiótica. Os fenómenos de resposta bipartida dos porta-enxertos de videiras expostos à escassez de ferro e ao stress da seca foram examinados a fim de investigar mais aprofundadamente as conclusões sobre a reciprocidade entre as melhorias das paredes celulares, efluxo de exsudado, disponibilidade de ferro, hidráulica radicular e, por conseguinte, sistema radicular de arquitetura (RSA).

A este respeito, a formação da faixa Casparian e o apoio suberina em áreas de intersecção dérmica das raízes principais, bem como o desempenho da arquitetura do sistema radicular (RSA) foi determinado para os porta-enxertos Fercal e 3309 Couderc obtidos a partir de uma preparação de teste in vitro.

Foi utilizado um meio de cultivo sem ferro (NOFE) para simular o stress da cal, enquanto que a escassez de água foi produzida através do uso de osmólitos (PEG). Num terceiro tratamento, ambos os fatores de stress foram combinados (NOFEPEG). Investigando se os resultados podiam ser aumentados para padrões maiores e mais naturais, foi realizada uma experiência sucessória com aplicações de stress ajustadas para uma mistura solo-perlite em rhizoboxes.

A subsequente avaliação de impacto por análises RSA e avaliação micrográfica de tecidos celulares tratados com corantes fluorescentes, tornou rastreáveis desenvolvimentos graduais e específicos da parede celular do porta-enxerto. As estratégias de resposta entre Fercal e 3309 C são, comprovadamente, divergentes. Fercal é mais eficiente na distribuição de biomassa, funciona mais energeticamente equilibrado por unidade de superfície radicular e desvia-se de o comportamento radicular habitual encurtando a zona de alongamento sob deficiência de ferro.

Uma elevada variabilidade entre os porta-enxertos indica ainda mais adaptações de estratégias específicas individuais, de modo que uma inclusão de parâmetros radiculares adicionais e uma análise do valor da cor das amostras tingidas poderia ser vantajosa.

Palavras-chave: faixa Casparian, suberina, arquitetura do sistema radicular, stress abiótico, fenética

Table of content

List of figures

List of tables

List of abbreviations

ABA	ABSCISIC ACID
C	CONTROL
CASP	CASPARIAN STRIP MEMBRANE DOMAIN PROTEIN
CCE	CALCIUM CARBONATE EQUIVALENTS
CPI	CHLOROTIC POWER INDEX
CS	CASPARIAN STRIP
cv.	CULTIVAR
FCR	FERRIC CHELATE REDUCTASE
i.a.	INTER ALIA
IAA	INDOLE-3-ACETIC ACID
IBA	INDOLE-3-BUTYRIC ACID
IRT	IRON REGULATED TRANSPORTER
L_{Pr}	ROOT HYDRAULIC CONDUCTIVITY
NADH	NICOTINAMIDE ADENINE DINUCLEOTIDE
NADPH	NICOTINAMIDE ADENINE DINUCLEOTIDE PHOSPHATE
NOFE	NO IRON
NOFEPEG	NO IRON / POLYETHYLENE GLYCOL
P-ATPase	PLASMA MEMBRANE PROTON-ADENOSINETRIPHOSPHATASE
PEG	POLYETHYLENE GLYCOL
PIP	PLANT PLASMA MEMBRANE-TYPE PLASMA MEMBRANE INTRINSIC PROTEIN
P_r	ROOT PRESSURE
$-P_r$	NEGATIVE ROOT PRESSURE
ROI	REGIONS OF INTEREST
ROS	REACTIVE OXYGEN SPECIES
RSA	ROOT SYSTEM ARCHITECTURE
SPAC	SOIL-PLANT-ATMOSPHERE CONTINUUM
SUB	SUBERIN
subg.	SUBGENUS
viz.	VIDERE LICET
WUE	WATER USE EFFICIENCY

I. Objectives

Regarding iron deficiency and drought stress, the aim of this work is to investigate the responses of the rootstocks Fercal and 3309 C at the cellular level (endomorphological) and phenetically (RSA) and, if present, to show correlations. For this purpose a method is established, which includes both an in vitro experiment and a greenhouse approach in order to gain insights into the dynamics between micro- and macromorphology.

In addition, advances in the upscalability of a laboratory method to more natural levels could be made possible. This would accelerate important work steps in phenotyping and genotype x environment variability. The anticipated reciprocities could also be exploited for soil cultivation, intercrop design, rhizosphere engineering, breeding decisions, and the better understanding of holobionitically organized systems.

The first corresponding research question in this context asks whether rootstocks will adapt fine root differentiation to varied and combined stresses on an in vitro scale. And if the respective findings are interpretable for more natural environments.

Secondly, it is inquired how different genotypes specify or counter control general adaptation strategies for iron (lime) stress and drought mitigation.

And finally, it is to be clarified, in how far dermal cell wall lignification and suberization influence the root system architecture.

The answer to these questions and the methods and means used for this purpose are presented in detail after a thorough introduction to the global, eco-spherical environments and pedobiomes, as well as to root ontogeny, anatomy and nutritional contexts.

II. Deductive coverage of the subject area: a survey

This overview deductively organizes the relevant peripheries, preconditions, and environmental related domains around the core issue. Casparian strip development, suberic cell wall lamination or rooting pattern dynamics, viz. endorhizomatic adaptation mechanisms and phenom alteration under stress- or austerity conditions cannot be understood and scaled in isolation from ecological, geo-pedological or agro-meteorological long-ranges; at least not if the associated fields of study are attempting to run along agroecological targeted, i.e. sustainable, mitigative and ameliorative orientation lines.

Lime stress or iron deficiency and drought stress are heterogeneously integrated into bigger natural contexts. Within this meta-setting, the various macro-, meso- and microtopics are to be brought under closer scrutiny.

1. From viticultural-ecological fundamentals to abiotic and biotic challenges.

Sufficient nutrient availability and a balanced water use efficiency, along with adequate climatic contexts and the resulting weather and atmospheric conditions with their photobiological and photochemical relevance, are the phyto-physiological basis of the world's agricultural economy. This also

applies in particular to viticulture, which stands in a prominent position at the focus of numerous ecological, economical and sociological interests (Petti et al. 2006, Slattery and Ort 2015, Gilinsky et al. 2016, Brunori et al. 2016, Fraga et al. 2016, Salomé et al 2016).

In this context and with regard to the optimization segments of site selection, row orientation, row and vine spacing (planting densities), cover cropping, machine use, manuring regime, soil health and, where applicable, irrigation approach, a knowledge enhancement in the field of root research can hardly be overestimated (Smart et al. 2006, Jeudy et al. 2016, Pierret et al. 2016, Bernardo et al. 2018, C. van Leeuwen et al. 2018, Costa et al. 2020). Future intensification of viticultural challenges are to be expected in particular from alkaline, well-draining soils. Their share of 25 % of the soil surfaces worldwide makes their importance obvious (López-Bucio et al. 2000). All the more so, as they contribute to the *terroir*, thus to distinctive wine quality, e.g. in the Thermenregion, in Franconia, Burgundy, Pomerol, in parts of the Languedoc and southern Spain (Imerson and Verstraten 1984, White et al. 2007).

Such vineyards may be problematic because even at slightly elevated pH values of the soil solution, essential iron and other vital nutrients can only be imbibed with difficulty (Keller 2015). Furthermore, with simultaneous intensifying water shortage, the according acquisition additionally is dependent on adaption strategies which possibly may lead to irreversible degeneration cascades, but at any rate, however, to a reduction of performance capacities (Simonneau et al. 2017, Ding et al. 2018, Gambetta et al. 2020, Prinsi et al. 2021).

The bi-genomic interrelations between the fructiferous scion, i.e. in particular the economical sustainability, and belowground conditions, are to a decisive extent co-orchestrated by the rootstock DNA (Lovisolo et al. 2010, Prinsi et al. 2018, L. Zhang et al. 2020) and thereby not least by the corresponding phenes and species-specific readiness to reactively enter into communication with soil environments (Giehl and von Wirén 2014, Berlanas et al. 2019, Yan et al. 2020).

As a pedo-biotopic associated interface between lithosphere, hydrosphere and atmosphere (Stahr et al. 2016), rootstocks show highly dynamic potentials in the adaption services, the resilience stability, resistance intensity and thus in the maintenance of plant health and crop quality (Warschefsky et al. 2016, Gautier et al. 2020).

Pertaining to viticultural objectives, thus to the expected biotic and abiotic problems as well as to climatic and macro-spatial conditions, there is, theoretically, a wide bandwidth of agriculturally exploitable rootstock functional-, response- and effect traits (Yıldırım et al. 2018, Cochetel et al. 2020, Kalcsits et al. 2020). Particularly against the backdrop of climate change, these environmental reactive phenes need to be much better understood regarding their morpho-physiological inherence and their inter- and intra-factorial reciprocity (Harris 2015, Shkolnik and Fromm 2016, Canarini et al. 2019, Gambetta et al. 2020). Such insights may reveal or possibly even increase the ecologic-economical capital of roots with a view to a future-proof, i.e. sustainable plant and soil deployment.

However, Ollat et al. (2016) and Gautier et al. (2020) indicate, that 90 % of vines worldwide are grafted on a selection of ten rootstock species or interspecies respectively. In Europe the potential of the 83 rootstocks listed seems not yet been fully explored.

Finding a best practice here is not trivial, and the already indicated complexity makes breeding efforts a challenging task (Cousins 2005, Zhou et al. 2019), particularly with regard to the perspective

dimension of agricultural and hence viticultural developments (Heinitz et al. 2015, Waite et al. 2015, Santos et al. 2020). The restriction to a few rootstocks is re-considerable in view of the soil diversity, the intra-annual soil-climatic variability and the alpha- or beta-zonal relevance mentioned also in the climate change context by Jackson and Lombard (1993) or C. van Leeuwen (2010), among others. With regard to grape constituents, must qualities and wine styles rootstocks will have to be patterned more variably in the future by co-relying on the rapidly developing possibilities of precision farming for the benefit of a more *terroir* convenient and resource-saving production (Brillante et al. 2016, Brillante et al. 2020).

Soil biodiversity, soil health, depletion backstop and preservation of natural cycles in directly or indirectly providing biotopes, i.e. also the restructuring of hitherto valid farming and landscape design patterns (Moser et al. 2002, Culman et al. 2010, Wu 2013, J.P. van Leeuwen et al. 2019), are always directly linked to biotically and abiotically motivated nutrient provisioning mechanisms and nutrient acquisitions (Winter et al. 2018, Kalcsits et al. 2020). These dynamic eco-zones are therefore important augmentation, at least adaptation and mitigation domains. Accordingly, they cannot be conceived without an interdisciplinary networked understanding of the ectorhizosphere, rhizoplane and endorhizosphere (McNear 2013, Yıldırım et al. 2018), where trophic cycles as well as protection and equilibria mechanisms interlock via signal control (Abisado et al. 2018).

Considering, that three domains (Bacteria, Archaea, Eukarya) inter and intra-act down to genus and species level (Woese et al. 1990, Ottow 2011) which are simultaneously connected to various abiotic realities like pore volume decrease, anoxic conditions or osmolyte accumulation due to inexpert irrigation practices etc. (Kibblewhite et al. 2008), while being of reciprocally relevance up to the final crop quality and socio-ecological aspects (Pomarici and Seccia, 2015, Mohanram and Kumar 2019) the includability of specifying and exclusive research may not seem instantly evident or even always advisable (Heberlein 1988, Wilson 1998, Brevik et al. 2015). However, interrelating niche studies will albeit need intensification as long as specificity and ultra-specialized research can at least contribute to the attempt of eventually completing the puzzle (Heberlein 1988; Wilson 1998, Spelt et al. 2010; FAO 2017, Acevedo et al. 2018, Ferguson 2021).

2. Pedobiome, atmosphere and water relations

Imagining viticultural used soils and subsequently the endomorphological reaction rooms of the root in multi-annual cycle series (Oburger and Schmidt 2016, Sun et al. 2016) as distinctive spots in a three-dimensionally organized pedo-phytotype extended by space-time (Hoosbeek and Bryant 1994, Minasny and McBratney 1999, Grunwald 2006), requires an initial awareness of geological, pedological and in consequence agropedogenic factors (Kuzyakov and Zamanian 2019).

Thus, as a fundament of viticulture, which is often thought from localized quality indicators (Bonfante et al. 2011, Brillante et al. 2020), the first aspect to be approached should be the pedo-biotopic circumstances that, if occurring to be a stress cause or providing physiologically effective malfunctions, lead to unfavorable consequences for functional trait development and ecological performance (Negin and Moshelion 2016). Again, in these considerations the mutual interspheric influence i.a. driven by spatio-characteristic energy rotations like the carbon or water or nitrogen cycle (Gao et al. 2013, Sun et al. 2016) must, of course, always be taken into account; *vide supra*.

For a superordinate consideration in the given context, particular interest would be attended to calcareous soils, notably including those of the arid and semi-arid zones being exceedingly susceptible to drying and to other drought-prone soil types such as coarse sandy soils or very fine-grained substrates as for example defined by high clay contents (Läuchli and Grattan, 2012, J-F. Liu et al. 2016, Scheffer et al. 2016).

2.1 Calcareous soils and alkalinity

For calcareous, alkaline soils, calcium is of course the key element. Calcium oxide or quicklime (CaO) contributes mineral bound to about 5% of the earth's surface crust. Chalk, i.e. the carbonate bond forms of calcium (Ca) is abundant as the mineral calcite (calcspar) and less prevalent as that of aragonite. Both are also crystallization forms of calcium carbonate ($CaCO_3$), i.e. a salt of carbonic acid (H_2CO_3). The iron containing siderite ($FeCO_3$) is emerging in comparatively minor proportions, particularly versus the frequently occurring dolomite ($CaMg(CO_3)_2$), which exhibits several cations and bears the same name as the corresponding carbonate parent rock. However, carbonate rock (e.g. limestone and dolomite) can be further subdivided into lime rock (>75 % carbonate) and marl (25 – 75 % carbonate), which is characterized by higher proportions of clay minerals.

As a chemo-biogenic rock, carbonate rock is formed in seas by sedimented corals and mollusk shells or, more rarely, as a terrestrial form in groundwater and backwater areas (Nieder 2008, Galler 2013, Scheffer et al. 2016).

Carbonates usually are introduced into soils via physico-chemical process paths from carbonate rocks while the non-carbonate residue (such as phyllosilicates) will be incorporated as clay-mineral-components. In broad terms and with a view to the minerals mentioned so far, it can be inferred, that a considerable part of the natural nutrient composition (e.g. for Mg, Ca, Fe) of developed soils is highly dependent on the minerals provided by the parent rock. Incidentally, the clay minerals, mostly alluvially disseminated into the carbonate rock layers, are of considerable importance for calcareous soils' inventory of sulfides, phosphorous or potassium. The latter can be contributed almost exclusively by illite[1], which is not sufficiently present in all carbonate-born soils.

The actual soil formation proceeds via chemically motivated weathering, e.g. by CO_2 saturated water and later by the CO_2 released in the soil solution by root- and microorganism respiration. In the process the readily soluble calcium hydrogen carbonate ($Ca(HCO_3)_2$) is formed while incrementally humus accumulation and bioturbation provide carbon admixture and aggregate formation (Stahr et al. 2016).

However, unlike limestone or more exactly calcit ($CaCO_3$) that provides the corpus of Ca^{2+} ions contributing to plant nutrition and soil structuring via bridging within clay-humus-complexes, gypsum ($CaSO_4$) is not lime but calcium sulfate and does not have alkaline activity, i.e. it has no pH raising influence. In the very context it may still be employed to reduce irrigation water corrosivity and to prevent incrustation, pore clogging and siltation, or further suit as a soil conditioner to palliate excessive sodium,

[1] Sublett et al. (2018) describe the range of illite as $K_{0.6\text{-}0.85}(Al,Mg)_2(Si,Al)_4O_{10}(OH)_2$

potassium or magnesium ratios (Galler 2013, Wheaton et al. 2008, Blum et al. 2011). Regardless of the feed source, the importance of Ca becomes evident.

For the purpose of agronomic assessment and adjustment of reference values, farmland soils are therefore frequently ranked into lime content groups, which provide information on the amount of CaO ha^{-1} present; similar contexts often refer to other lime compounds as to calcium carbonate equivalents (CCE), which essentially describes the percentage of carbonates of the < 2mm size fraction; *alias* active lime an important assessment variable in soil analysis and rootstock choice (Tagliavini et al. 2001, Spring et al. 2003, Bast et al. 2011, Beach et al. 2018).

If advised, soil liming will cause the lowering of the H^+ ion concentration, or neutralization of protons (hydrons) by raising the hydroxide ion concentration. In any case, due to the multidimensionality and diversity of soils and the manifold agricultural land use options, an optimum carbonate content can merely be given approximately and only in line with the respective site conditions (Schubert 2018, J. Holland et al. 2017).

However, calcareous soils inherently exhibit $CaCO_3$ equivalent ranges between 10 and almost 1000g kg^{-1} and therefore promote equilibrium reactions between carbonic acid (H_2CO_3) and $CaCO_3$ or Ca^{2+} and hydrogen carbonate (HCO_3^-) respectively. As calcium ions or hydroxide ions will remain in the soil while CO_2 discharges when reverse reactions remain improbable or are not intentionally induced, the result is a high buffer efficiency as against acidification (Läuchli and Grattan 2012, Stahr et al. 2016). Contrariwise, a high CCE range corresponds to alkaline pH values which have significant effects on soil biogeochemical interdependence concatenation and rhizosphere trading strategies. Thus, by influencing the soil acidity or alkalinity respectively, the lime content has direct impact on nutrient acquisition and mobilization. (Morrissey and Guerinot 2009, Miller 2016, Neina 2019).

It appears that lime deficiency is just as much a physiological relevant stressor or at least a game-changer in phyto-physiological and pedo-chemical realities as a plethora of calcium carbonate derivatives (Loeppert and Suarez 1996, Hinsinger et al. 2003, Neina 2019). While the calcium fraction in soils with elevated pH is often expectably high, the plant accessible Ca^{2+} can be rare for being sparingly soluble bound to minerals (Läuchli and Grattan 2012). Likewise, the probability for a shortcoming of phosphorous viz. $H_2PO_4^-$ and HPO_4^{2-}, manganese viz. Mn^{2+}, Zink viz. Zn^{2+}, Copper viz. Cu^{2+} and Bor viz.H_3BO_3 increases due to bonds of low solubility. In addition, of course, iron viz. Fe^{3+} and the finally exploitable Fe^{2+} represent a key point in the context given as it has major influence on plant homeostasis and sound crop yields for being a setscrew in the mechanism of chlorosis evolution. Apart from this, a substantial trade-off affects other deficiency-prone nutrients and elements tending to toxicity (Y. Chen and Barak 1982, Morrissey et al. 2009, Schubert 2018).

In spite of other, e.g. sodic soils may range in the alkaline spectrum as well (Proffitt and Campbell-Clause 2012), where ion and iron acquisition disturbance can also be observed accordingly, the total chemism however, and therefore the impacts on plant foraging and adaptiveness differ clear enough to address lime-borne alkalinity exclusively (Richards 1954, Y. Chen and Barak 1982, George et al. 2012, Contin 2020).

2.2 Dry soils and water deficiency

2.2.1 Circular approach

Allowing to consider the soil-plant-atmosphere continuum (SPAC) the most evident interspheric circuit design, it may serve as a primus inter pares exemplification of phytom-controlled energy flux transformation with hyperglobal balancing effects. Although water appears to be the cardinal variable here, drought, drying and climate-induced site alterations promote the effects in cross-amplifying dynamics. Intake of mass and energy via stomatal aperture, foliar surface or wooden parts is co-orchestrated by the physico-chemical transitions in the rhizosphere (Düring, 2003, Limm et al. 2009, Bonan et al. 2014, Evaristo et al. 2015, Silva and Lambers 2018, Fuenzalida et al. 2019). No roots, no rain. (Freschet et al. 2017, Freschet et al. 2021).

Indeed, the rough process of water and energy circulation in its different manifestations is fairly apprehended (Kozlowski 1964, Hanson 1991), but the orchestrated entirety of functional multi-interdependences within developing or degenerating ecosystems eludes supra-systemic traceability and cross linkable certainty in numerous aspects regarding landscape ecology and thus agri- and more specifically viticulture with all associated sub-disciplines included (Culman et al. 2010, Fraga et al. 2012, Hatfield and Dold 2019, Santos et al. 2020).

As complexity seeks invention and area thinking, Lovelock (1987, 2003) referred to the planet as being organized like a living holo-organism. In point of fact, while knowledge increases, a turn to holistic concepts seem to gain broader acceptance. Norman and Anderson (2005) affirmatively exemplified the global air and water streams or atmospheric climate cells as vessels and veins like the plants' xylem or phloem. Thinking this out, it seamlessly anastomoses into the laws of physics, where barometric and osmotic pressure, redox-potentials, water potentials, suction, adhesion, resistance and other promoters of gradient based systems propel the wheelwork of life-cycles; may this relate to the mitochondrial respiratory chain, the gulf stream or the water balance. Particularly for plants the source-sink principle is taking effect here, where the soil is the main source and the atmosphere is the main sink, while roots and aerial plant parts serve as transient or intermediate sources and sinks (Anderson et al. 2003, Norman and Anderson 2005, Scholz et al. 2011, Deng et al. 2017, Deloire and Pellegrino 2020).

In relation to drought and drying soils consequently two atmospheric supra-variables are pivotal: temperature in connection to humidness and precipitation. More unpredictable heat events and deregulated rainfall patterns will severely affect the unbroken consistency of circular flows in all sub-variables of the total system including root vessels, soil structure, soil biota and hence, the geospheric main variable as a whole: the soil with all associated ecosystem services (Hansen et al. 2012, T. Holland et al. 2013, Lerebroullet et al. 2013, C. van Leeuwen et al. 2019).

2.2.2 Budget approach

While on the one hand there is a clear dependence of the soil water budget on atmospheric inflows (e.g. precipitation) and outflows (e.g. evapotranspiration), the budgeting and distribution of this disposability in turn depends again on hydraulic and capillary gradients and thus on the soil structure, i.e. essentially on grain sizes and pore volumes.

The water potential in the soil (Ψ_s) consists of two partial potentials as well as the water potential in the plant (Ψ_p). Where Ψ_s consists of the matrix potential (Ψ_m) and the osmotic potential (Ψ_o) and can be formulated as $(-)\Psi = (-)\Psi_m + (-)\Psi_o$; in relation Ψ_p consists of the Ψ_o and the turgor pressure potential Ψ_t and can be displayed as $(-)\Psi = (-)\Psi_o + (+)\Psi_t$. The dependencies within Ψ_o are basically explained by the saturation gradient (quantity of ions or sugars in soil solution or cytosol and vacuoles) on the one hand and within the plant by the gradient between saturation in the vascular tissue or cells respectively or within apoplast and protoplast; a functional complex which in turn is closely linked to hydraulic conductivity, L_{Pr}, where P_r is designated as negative root pressure ($-P_r$). Water concentrically is transferred through root tissues to the xylem for axial exhaust (de Herralde et al. 2006, Scheffer et al. 2016, Schubert 2018).

Based on the reliable model of soil water holding capacity (Boussinesq 1885, Richards and Weaver 1944), Geng et al. (2015) set marginal conditions at 10 % water (v/v) for agricultural soil in general and remind irreversible soil degradation below this threshold. However, to ensure rehabilitation processes after drought occurrence, ≥ 14,3 % are set as a minimum value of constant water proportion. Summarizing, Osmolovskaya et al. (2018) assign drought set in for Ψ_s falling below -0,4 MPa, whereas intense to threatening unavailability ranges between -1,5 MPa to -2 MPa, for which reason experimental set ups are generally to be carried out in a scope of -0,3 MPa to -0,8 MPa. Of course, for homeostasis purposes, the time endured in drought conditions is a pivotal factor too (Fort et al. 2017, Razmkhah 2017). Merging intensity and duration a general response strategy classification subdivides into drought elopement, drought prevention and drought tolerance (Yıldırım and Kaya 2017, Osmolovskaya et al. 2018). This might be termed up by drought recovery (Fang and Xiong 2015) which, along with the aforementioned behavior patterns, is a functional response trait of crucial value for rootstocks and rootstock breeding in viticulture (Vandeleur et al. 2009, Cochetel et al. 2020, Frioni et al. 2020).

Doubtless, vineyard soils, although still cropland, are being appraised differently (Huggett 2006, Brillante et al. 2020, Lazcano et al. 2020). A mild to moderate water shortage is often considered beneficial to high quality grapes especially from red cultivars (Chaves et al. 2010, Shellie 2014, C. van Leeuwen et al. 2018). If, conversely, the progressive climatic changes and the maintenance of certain wine styles are considered, the dryness to quality ratio needs increased spectralization. By implication, many authors (Fraga et al. 2015, Bernardo et al. 2018, Koch and Oehl 2018, C. van Leeuwen et al. 2018, Gambetta et al. 2020, Lazcano et al. 2020, Santos et al. 2020, Venios et al. 2020) clearly advocate for a research increase with regard to adaptation, mitigation and amelioration strategies at the level of plant physiology, breeding, soil science, agroecology and, consequently, everyday practice. Roots, root proprioception in general and root response traits in sensu stricto are significant sub-values of this prospective empowerment of viticultural organized nature (Woods et al 2010, Ollat et al. 2016, Lynch 2019, Freschet et al. 2020, Strock and Lynch 2020, Marin et al. 2021).

Just as dynamics of water distribution patterns on various spatial scaling scopes become the focus of corresponding remote sensing disciplines (Brillante et al 2016, Babaeian et al. 2019), experimental in-field respectively in-situ data provision continues to be challenging (Schultz and Stoll 2010, Yu et al. 2020). Mainly because of the many contributing and aforementioned abiotic or biotic variables respectively, that are difficult to predict and that interact at numerous levels of motivation (Ottow 2011,

Bünemann et al 2018, Marin et al. 2021). To illustrate this complexity, Kibblewhite et al. (2008b), Brussaard (2012) and Bünemann et al. (2018) elaborated a linkage model between soil threats, soil functions and soil based ecosystem services, which in Figure 1 is expanded by corresponding root involvements.

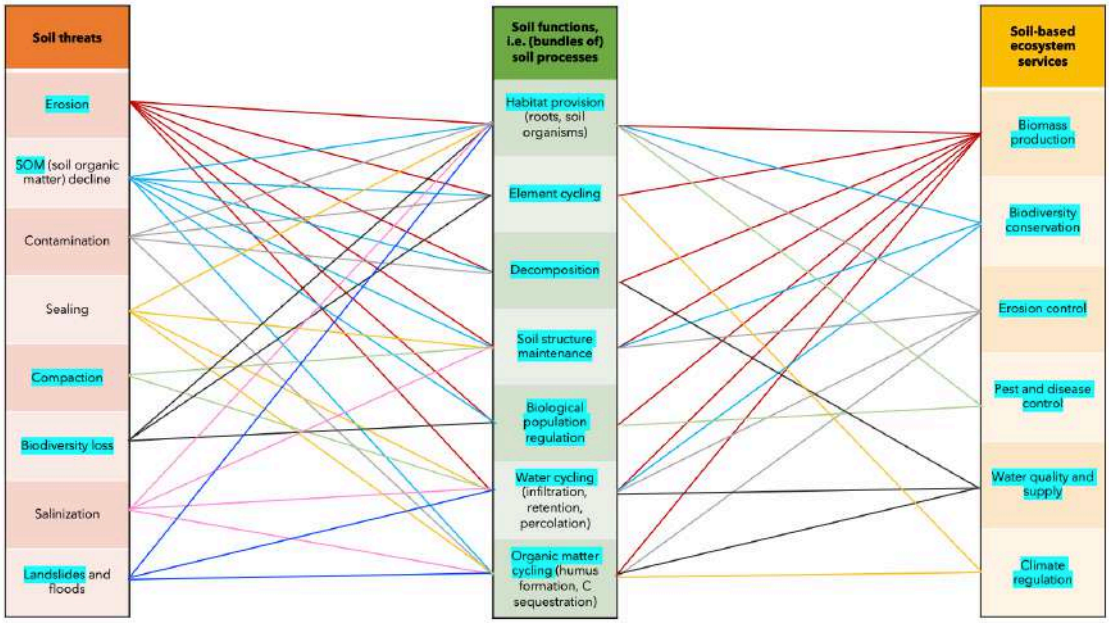

Figure 1 Interactive links between soil threats, soil functions and soil-based ecosystem services. Certain interrelations or impacts and amplification effects could be added depending on the definition. Flooding, for example, would also negatively affect the maintenance of soil structure; furthermore, reciprocal amplifications within the columns of variables are likely to be incorporable. The motivation complexes in which roots or the resulting ecosystem properties and parameters are directly or indirectly involved are highlighted in color (amended from Kibblewhite et al. 2008b, Brussaard, 2012, Bünemann et al. 2018).

However, evolving techniques with regard to water economization and sustainability improvement show promising possibilities (Lopes et al. 2018, Babaeian et al. 2019, Yu et al. 2020) and already complement the efforts towards water use efficiency (WUE) enhancement ventured by rootstock breeding, rootstock choice and realignment to accumulating soil data and progressing belowground phenomics (Zhu et al. 2014, Pagay and Kidman 2019, Falk et al. 2020, Frioni et al., 2020).

Benefit is also envisaged by Radville et al. (2016) with regard to the carbon sequestration capacities of subsurface plant parts, yet reminding the still incalculable effects of global warming on seasonal synchronization of root growth with aboveground developments and general growing patterns; which, of course, in turn are likely to have impacts on nutrient acquisition and whole plant endurance (Nord and Lynch 2009). Responding to this admonition, it can at least be said that within the last few years the efforts and the prolific scrutinies and counter-scrutinies yielded a considerable knowledge increase, which in turn contributes to new horizons in understanding the hidden half (Atkinson et al. 2019, Ephrath et al. 2020).

3. Root histology, nutrient pathways and stress responses

Approaching the target material, roots and rootstocks in their environment are focused in terms of function, general morphology, distribution and architecture. A specifying view applies to endodermis,

exodermis and their lignin-like or suberin-like cell wall enhancements. The corresponding interaction with environmental or nutritional conditions and constraints are surveyed in both micro-endomorphologic and macro-phenomic response characteristics.

3.1 Roots

3.1.1 Blueprint and development

Towards the proximal end, primary roots are basipetally organized in four sections, of which the first is the root tip meristem consisting of columella root cap, peripheral lateral root cap and quiescent center, a cell layer with unregulated and rather merismatic emergency scheduling ability. While haphazard cell division is passing off (Hayashi et al. 2013), Golgi apparatus mediated mucilage exudation of both hypersecretory root tip cells and associated soil bacteria ensures sustained root-soil contact. Hydraulic conductivity maintenance and tissue are protected simultaneously as the gelatinous-like polysaccharide-acid mix turns to a mucigel called lubricant by incorporating particles of rhizosphere soil and lysed microbe or plant cells respectively (Bending 2003, Neumann and Römheld 2012).

Furthermore, the columella meristem holds statocysts with statoliths for gravitropic growth orientation and not yet specified H_2O sensor-synergies. This complexity, inducing cytosolic Ca^{2+}, abscisic acid (ABA), reactive oxygen species and auxin counter-action for hydrotropic root growth by accelerated amyloplast expression and autophagy, would neglect the Cholodny-Went theory for hydrotropism decryption (Shkolnik and Fromm 2016, Jiménez-Nopala et al. 2018). However, this pioneering region subsumed as calyptra indeed has already veritable influence on total root architecture due to its signal cross-point function. Figure 2 here underlines the remarkable fact, that all other root cells will form from this initial part in later stages throughout root maturation, where all tissues are organized in concentric cylinders one around the other (Gambetta et al. 2013, Keller 2015, Kumpf and Nowack 2015).

First cell division is a transversal reduplication into a second regenerative cell to retain renewal qualities. Successively, a second but longitudinal dissection origins an epidermal cell and a cortex cell. The outermost layer of this cortex tissue will develop into the endodermis with consecutive Casparian strip

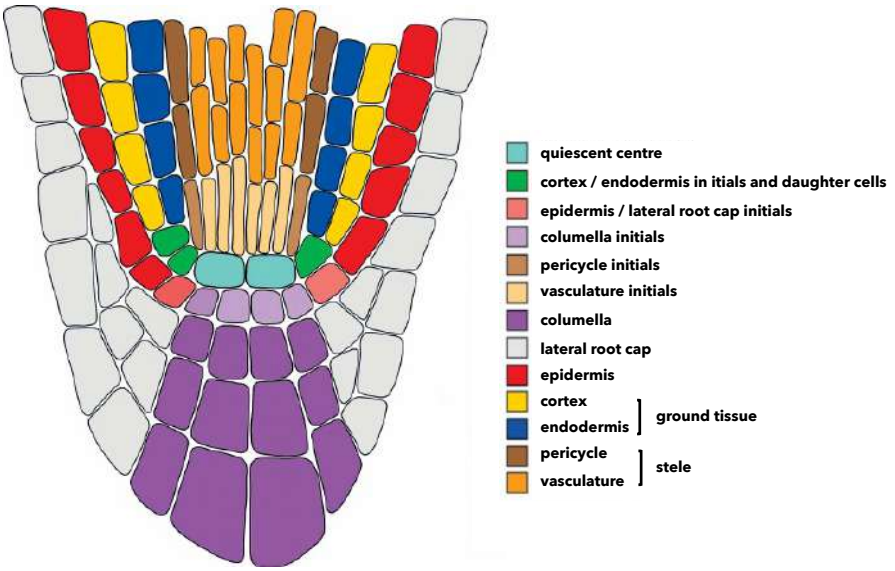

Figure 2 Ontogenetic organization of meristems in the root tip of a dicot. Amended from Stahl and Simons, 2005.

(CS) formation (Benfey and Scheres 2000, Augstein and Carlbecker 2018).

In this primary meristem all functional tissues of the root entity have their origin already as procambium (vascular tissue formation), ground meristem (cortex formation) and protoderm (epidermis, rhizodermis and exodermis blueprints). It becomes evident, that all types of cells are present in every developmental stage along the same root axis. This, in turn, allows the formation of Casprian strips from a certain point within the overall root design to be conceived as distinctive chrono-spatially adaptation of the endo-micromorphology to first rhizophenological necessities and then to environmental realities; *vide infra* (Benfey and Scheres 2000, Kumpf and Nowack 2015, De Rybel et al. 2016).

The elongation zone hereupon is adjacent to the meristematic active root tip in the axial direction towards the soil surface. According to Larkins et al. (2001), Hayashi et al. (2013) or Shu et al. (2018), for many plants this space-gain to some extent is achieved by cell volume enlargement. Quite often this might at least partly be ascribed to endoreduplication effects operated by a mitotic cycle contraction resulting in DNA content increase without cell division. Anyway, the general cell size enlarges progressively from the bottom half of the meristem and then increases significantly from the transition to the elongation zone where rhizoderm and vascular tissue formation originate. It remains to be seen whether this phenomenon initially is due to escalated cell expansion or to endoreduplication (Beemster et al 2003, Hayashi et al. 2013). Nota bene, while this biomechanism is very common throughout the phylogenetic tree, grapevine does not show any evidence for endoreduplication (Chevalier et al. 2011), yet still exhibits comparable growing patterns and cell sizes; i.e. cells of the elongation zone do not grow by number but about ten times faster in length as compared to meristematic cells (Baskin et al. 2020). In the context given it is of relevance, that root elongation and consequently sustained cell wall distensibility and permeance are crucial factors for drought tolerance or recovery respectively (Prinsi et al. 2018).

In terms of chronological and endo- or exo-spatial distribution, the transition zones of roots and their tissues are not strictly definable. Nevertheless, an operative order applies according to which the maturation zone emerges functionally from the elongation zone (Archer and Saayman, 2018, Baskin et al. 2020), which corresponds with the findings of Sánchez et al. (2018) for *Arabidopsis thaliana*, according to which cell elongation to some extent continues even after the first root hair convexities indicate a beginning maturation zone.

However, in this section functional accrual is achieved by the differentiation of pericycle, primary phloem, primary xylem, and endodermis (Gambetta et al. 2013, Keller 2015). Successively, the trichoblast cells of the rhizodermis protrude as root hairs having water and nutrient uptake from the rhizosphere as their main purpose and the bonus effect of soil structure stabilization. Archer and Saayman (2018) together with Winkler (1962) and Cailloux (1972) validate an influence of soil pH on root hair abundance but object to the importance of root hair patterns for nutrient acquisition or plant growth under field conditions. May this, together with mycorrhizae as a possible substitutional player in root-surface-enlargement, be further fathomed (Lakso and Eissenstat 2012, Bengough et al. 2016, Correa et al. 2019).

Transitioning from maturation to secondary growth, progressively exodermis appears due to rhizodermis stalling and as the last step in primary growth, secondary phloem and xylem formation from the vascular cambium initiates the secondary growth phase. Here, root branching may occur due to lateral

root formation from the pericycle. As the pericycle actually is a primary meristem, the integrity of the concentric tissue layers of the whole root surface is not violated by transversal main mother-root perforation (De Smet et al. 2006). In assumed contrast, Barberon and Geldner (2014) note that a pure apoplastic passage can only result from unaccomplished CS formation in early developmental root stages or from barrier disruption e.g. due to lateral root emergence. However, it is rarely stated that endodermis will re-reconfigure from the pericycle to close that unprotected flank, a publication from the environment of the latter authors has shed light on these relationships (Vermeer et al. 2014). In a study co-authored or respectively edited by the same institute, Vilches-Barro and Maizel (2015) again indicate that the isolation of the stele from the cortex is preserved. The orchestration of phytohormones, protein regimes and biomechanics is extremely complex here (Lucas et al. 2013, Du and Scheres 2018) and many aspects are still difficult to understand.

Growth in total is ensured by cell wall softening, cell expansion and turgidity amongst other factors (Vilches-Barro and Maizel 2015). Since the lateral roots are symplastically disconnected from the mother root, the only support may be given via plasma membranes, hence aquaporins. Knowing this and already anticipating suberization under malconditions, it becomes clear that total root elongation and formation of lateral roots (volume expansion) under drought stress is already mechanically restricted. Genetic tooling and architectural intelligence of the (individual) plant make the difference here (Vilches-Barro and Maizel 2015, Du and Scheres 2018), which is especially true for grafting ambitions and grapevine rootstock choice, because two genomes have to coincide (Marguerit et al. 2012, Cookson et al 2013, Melnyk 2017).

However, neither endodermis nor exodermis follow the increase in girth initiated by secondary growth progression. In fact, a third terminal tissue is formed with the periderm. Here, the root will lignify, form bark (Beck 2010, Keller 2015) and finally, all this contributing features will cross-link into either allorhizic root systems for dicotyls (as e.g. grapevine) or homorhizic root systems for monocotyls via inter- and intradependently dynamizing reciprocities.

3.1.2 Endo- and exodermis. Magnifying Casparian strips and suberin lamellae. Function and performance

As a matter of fact, each cell of the endodermis is endowed with Casparian strips following the transverse primary cell wall tangentially and the radial oriented primary wall axially (Beck 2010). These bands are rarely measuring more than a third to a half of the anticlinal wall structures. Casparian strips in the exodermis in contrast may spread over the entire area of the respective walls but remains rather patchy and is at least partly subjected to stress dynamics (Enstone et al. 2003, Gambetta et al. 2013).

Because many, especially graphic, orientation aids for locating and assigning the CS are somewhat vague, it should be said that the corresponding polymers bind to the plasma membrane and infiltrate the cell wall interstices (Roppolo and Geldner 2012, Simpson 2018), meaning that they are not actual deposits but, in a sense, extensions of the plasma membrane or cell walls (Figure 3). In this context, it should also be noted that the apoplast includes both the space within (between) cell walls and the intercellular space, which also contributes to undirected water inflow (Zarebanadkouki et al 2019). CS barriers must therefore also penetrate the middle lamellae to seal the steles (Roppolo and Geldner 2012, Z. Liu et al. 2015).

After protracted disagreement regarding the composition of this hydrophobic barrier, now everything except lignin or a polymer highly related to lignin can be rejected (Naseer et al. 2012). Indeed, it was a leveraging conclusion, that polymer biosynthesis initiating and the actual accretion of the lignin-like polymer to the functional barrier of the Casparian strip is effectuated by the CS membrane domain proteins. But nevertheless, the accumulation dynamics of CASPs, the processes of the CS lignin-type polymerization and the subcellular organizational hierarchy of the literal production seem to be still unclear (Benfey and Scheres 2000, Lee et al. 2013, Ropplolo et al. 2014, Lee et al. 2019).

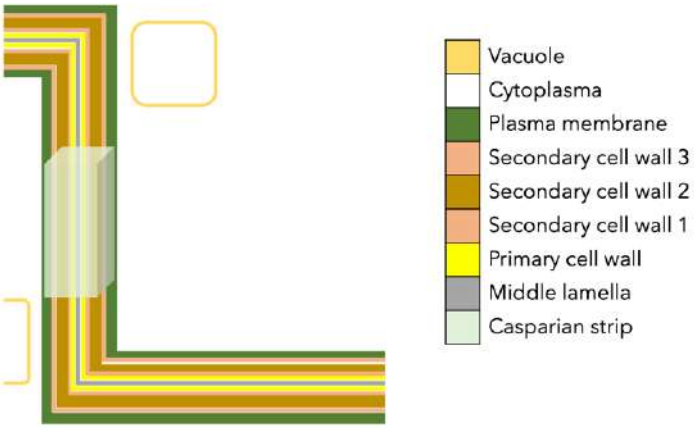

Figure 3 Schematical top view in acropetal direction on two adjoining root cells. Commencing with the spotting of the Casparian strip domain proteins (CASPs) in the plasma membrane, the accumulation of the lignin-like polymer will successively build the Casparian strips. To ensure barrier function, the total apoplast needs to be blocked. However, the multi-part and multilane synthesis and accumulation process remains in need of further elucidation in numerous domains.

The general synthesis pathways of lignin itself however, seems to be relatively well understood; nevertheless they are extreme multi-laned and again, the exact composition of the respective fractions remains mostly untraceable due to its reactive polymerization randomness (free radical coupling). This would play a role for the residue-free depolymerization into products like biofuel, biogas or bioethanol (Welker et al. 2015), but can also be important for enological issues (Le Floch et al. 2015).

Kreszies et al. 2019, for their part, are submitting distinct observations with reference to Bernards (2002), Garca (2015) and Lupoi et al. (2015) when describing lignin or rather the CS as a complex aromatic biopolymer formed by syringyl, guaiacyl and p-hydroxyphenol monomers; and suberin lamellae as a composition of polymerized polyaliphatics (i.e. primary alcohols, fatty acids, α-ω dicarboxylic acids and ω-hydroxy acids) and polyaromatic domains (i.e. ferulic and coumaric acids). In addition to further advantages of a precise knowledge of the CS and SUB components, this would also allow optimizations to be derived for histochemical staining methods, which are an important feature of microscopic morphology research (Baldacci-Cresp et al. 2020).

However, a possible source for biased earlier attempts of compound determination or simple misnomer is the fact that as maturation of the lignified cell wall sites progresses, suberin (SUB) will successively but possibly non-contiguously be laminated as well (T. Chen et al. 2011, Halpin 2013, Kreszies et al. 2019). Indeed, suberization is performed independently via other, process-intrinsic albeit partly still elusive pathways. Suberin occurrence is either due to root maturation or stress-responsive mechanisms or both (Kreszies et al. 2019, Cohen et al. 2020, L. Zhang et al. 2020). Suberin lamination for stress mitigation is indicating a presumed strategy change from an actively selecting (CS) to an indiscriminative (SUB) defense (Barberon et al. 2016). Although the expression occurs always qualitatively independent of biotic or abiotic demands in roots of higher plants (disregarding mutations in which e.g. hormone

peptides are not provided or the transcription factor MYB36 remains defective), it is quantitatively controlled by reaction response. The pattern as well as the chrono-spatial positioning within the root are thus induced by stimuli syndromes (Karahara et al. 2014, Kamiya et al. 2015, Líška et al. 2016). Furthermore, the exact composition, individual histogenesis, or stimulus-dependent initiation times for expression and intensified expression of polymers seem to be species-dependent and can sometimes vary significantly (T. Chen et al. 2011, Ranathunge and Schreiber 2011); all the more so when the diversity and adaptivity of stress strategies are factored in, even over only small spatial gradients. Song et al. (2019) for example found evidence for simultaneous accumulation of both lignin-and suberin-like primary wall enhancing compounds at protoplast surfaces in Chinese fir.

The endodermis as a selective barrier tissue and root hair development occur during the same chrono-spatial unit formation. With further inclusion of the fact, that total root plasticity is explicitly codetermined by signaling pathways of the stress hormones ethylene and auxin, e.g. geared by N, Fe, P or H_2O deficiency, the endodermal CS contribution to plant homeostasis may become conceivable (Grierson et al. 2014, Karahara et al. 2014, Marzec et al. 2014, Robbins et al. 2014, Shibata and Sugimoto 2019).

In principle, the controllability of the influx into the vascular tissues is achieved by pathway regulation. Water and solutes or pathogens can no longer enter the stele apoplastically and must therefore be introduced either symplastically (through plasmodesmata) or transcellularly via plant plasma membrane-type plasma membrane intrinsic protein (PIP) transport (Gambetta et al. 2013, Robbins et al. 2014). Whereas the root hydraulic conductivity of the apoplast can be rigidly modulated by CS or SUB charged endo- and exodermal cells, the root hydraulic conductivity (Lp_r) of the transcellular pathway can be counter-controlled by the plasmodesmata as well as additionally or alternatively by aquaporins, whose efficiency performance is positively linearly correlated with their activity and abundance.

According to Steudle and Peterson (1998), Vandeleur et al. (2009) or Ranathunge and Schreiber (2011) in turn, the symplastic and the transcellular pathway are not effectively distinguishable as inflow pathways; at least not for water due to its high permeability. Other substances, however, can be actively selected and, if necessary, vacuolated or discharged by means of energy investment (Diener et al. 2001, Weston et al. 2012, Song et al. 2019).

Understandably, up- or downregulation of PIPs, i.e. aquaporin gene expression and activity intensities, are dynamically controllable in the short term (hours); whereas lignin or suberin accumulations are medium term manoeuvers and of limited reversability (Gambetta et al. 2013, Gambetta et al. 2017, Kreszies et al. 2019), which for the CS seems to be less rigid in terms of construction and more flexible in selective flux control than previously assumed (Wangenheim et al. 2017). This makes particular sense when considering that additionally to a controlled mass transfer, pathway regulation also adjusts resistivity and negative pressure to changing conditions. Analogously, but more undirected, the formation of CS in anticlinal walls of the exodermis contributes to resistance adaptation to radial water flow and presumably again to total root plasticity under rhizospherically unfavorable conditions (Hose et al. 2001, Song et al. 2019). Furthermore however, Casparian strips, both in endodermis and exodermis, cannot be appropriately conceptualized without their (albeit time-delayed) dynamic dialogue with suberin about functional balancing. Since CS in exodermis are not continuously

expressed and suberin lamellae appear to be accumulated effectively on demand (sometimes even before CS occurrence) and considering the existence of non-laminated passage cells within the barrier ring, it seems, that no exodermal enhancement strategy targets a hermetic sealing even under severe strain, but rather always intends to screen solutes for hazardous compounds or, in agreement with the two most commonly expressed PIPs (VvPIP1;1 and VvPIP2;2), to regulate root water potential (Enstone et al. 2003, Tyerman 2010). Figure 4 surveys the most important details.

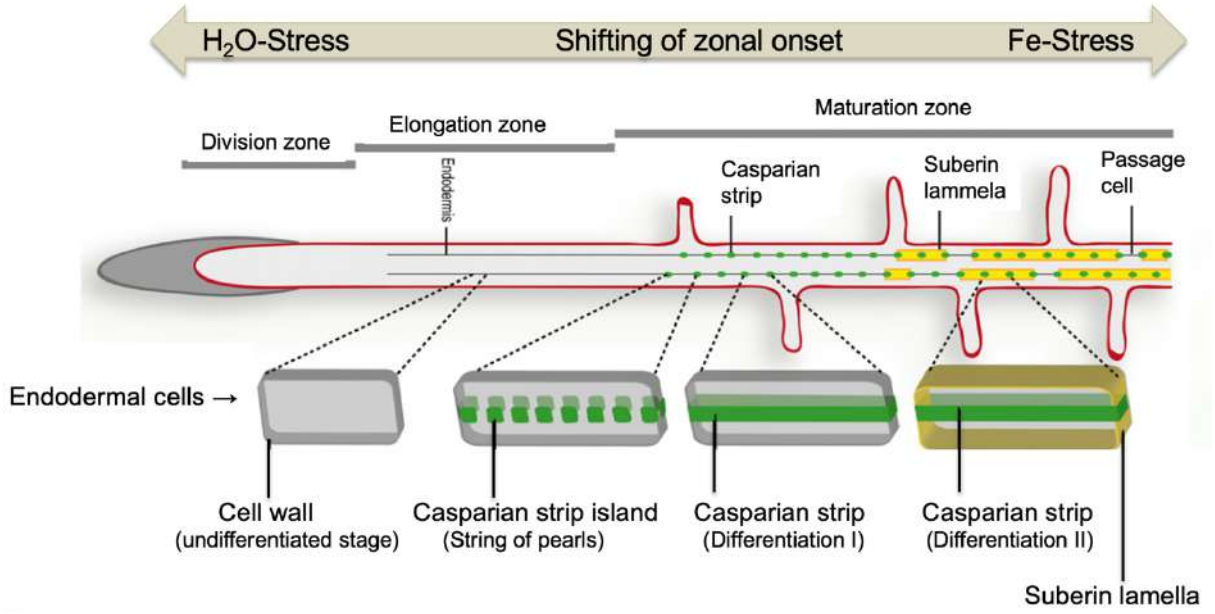

Figure 4 Occurrence of Casparian strips and suberin lamellae. Both polymers will develop acropetally under fulfillment of several, chrono-spatial tasks or as responses to detected strains. In general, the elongation zone of plant roots is shortened when water shortage occurs; in the case of iron deficiency, however, incrustation and maturation usually start later. Amended from Barberon and Geldner 2014.

Instancing integrity losses, an intelligent communication sequence can also be observed for the endodermis, where damage to the lignin-like belt allows signal peptides to pass from the stele into the cortex, which cause a reduction of the aquaporin share in total transport and thus lower the hydraulic conductivity. By further inducing suberization, the osmotic potential is maintained and ion leakage is avoided. Similarly, the stomata are adjusted via long-distance signals (Wang et al. 2019). Kreszies et al. (2019), on the other hand, recognize that suberin production is stimulated by osmotic stress, but not that aquaporin expression is markedly reduced. However, increasing suberin also seals the membrane channels (Wang et al. 2019). Hence, the latter authors consider whether the sheer amount of aliphatic substance application must always be negatively correlated with water permeability and conclude that this appears to be short-sighted due to the highly diverse monomer combinations and thus the microstructure of individually or species-specifically expressed suberin substances. Schreiber et al. (2005) and Gambetta et al. (2013) could pre-confirm this assessment.

In the given context it is also worth pointing out once again, that Casparian strips may as well signify axial maturation processes for only occurring when the cells of the endodermis are terminally mature (Figure 4) and hence not further elongate (Karahara et al 2014). Along the physically embodied timeline of roots, therefore a primary, a secondary and a tertiary endodermis can be distinguished, which, except

for the primary endodermis although is not universally observable for all plants. The distinction can be made by both, intensity of incrustation and polymers employed; as well as, of course through the chrono-spatial position.

In summary, lignification or suberization or combined polymer infiltration and lamination of exo- and endodermal cell walls can be defined as prominent formulations of stress responses of plant roots to drought or toxicity hazards (increased salinity, heavy metal accumulation in the rhizosphere etc.). By impregnation of the according cell walls with a selective, respectively hydrophobic protection layer, the dermal tissues enhance their resistivity to degradation phenomena. Further, they increase flow control in root sections above the meristematic zone (Naseer et al. 2012) by sheathing more sensitive tissues with dynamic, i.e. cutoff-variable cylinders, whose properties and micro-spatial development can be further interpreted in the direction of homeostasis safeguarding and RSA influence in grapevine rootstocks (Gambetta et al. 2013, Chaparro et al. 2014; Tylová et al. 2017, Barrios-Masias et al. 2015, Marastoni et al. 2020, Namyslov et al. 2020).

3.1.3 Iron deficiency. Organization of the rhizosphere emporium

Sufficient presence of iron is assured due to the sheer abundance in the earth's crust and thus in the soils. Since elemental iron in contact with water and oxygen first oxidizes at high rates to Fe^{2+}, which then reacts with hydroxide ions from the soil water to form Fe^{3+}, the uptake of this micronutrient is again often limited (Pérez-Guzmán et al. 2010). Iron is essential for the plant not only for the maintenance of photosynthesis performance as a protein cofactor (Kroh and Pilon 2020), but also for respiration, sulfur or nitrogen metabolism, electron transport chain functioning and in the transposition between iron oxidation states, which is a crucial factor in CO_2 emplacement. Hence, the efforts of the plant itself and the agro-cultural ambitions to make iron from the soil available for roots are intense . But as with any nutrient, too much iron can be just as deleterious as too little. In hypoxic soils, e.g. introduced through water logging or compaction and surface luting (Morales-Olmedo et al. 2015, Loreti and Perata 2020) it i.a. leads to hydroxyl radical formation via Fenton reaction (Krohling et al. 2015). However, to overcome a shortage of iron, plants can either protonate, chelate, or reduce the Fe^{3+}; where one step may prepare the others (Guerinot and Yi 1994). Basically and generally, however, iron can be absorbed as Fe^{2+}, Fe^{3+} and as iron chelate.

Plasma membrane proton-adenosinetriphosphatase (P-ATPase) mediated exudation of protons by roots that acidify the rhizosphere (and promote Fe^{3+} reduction) is the strategy I of eudicotyledons (grapevine) and non-monocot grasses (Ramos et al. 2009, Krohling et al. 2015). In this process, P-ATPase increases the solubility of ferric iron (Fe^{3+}) and ferric chelate reductase (FCR) reduces the dissolved Fe^{3+} to the plant available Fe^{2+} with an additional increase in uptake by the iron regulated transporter (IRT) on the rhizodermis (Krohling et al. 2015) while nicotinamide adenine dinucleotide (NADH) or NADPH cater the electrons. In fact, carbonic acids also seem to be formed by respiration and exudation of boron CO_2, which in turn can raise the pH to some extent when dissociating under alkaline conditions (Hinsinger et al. 2003). Accordingly, different root exudates, like malic acid, citric acid, phenolic acid and piscidic acid can form stable iron chelates (Guerinot and Yi 1994; Marschner et al. 2011). Whether a (drought-)stress induced shift of the maturation zone could have an effect here might have to be

considered, since iron (also Zn and P) undersupply provides a retardation of suberization processes and increased integration of passage cells as a palliative strategy (Odgen et al. 2018). Here, a simultaneous inhibition of root elongation due to ethylene (J. Li et al. 2015) contributes in functional congruency and may result in CS formation disturbance or a resistor to elongation termination.

Although iron deficiency mediated by alkaline root environments and drought phenomena determine the development of different approaches with regard to defense reactions and strategic morphological maneuvers respectively (Bert et al. 2013, Fort et al. 2017, X. Zhang et al. 2019), grapevines do not infrequently have to endure both malconditions at the same time (Tagliavini and Rombolà 2001, Kocsis et al. 2009, Pavloušek 2010). In this context, rooting pattern differentiation and lignification or suberization properties are processing resilience enhancements of rather lime tolerant varieties as evidentially as of representatives being rather unsusceptible to drought (Smart 2006, Connorton et al. 2017), interestingly, however, often in apparently opposite ways concerning barrier layer reinforcements (Vigani et al. 2012, Marastoni et al. 2020). The latter studies point to dicot representative strategy I responses like intensified H^+ release to the rhizosphere along with FCR upregulation and increased root exudate effluence. For these mechanisms Casparian strip formation and other cell wall strengthening would be unfavorable as barrier formation especially in lateral fine root dermal layers interferes with rhizodeposition measures mediating the iron uptake (Barberon 2017, Tylová et al. 2017, De-Jesús-García et al. 2020).

On this account, morpho-adaptive root-tip behavior is particular important and requires micro-segmental observation since metabolites primarily diffuse osmotically through the apoplast of undifferentiated root tip tissues, while contrary to this, protectional layer formation is extended toward the elongation zone under abiotic stress, *vide supra* (Enstone et al. 2003, Naseer et al. 2012, Canarini et al. 2019).

Finally it has to be mentioned, that Fe deficiency is not synonym to elevated pH values which are not synonym to lime which again is not synonym to rhizosphere realities resulting in an iron undersupply or an acquisition obstruction. However, in this context, Hsieh and Waters (2016) give rise to the remark that Fe shortage and elevated pH values or alkaline lime soils seem not to have been investigated as discrete parameters in molecular physiological research so far. The bio-physico-chemical gene-to-phene mechanism in root-substrate-interdependencies, also referred to as the rhizosphere effect, still keeps offering many blind spots to plant research ambitions (Hinsinger et al. 2009, Ottow 2011, Schneijderberg et al. 2020).

3.1.4 Root system architecture. Responsivity and foraging performance

Successful water supply and nutrient uptake in the ecological and agricultural sense always has to do with plant intelligence, i.e. the ability to colonize and forage in the right soil spaces at the right time with the right roots (Wangenheim et al. 2020). In addition to water, nitrogen, phosphorus and potassium, it is notably magnesium and calcium (in acidic environments) and iron and zinc in alkaline environments that need to be acquired. The corresponding traits can be evaluated with the assist of phenomics and phenotyping measures, and the results can be used for smart and precision viticulture in coordination with accurate soil information. Straight, fast and deep growing ideotypes, for example, promise efficiency towards water and nitrogen. On the other hand, superficial branching and lateral formation in turn

procure phosphorus, magnesium or newly-mineralized nitrate, etc. A successful rhizosphere-trading, in turn, is promising for assured iron uptake (Lynch 2019, Daldoul et al. 2020).

Combined stress effects thus pose a particular challenge. For example, a low-energy, fast-growing root architecture specialized in water sourcing would be significantly more expensive and demanding in terms of energy technology and construction mechanics, if they had to be achieved under adverse or poor biotope realities (Suarez et al. 2019, Strock and Lynch 2020, Freschet et al. 2021). Here, some modules had to be laboriously collected. Moreover, Correa et al. (2019) interestingly make the rare but essentially imperative distinction between strain and stress when, together with Blum (2016), defining strain as the primary symptom of stress, i.e. as the pre-collapse effect of a stressor on the plant and thus as the phenotypic expression of this specific stress. The strain itself may be reversible or irreversible, meaning elastic or plastic respectively. Only by indirection of the strain can stress actually be phenotyped. In this dynamic, strain can also be referred to as stress response; representable and evaluable in constitutive traits, performance traits, response traits and effect traits (Violle et al. 2007, Blum 2016, Correa et al. 2019).

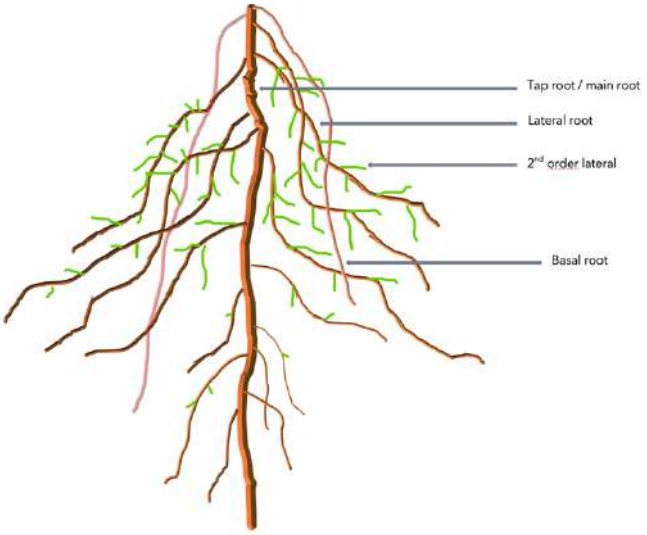

Figure 5 Allocation of the main root contributors to total RSA of a dicotyledonous plant according to the ISRR (International Society of Root Research). For the taxonomy a further look may be taken at Zobel and Waisel (2010). The above pattern is random and does not refer to any soil, stress (strain) or plant species.

In agreement with Comas et al. (2013) and Schnepf et al. (2018), root architecture and root traits are ordered multidimensionally. The root system for a dicotyledonous plant (Figure 5) consists of up to three root organ main types. The framework of woody roots, popularly referred to as the root, which more or less allometrically reflects the aboveground branching of the shoots and, as a perennial plant part, provides anchorage, compound storage and compound or water transport and redistribution. This network usually consists of the tap root (first root of the seed or seedling) and possibly basal roots (emerging from hypocotyl or mesocotyl); both are often summarized as adventious roots when referring to grapevine rootstocks (Smart et al. 2006). It also includes the lignified laterals, which may be further subdivided into fine roots, when diverging non-lignified as the first branching from the main root and the first branching from the first lateral (Schnepf et al. 2018, Freschet et al. 2021).

Of course, the root systems of plants are very dependent on the species, the soil and climatic conditions, and the supply or undersupply in agricultural contexts. For drought-related problems, other regions of interest (ROI) would have to be focused on than for phosphorus or iron, or they would have to be combined depending on the problem and the influencing intra-reciprocities would have to be observed accordingly. Which parameters are considered therefore depends on the research question.

However, important parameters can be: length, average diameter, surface area, volume. Initial growth speed, length of basal zone, length of apical zone, branching distance, number of branchings or laterals and angle can provide further information about the function (Julkowska et al. 2014, S. Li et al. 2015, Shahzad et al. 2018, Seethepalli et al. 2021). RSA studies thus offer a favorable perspective for the consideration of the multi-chrono- and multi-spatial dimensioning of the root.

For a better arrangement of the parameters in space, various methods have been established and improved in recent years, trying to transilluminate the fundamental seclusion of the root systems in their natural environment. Classical phenotyping is still laborious and often destructive, especially under field conditions (De Herralde et al. 2010, Dumont et al. 2016, Jeudy et al. 2016).

This is where various new or improved imaging, screening, and computed modeling approaches come to the fore. They will gradually gain in importance with refinement of applicability (Li et al. 2015, Dumont et al. 2016) and are likely to evolve from single root observations to rhizosphere models in which all parameters (i.e. holobiontically including other biotic and abiotic contributors) are taken into account. By this means, adaptation approaches on patterned landscape-scales should become more reliable (Tracy et al. 2020).

Nevertheless, rhizoboxes or rhizotrons and 2D or 3D scanning methods are continuing to be a good tool. However, i.a. Varsheny et al. (2018) prophesy many old and new challenges on the way from the dynamic phenotype to the comprehension of the inherent mechanics and gene-protein assemblies that will ensure appropriate adaptive performance. Or vice versa?

According to Negin et al. (2016), this also relates to the fact that controlled conditions and field conditions are still difficult to reconcile and the hard to calculate genotype x environment interaction is almost limitless in its factor interdependence. It must be understood, that both morphological and phenomic adaptations cannot be regarded as decoupled singularities of functionality; they are systemic or partial systemic mitigation syndromes that must be counter-controlled at the whole plant level. In this context, phenotypes are highly complex - they are the result of extremely variable reciprocities between genotypes and envirotypes (Xu, 2016, Gazengel, et al. 2021, Lecarpentier et al. 2021). Anyway, complexity also requires research flexibility.

In this regard, the introduction of certain ontological elements into the root-existence is at least to be considered (Witzany 2006, Ginsburg and Jablonka 2009, Gorzalek et al. 2015, Calvo-Garzón and Keijzer 2011, van Loon 2016, Correa et al. 2019, Calvo et al. 2020) and could possibly be referred to as root proprioception (*vide supra*), inherence, or, more daringly, as the integration of a mechanical intelligence into the reverse bionics of plant consciousness.

However, expressed genes render morphological or physical response-action which is a performative act. And genes, in the context given, are expressed as a reaction to environmental stimuli. Sincerely a topic to be further discussed (Sheth and Thaker 2014, Joshi et al. 2016, Heslop-Harrison 2017).

3.1.4 Rootstocks. Root design in viticultural contexts

Long before Degrully and Ravaz (1905), the choice of the rootstock was understood not only as an alternative or stress regulator, but also (not only in viticulture) as a chance. The initial spark to rootstock use for *Vitis vinifera* cultivars was, of course, the need for a phylloxera (*Daktulosphaira vitifoliae* (Fitch))

tolerant material. In modern breeding approaches *Vitis riparia* and *Vitis rupestris* (which, with individual exceptions, exhibit good rooting qualities from dormant cuttings) and *Vitis berlandieri* are still the most used Americana species (Gautier et al. 2020). Nevertheless, more and more *Vitis mustangensis* (e.g. Matador) or *Vitis candicans* (e.g. 116-60 Lider) respectively, as well as *Vitis champinii* (e.g. Dog Ridge, Ramsey, Freedom, Harmony) or *Vitis rotundifolia* (e.g. VR O39-16), which disadvantageously has poor rooting and grafting properties (Cousins and Striegler 2005, Cousins 2011), and other representatives of the genus are included in cultivation efforts (Arnold and Schnitzler et al. 2020).

Rootstocks, however, as said, do not convey their capacity in rebus but only in connection with a particular holo-biotope and under consideration of the *terroir* (def. pro re nata). According to their origin and their crossed partners, they basically fulfill requirements such as nematode or phylloxera tolerance, salt resistance, insensitivity to waterlogging, drought tolerance and WUE or indeed Fe-safeguarding in alkaline soils and nutrient foraging under adverse conditions. Thus, rootstocks have different strategies and response mechanisms in terms of RSA, lignification and suberization respectively osmoregulation and hydraulic adjustment etc. (Cousins and Striegler 2005, Ollat et al. 2016, Kahn et al. 2020).

Interestingly, the assessment of performance qualities often diverges somewhat depending on the source; while occasionally, for example, 1103 P (*V. berlandieri* x *V. rupestris*) is described as very drought tolerant or only medium to very drought tolerant, 3309 C (*V. riparia* x *V. rupestris*) is listed as both medium and low-medium drought resistant. The performance is therefore dependent on the situation, although the basic parameters remain perfectly reliable.

In connection with the present work, two rootstocks will be briefly presented in more detail. 3309 C is a crossbreeding of *Vitis riparia* (*tomentosa*) and *Vitis rupestris* cv. Martin. The chlorosis tolerance is rather low or medium and resists up to 20% of total limestone, 11% of active limestone and an CPI (chlorotic power index) of 10. 3309 C is well suited for acidic soils, poorly suited for drought prone soils, especially when drought stress sets in abruptly during vegetation, which is partly due to its flat, i.e. shallow-angled root architecture (Smart et al 2006, Schmid 2018).

The pedigree of Fercal is more sophisticated, according to genetic analyses it is a variety resulting from a cross between Berlandieri Colombard N°1 B (actually a cross between *Vitis berlandieri* and *Vitis vinifera* cv. Ugni blanc) and 31 Richter (derived from a cross between *Vitis berlandieri* cv. Rességuier N°2 and *Vitis longii* cv. Novo-mexicana). In accordance with the name (composed of Fer + Cal), the main feature of Fercal, however, is its tolerance to lime-induced stresses (strains) and thus its ability to make iron available under difficult conditions. It resists up to 60% total limestone, 40% active limestone and shows a CPI of 120. This rootstock is fairly tolerant of wet conditions in spring and its resistance to drought is average to comparatively good as long as the rooting is deep enough, nevertheless, it belongs rather to the semi-deep-rooted types (Galet 1988, IFV 2007, Schmid 2018).

In principle, of course, it is not necessarily the quantity of rootstocks available and yet to be bred that are important and necessary, but above all the knowledge of the traits of those rootstocks and those cultivars and those soils that actually converge to produce grapes in a sustainable, plant-safe, i.e. grapevine preserving and economically as well as oenologically advantageous way for a wine whose other parameters may be left to the winemaker himself.

III. Material and methods

1. Preliminary remark on the methodological approach

The experimental work had an establishing character in numerous aspects and required multiple adaptations until it was satisfactorily applicable. Where not explicitly indicated, all steps of this pilot study are described according to the final procedure used for data collection. The original recipes and protocols, part of which were used, were added to the appendix whenever text extraction and part-wise insertion appeared to be indicated. If adapted versions were used, they are both integrated into the text and separated in the appendix for independent reference.

The general idea was to expose the two chosen rootstocks (Fercal, 3309 C) to three different in vitro stress media and to conduct a control group. The stressors chosen were: Iron deficiency in place of lime stress (NOFE = no Fe), a combination of iron deficiency and drought or osmotic stress (NOFEPEG = no Fe / polyethylene glycol as an osmolyte) and drought or osmotic stress as a single stress (PEG = polyethylene glycol as an osmolyte).

As initially mentioned, it was intended to visualize the effects of this stress exposure on the dermal tissues (endodermis and exodermis) in terms of Casparian strip formation (lignin-polymers) and cell wall laminations (suberin-polymers) along the root axis section by section (Chapter 5.5). Several preparatory steps were necessary to finally make either fluorol yellow (FY 088) stained whole root samples for suberin control of the exodermis or berberine-aniline blue-stained cross sections for suberin and lignin interpretation of endo- and exodermis microscopically assessable.

2. Materials and equipment

2.1. Chemicals, reagents and products

Table 1 Chemicals, reagents and general products used in laboratory and greenhouse with corresponding supply source.

Product	Supply source
Ammonium nitrate	Carl Roth GmbH & Co. KG, Karlsruhe, Germany
Aniline blue	Sigma-Aldrich Chemie GmbH, Steinheim, Germany
Berberine hemisufate salt	Sigma-Aldrich Chemie GmbH, Steinheim, Germany
Boric acid	Carl Roth GmbH & Co. KG, Karlsruhe, Germany
Calcium nitrate tetrahydrate	Carl Roth GmbH & Co. KG, Karlsruhe, Germany
Copper sulfate monohydrate	Carl Roth GmbH & Co. KG, Karlsruhe, Germany
Ethanol 99%	Carl Roth GmbH & Co. KG, Karlsruhe, Germany
Fluorol yellow 088	Santa Cruz Biotechnology, Inc., Heidelberg, Germany
Gelrite™	Duchefa Biochemie B.V., Haarlem, Netherlands
Glycerol, Rotipuran®	Carl Roth GmbH & Co. KG, Karlsruhe, Germany
Indole-3-acetic acid	Duchefa Biochemie B.V., Haarlem, Netherlands
Indole-3-butyric acid	Carl Roth GmbH & Co. KG, Karlsruhe, Germany

Magnesium sulfate heptahydrate	Carl Roth GmbH & Co. KG, Karlsruhe, Germany
Manganese (II) Chloride Tetrahydrate	Carl Roth GmbH & Co. KG, Karlsruhe, Germany
Murashige & Skoog medium (including vitamins)	Duchefa Biochemie B.V., Haarlem, Netherlands
Murashige & Skoog medium (including vitamins) without iron	Duchefa Biochemie B.V., Haarlem, Netherlands
Polyethylene glycol, PEG 1500	Carl Roth GmbH & Co. KG, Karlsruhe, Germany
Polyethylene glycol, PEG 400 (liquid dosage)	Carl Roth GmbH & Co. KG, Karlsruhe, Germany
Polyethylene glycol, PEG 8000	Carl Roth GmbH & Co. KG, Karlsruhe, Germany
Potassium dihydrogen phosphate	Carl Roth GmbH & Co. KG, Karlsruhe, Germany
Potassium hydroxide	Carl Roth GmbH & Co. KG, Karlsruhe, Germany
Potassium sulfate	Carl Roth GmbH & Co. KG, Karlsruhe, Germany
Roti® -Mount FluorCare	Carl Roth GmbH & Co. KG, Karlsruhe, Germany
Saccharose	Carl Roth GmbH & Co. KG, Karlsruhe, Germany
Sodium hydroxide	Carl Roth GmbH & Co. KG, Karlsruhe, Germany
Sodium molybdate dihydrate	Carl Roth GmbH & Co. KG, Karlsruhe, Germany
Type 1 Substrate, Einheitserde, group II	Werner Tantau GmBH, Uetersen, Germany
Varnish (Nail polish)	Different common brands
Zinc sulfate monohydrate	Carl Roth GmbH & Co. KG, Karlsruhe, Germany

2.2. Expendable items

Table 2 Expendable items used in the laboratory with corresponding supply source

Product	Supply source
Cell sieves, EASYstrainer™ 100 µm	Greiner bio-one GmbH; Kremsmünster, Austria
Cover glass plates long	Fischer Scientific GmbH, Schwerte, Germany
Cover slips, Menzel-Gläser	Fischer Scientific GmbH, Schwerte, Germany
Falcon™ tubes 50 ml	Fischer Scientific GmbH, Schwerte, Germany
Glass jars, Rundhalsglas 580 ½ l	J. Weck GmbH u. Co. KG, Wehr, Germany
Microscope slides	Karl Hecht GmbH & Co KG, Sondheim, Germany
Parafilm®	Sigma-Aldrich Chemie GmbH, Steinheim, Germany
Petri dishes, glass, ⌀ 145 mm BIG	Greiner bio-one GmbH; Kremsmünster, Austria
Petri dishes, glass, ⌀ 60 mm small	Greiner bio-one GmbH; Kremsmünster, Austria
Pipette tipps, Eppendorf	Sigma-Aldrich Chemie GmbH, Steinheim, Germany
Razor blades	Different common brands
Specimen holder, 50 ml	Sigma-Aldrich Chemie GmbH, Steinheim, Germany
Sterile polystyrene Petri dishes, ⌀ 145 mm	Greiner bio-one GmbH; Kremsmünster, Austria
Sterile polystyrene Petri dishes, ⌀ 60 mm	Greiner bio-one GmbH; Kremsmünster, Austria

2.3. Equipment, devices and software

Table 3 Equipment and devices used in laboratory and greenhouse with corresponding supply source

Product	Supply source
Binocular, Olympus SZ61	Olympus GmbH, Hamburg, Germany
Camera, Olympus E-620	Olympus GmbH, Hamburg, Germany
Electro pipette (Easypet)	Sigma-Aldrich Chemie GmbH, Steinheim, Germany
Growing chamber	Hauser GmbH, Linz, Austria
LI 600 porometer/fluorometer	Li-Cor Biosciences GmbH, Bad Homburg, Germany
Microscope, Fluoview FV1000, BX	Olympus GmbH, Hamburg, Germany
Microscope, SP8-STED	Leica Camera AG, Wetzlar, Germany
pH 211 Microprocessor pH meter	Hanna Instruments GmbH, Graz, Austria
Pipettes, Discovery Comfort	HCT, Corning HTL SA, Warszawa, Poland
Rhizoboxes	Vienna Scientific Instruments GmbH, Alland, Austria
Scales, Sartorius GP 5202	LTF Labortechnik GmbH & Co. KG, Wasserburg, Germany
Special accuracy weighing machine, Kern 770	Kern & Sohn GmBH, Balingen, Germany
Sterile bench (TYPE?)	Clean Air Products, Minneapolis, U.S.A. (?)
Thermomix, ThermoStat plus 50ml	Sigma-Aldrich Chemie GmbH, Steinheim, Germany
Warming cupboard	Tecan Group Ltd., Männedorf, Switzerland

Table 4 Software employed for data evaluation with project-related purpose of use

Name	Purpose of use
Fluoview software, Olympus	Visualization
LAS X (Leica Application Software X)	Visualization
ImageJ	Visualization
Microsoft Excel	Data exploration, data operationalization
R	Data exploration, data operationalization
R Commander	Data exploration, data operationalization

3. Methods I: Plant material, propagation media and pre-organization for the in vitro approach

All plantlings were initially obtained as one or two node cuttings from greenhouse grown 3309 Couderc and Fercal rootlings. For the further use of plant material that is as homogeneous as possible, two or three of these cuttings were placed in glass jars (Weck Rundhalsglas 580) containing 100 ml control medium 1 (Table 5) and Parafilm®-sealed. All direct plant handling subsequent to the pre-prep-

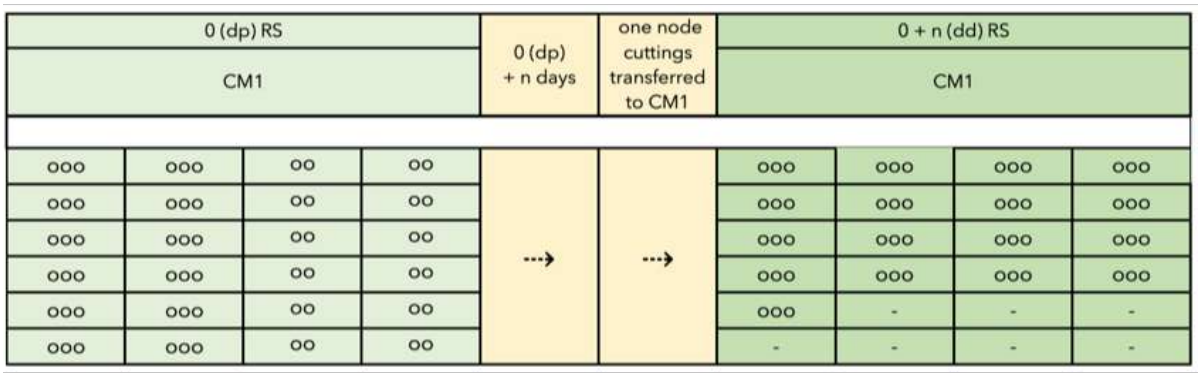

Figure 6 Overview schematically showing the preliminary work steps of plant propagation and provision. On a given day of planting (dp), young shoot cuttings from rootstock rootlings (initial step) or plantlings (successive propagation steps) are put to a propagation medium. After a time to specified (approx. 30 - 40 days) homogeneous one node cuttings are dissected and planted to encoded jars, which are then already part of the actual main experiment.

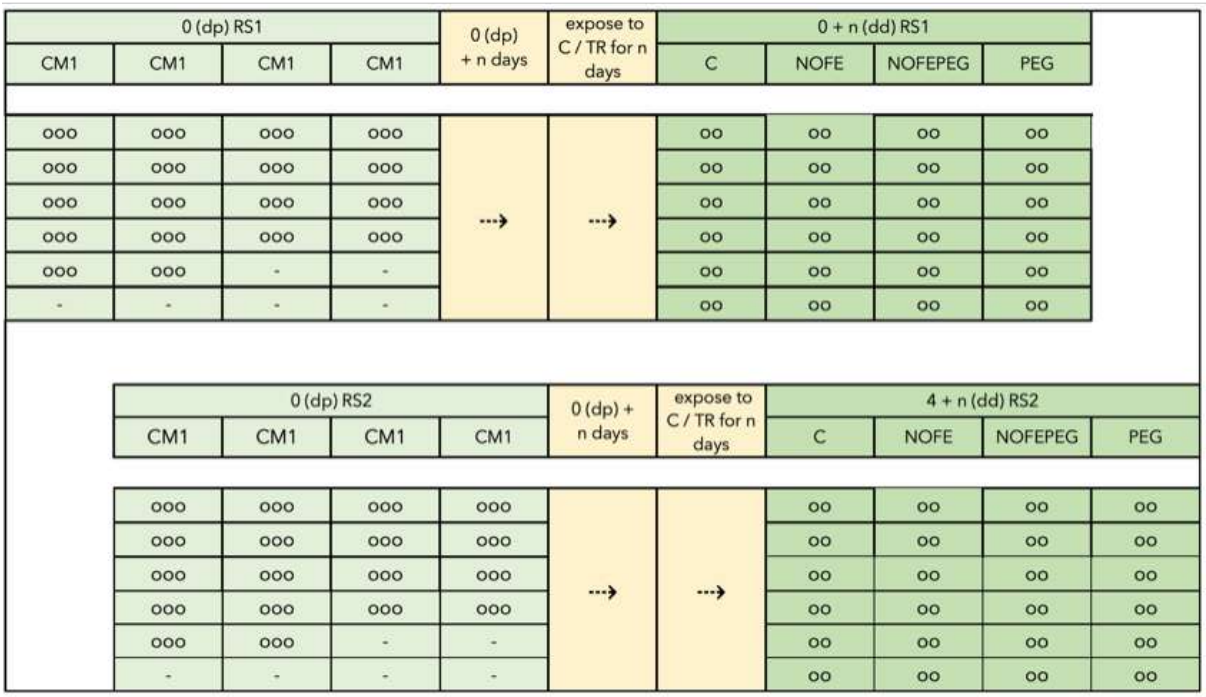

Figure 7 Experimental design for the in vitro setting organized by rootstock types. First, rootstock 1 cuttings are planted to the control medium (CM1) on a given day of planting (dp) for the individual time needed to obtain a suitable size (in the present case ca. 30 days for each batch). Here, 18 glass jars with 3 one node cuttings each seemed appropriate and hence resulted in a total of 54 plantlings; 6 of which were intended as standby material in case insufficient growth or fungal spoilage would occur. Then, 2 plants each were transferred to a 145 mm Petri dish either prepared with the CM1 for control (C) or to the individual stress treatments (TR: NOFE = iron deficiency, NOFEPEG = iron deficiency + drought, PEG = drought) respectively and kept exposed for another ± 14 days (in the present case stress exposure lasted 17 days for Fercal and 15 for 3309 C; where the duration difference was due to strict schedule logistics). All dishes were shaded with black cardboard envelopes up to the medium edge to support gravitropism. On dissection day (dd), roots were prepared for staining and treatment response visualization.

aration of the greenhouse rootlings for laboratory use and prior to the final root collection was carried out under the sterile bench. Initial fresh cuttings were propagated successively in the growing chamber (Table 6) until sufficient material was available (Figure 6).

Unlike the media of the trial stage, (Tables 7 - 10), the control medium 1 (CM1) contained the hormones IAA (Indole-3-acetic acid) and IBA (Indole-3-butyric acid) to ensure the targeted rootage.

Due to temporal and spatial logistic constraints, it was necessary to organize the experimental procedure in two batches (Figure 7). However, both batches were organized uniformly. That is, taking into account genotypically motivated growth characteristics, all plantlings had approximately the same age and phenotypical expression before they were introduced as basic material into the test set-up. The test set-up itself was prepared by a jar-wise equal allocation of the pre-propagated plantlings, subsequently each single step was carried out identically, yet time-shifted, in every single step for both batches.

Even under laboratory conditions, plants are living individuals; although genetically identical by means of propagation, deviating, e.g. epigenetic effect variants are morphologically and phenotypically to be expected (Miguel and Marum 2011, Us-Camas et al. 2014).

3.1 Recipe for the control medium 1 and growing chamber conditions

3.1.1 Control medium 1

For the production of the medium (and all other media), a laboratory bottle with the required amount of water was provided with a stirrer bar and placed on a magnetic stirrer, then the components were added in the order Murashige & Skoog medium (M+S), Saccharose, Gelrite™ via a funnel. Last, the plant hormone solutions are pipetted to the liquid media.

Each ingredient should be completely dissolved before adding the next. Heating the water is not necessary, but contributes to the solubility of the product. However, since Gelrite™ hardens after one heating and subsequent cooling and cannot be liquefied again afterwards, the handling seems to be more flexible at room temperature. Preliminary tests have shown that the medium solution can be stored at room temperature for one to two days, prompt processing is recommended nevertheless. Before use, the medium solution must be autoclaved. Afterwards, it should cool down to about 60 °C in the warming cupboard for further processing.

Table 5 Control medium 1 recipe. This medium serves for propagation and provision of the experimental plantlings

Name	Ingredients and ratios for 1 l double distilled water (ddH_20)	
Control medium 1	2,4 g	Murashige & Skoog medium (including vitamins)
	18 g	Saccharose
	5,3 g	Gelrite™
	1 ml	IAA (Indole-3-acetic acid)
	1 ml	IBA (Indole-3-butyric acid)
The medium was adjusted to a pH value of 5.75 by KOH addition		

3.1.2 Growing chamber conditions

The growing chamber was equipped with a three-shelfed storage rack on each long side of the room. To ensure equal conditions, the propagation containers and the test containers for each batch were kept on the same rack level and on the same chamber side.

Table 6 Growing chamber conditions. The conditions were set during all periods of growth, i.e. for the pre-propagation and plantlet provision as well as for both experimental batches

Feature	Settings and specifications	
Light yield	Long day	06:00 am – 22:00 pm
Light source	Tubular fluorescent lamps	PHILIPS cool white 28 W
Light source unit	6 Tubular fluorescent lamps	Per shelf compartment
Temperature	25° C	± 2° C diurnal fluctuation
Relative humidity	60 %	Diurnal fluctuation. possible

4. Methods II: Plant growth for experiment use, plant handling, plant preparation

4.1 Preparation and pre-growth of the experiment plantlings

In a first production step, 18 jars were filled with 100 ml CM1 under the sterile bench, numbered and encoded and kept for ensuing use.

For integration into the actual experimental method sequence, plants which had a previous growing time of about 30 to 40 days in CM 1 were employed. The jars holding the donator plants were unsealed in sterile setting, the aerial parts were captured with forceps and dissected with a laboratory scissors (all instruments and consumables have been autoclaved).

After leaf removal, the shoot parts were placed on a rectangular cardboard plate on which vital and passably uniform one node cuttings were fabricated by scalpel use. The cuttings were then transferred into the prepared jars, so that the lower, non-noded part was set upright in the medium. After carefully sealing the encoded jars, they were kept in the growing chamber for 17 days (Fercal) and 15 days (3309 C) respectively, were the difference in growth time resulted from immutable schedule obligations.

In the run-up it has been tested whether the one node cuttings would directly be growing in Petri dishes inclined vertically by about 60° with the aim of a more adjusted root system shape; while it seemed to be applicable for the control media and the NOFE approach, it failed for NOFEPEG and PEG.

4.2. Preparation of control medium and stress media

4.2.1 Control medium

For the preparation of the control medium (Table 7), the same procedure was followed as for control medium 1 omitting IAA and IAB. That is, gradual complete dissolution of the ingredients in the order given.

Table 7 Control medium recipe

Name	Ingredients and ratios for 1 l double distilled water (ddH_20)	
Control medium (C)	2,4 g	Murashige & Skoog medium (including vitamins)
	18 g	Saccharose
	5,3 g	Gelrite™
The medium was adjusted to a pH value of 5.75 by KOH addition		

4.2.2 Stress medium 1 (iron deficiency)

The previously explicated procedure also applies to the preparation of the stress medium 1 (iron deficiency = NOFE, Table 8), except that for Murashige & Skoog medium (including vitamins) the special preparation Murashige & Skoog Medium (including vitamins) w/o iron was used. Therefore, in this case, the unavailability of iron is absolute.

Table 8 Stress medium 1 recipe. Iron deficiency

Name	Ingredients and ratios for 1 l double distilled water (ddH_20)	
Stress medium 1 (NOFE)	2,4 g	Murashige & Skoog medium (including vitamins) w/o iron
	18 g	Saccharose
	5,3 g	Gelrite™
The medium was adjusted to a pH value of 5.75 by KOH addition		

4.2.3 Stress media 2 and 3 (iron deficiency and drought or osmotic stress, drought or osmotic stress)

Preparation and handling of the respective stress medium was organized along the split-up method (Figure 8, Appendix 1) established by Kreszies (2019) with only slight changes that will be indicated. With rapid material processing, the method appears to be excellently qualified to time-efficiently cast homogeneous plates. For individual adjustment the conversion of physical units to percentage might be desirable for simplification. However, in the following physical units are kept. Furthermore, in this context, and in accordance with the original recipe, it should also be expressly noted that Gelrite™ should in no case be replaced by common plant agar since it will prevent PEG from solidification.

Since preliminary tests with more severe water stress, i.e. with more negative water potentials, could not provide properly evaluable root material, an approximate target value of -0.55 MPa was finally set, for which a PEG amount of 100 g l^{-1} is required.

To prepare the split-up medium, the required amount of water was distributed in a 1:1 ratio to two laboratory bottles equipped with stirrer bars, i.e. 500 ml each for one liter. The required amount of 6 g Gelrite™ was completely dissolved in one bottle. Incidentally, bottles (or beakers, as described in the original protocol) of approximately twice the filling volume should be used, as PEG can increase the original volume by double-digit percentage values. In the second bottle, 100 g of PEG 8000 was

completely dissolved. Subsequently, both bottles were autoclaved, while then Gelrite™ containing bottle was kept in an oven at about 60° C (or in a water bath as described in the original protocol), the other bottle was filled with PEG 8000 under the sterile bench. Since PEG itself is not autoclavable, all other tools and equipment should either be autoclaved or carefully cleaned with 70% ethanol (v/v) beforehand. Since weighing and dissolving of the PEG also takes place under the sterile bench, balance and magnetic stirrer should have been prepared in time. After dissolving the PEG, the bottle was closed and also stored in the oven until both solutions had about the temperature of 60° C. The bottle containing the Gelrite™ solution was then placed back on the magnetic stirrer under the sterile bench and the PEG solution was poured in quickly but not gushily. At the highest temperature manageable, 100 ml of the medium was quickly measured in a beaker and poured into sterile Petri dishes under the sterile bench as rapid as possible, for solidification already begins during casting. During the hardening process, it is recommended not to close the dishes in order to avoid excessive condensation. As soon as the medium has solidified and cooled down, the transfer of the plantlings can be conducted.

The temperature of the medium and the sterile environment seem to prevent contamination incidents sufficiently reliable. These are also controllable in the further steps, but nevertheless occurred on one dish, which was probably due to a damaged Parafilm® seal.

It should furthermore be expressly noted, that PEG is available in widely differing average molecular weights, which are indicated by the according numbers.

Since PEG has a high negative osmotic potential (drought stress application) on the one hand and on the other hand is eligible to preserve the lipophilic organized cell structures by infiltration (sample conservation), where it in turn might bind tightly to hydroxyl groups of polyphenols such as lignin, the correct average molecular weight must be selected for each working step, e.g. to avoid interference in imaging procedures (Ferreira et al. 2014, Ferreira et al. 2017, Kitin et al. 2020). In addition to consulting the relevant literature, for the work present corresponding pre-trials verified the appropriate and fail-safe usage of the applied PEG. In this context, the choice of the corresponding molecular weight is always referred to hereinafter.

Table 9 Stress medium 2 recipe. Iron deficiency and drought or osmotic stress

Name	Ingredients and ratios for 1 l double distilled water (ddH_20)	
Stress medium 2 (NOFEPEG)	2,4 g	Murashige & Skoog medium (including vitamins) w/o iron
	18 g	Saccharose
	6 g	Gelrite™
	100 g	PEG 8000
The medium was adjusted to a pH value of 5.75 by KOH addition		

It will have become evident here, that the coupled stress comes into effect just by using the Murashige & Skoog medium lacking iron. For consecutive media production, contamination avoidance should therefore be taken into account.

Table 10 Control medium recipe. Drought or osmotic stress

Name	Ingredients and ratios for 1 l double distilled water (ddH_20)
Stress medium 3 (PEG)	2,4 g Murashige & Skoog medium (including vitamins) 18 g Saccharose 6 g Gelrite™ 100 g PEG 8000
The medium was adjusted to a pH value of 5.75 by KOH addition	

The pH measurement and corresponding adjustments were carried out right before autoclaving the split solutions. Any adjustments after the part quantities have been back-mixed would require extensive effort, not least because of the immediate solidification of the medium.

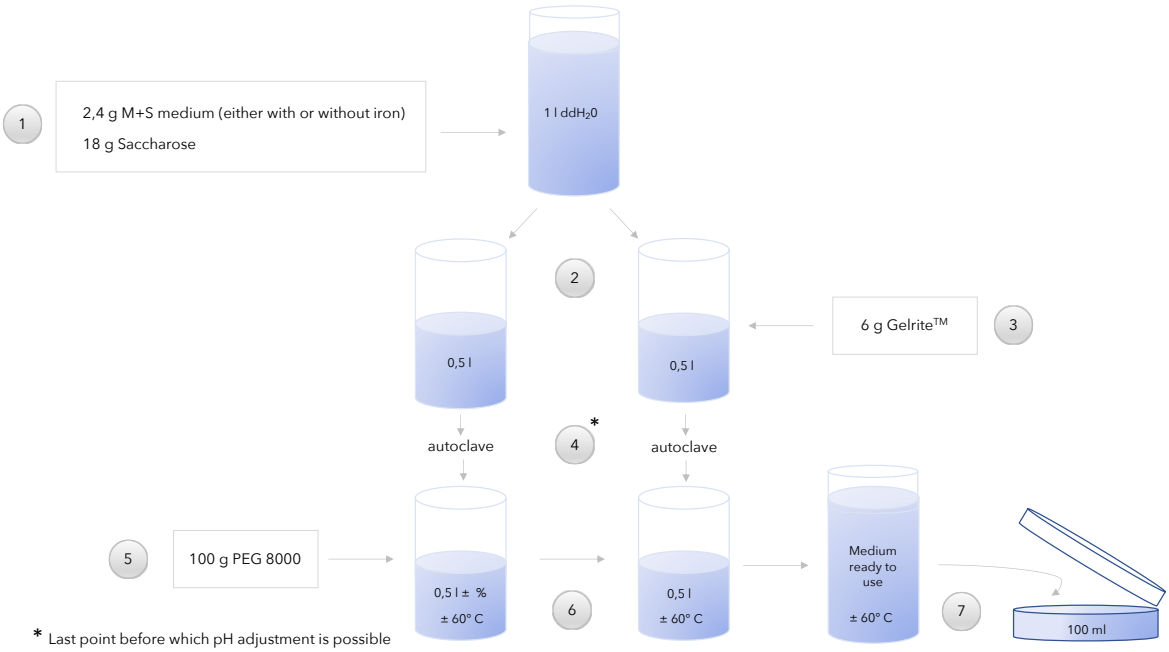

Figure 8 Flowchart providing a schematically overview of the Kreszies split-method for media containing PEG 8000. The amount of PEG added determines the osmotic stress level. According to Kreszies (2019), 100 g l^{-1} will result in a negative water potential of -0.55 MPa with SD ± 0,07 calculated from minimum 5 independent replicates. For the work present, higher portions of PEG 8000 lead to insufficient plant growth and consequently to unusable root specimen. From step 6 onwards a well-organized and rapid processing is recommended.

4.3. Transferring plantlings from jars to Petri dishes

Subsequent to a random assignment of the jars, any accumulations of weak- or strong-growing plantlings were deliberately leveled so that an approximate distribution of phenotypes per stress group was ensured. In a second preparatory step, a spatula (all instruments and consumables have been autoclaved) was used to remove the solidified medium about 1,5 cm from the center of the Petri dish, resulting in a transversally-edged planting area of about two-thirds dish area, the excess media was retained by first halving the quasi semicircle in the middle and then moving one part at a time to a spare,

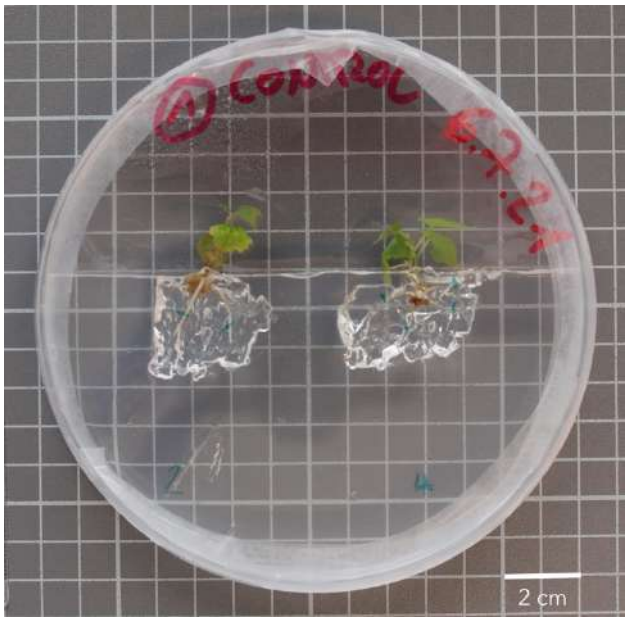

Figure 9 Plantlings freshly incorporated into the control medium. The roots have been covered up with a suitable quantity of spare media that had been cut out earlier with a sterile spatula.

not yet treated medium surface. In this way, the placement of one dish was always completed before the next was cut out. Accordingly, two planting areas were prepared by cautious loosening the medium at two spots oriented to the center and with a sense of proportion for the respective root size; a spatula or forceps tips will be suitable tools here. Now, using forceps, a plantling was taken out of a jar that had been unsealed prior to this work step under the sterile bench and by using a dull scraper the roots were rid of the control medium 1 (CM1).

In a next step the plantling was placed into the loosened medium with utmost care in order to prevent the roots from breaking. A pruning for obtainment of homogenized root parameters is unadvisable as plants exposed to at least NOFEPEG and PEG are very likely to not overcome this additional imposition.

Once the plantling was gently pressed into the medium, the one spare part was placed on the planting area so that the roots are fully covered with medium (Figure 9). Care has been taken, that between the cover-medium and the covered medium no cavitation occurred. After the second plantling has been incorporated the same way, the Petri dish was sealed with Parafilm®. Gradually, six Petri dishes containing two plantlings each were completed and restored into the growing chamber for the application phase. To support gravitropism, all dishes were shaded with black cardboard envelopes up to the planting surface.

5. Methods III: Root dissection, tissue fixation and tissue stabilization

Since the root material is henceforth intended to be processed for microscopic exploration, it is advantageous to stabilize the corresponding tissue in order to be able to observe intact morphological contexts. If fixation and stabilization steps are skipped, and fresh material is processed, even with direct processing, cell lysis, tissue degeneration and shape change due to biochemical and mechanical impact can hardly be avoided, as corresponding preliminary tests in accordance with the relevant literature have shown (Talbot and White 2013, Huang and Yeung 2015). Accordingly, numerous techniques exist, which can be roughly divided into chemical approaches, such as glutaraldehyde fixation or formaldehyde-aceto-alcohol (FAA) fixation, and physical methods, such as cryopreservation or microwave inactivation (Huang and Yeung 2015). Since it was the explicit aim of the method to be established without using toxic and highly toxic substances in any of the work steps, yet still to produce material that could be appropriately evaluated at a high throughput, it was decided to use WEG (water-ethanol-glycerol) according to the recipe of Kitin et al. (2020) for further whole root processing and, with regard to subsequent sectional treatment, a classic PEG (polyethylene glycol) infiltration after prior dehydration with

ethanol; corresponding instructions and specifications for implementation have been provided by Dr. Sabine Rosner, Institute of Botany, BOKU, Vienna.

5.1 Root evaluation and dissection

Prior to the dissection, for each plantling intended root parameters were obtained, i.e. number, length and increment were monitored for the main roots and number and length for first order laterals. As this was done manually (without software employment), for a lateral root count number greater than n = 35, an additional number of n = 5 was calculated and for a number greater than 40 also an additional number of n = 5. Here, for uncountable laterals, approximate length values were assumed in each case.

Subsequently, the Petri dishes were unsealed and the plantlings were cautiously collected from the media by using forceps. When necessary, media residues were removed and single main roots were chosen for cutting off. Desirable but not consistently available was a minimum length of about 5 cm and straight growth, as later placement on microscope slides and measurement would have been compromised by curved roots. To avoid later sample failures, up to 15 individual roots per treatment were collected and allocated to further procedures. However, both rootstocks showed limited selection, especially for NOFEPEG and PEG treatments.

5.2. WEG (water-ethanol-glycerol) fixation

WEG not only preserves the plasticity of the sample, but also facilitates the cutting of lignified and suberized tissue fractions (Kitin et al. 2020), which, however, was not decisive according to the present experimental setup. The recommended vacuum infiltration was omitted after preliminary tests for reasons of handling simplicity. Accordingly, about 4 – 5 fresh main roots per treatment were transferred to 50 ml specimen containers and submerged in a 1:1:1 WEG solution (Table 11) and stored at 4° C for later whole staining and evaluation (Chapter 5.6).

Table 11 WEG (water-ethanol-glycerol) recipe for a 1:1:1 (v/v/v) solution.

Name	Ingredients and ratios for 240 ml
WEG (water-ethanol-glycerol)	80 ml double distilled water (ddH_20) 80 ml Ethanol ≥ 99,5% 80 ml Glycerol
The fixation solution can be prepared in larger quantities and kept at 4° C	

5.3 PEG (polyethylene glycol) infiltration

Root sample dehydration was achieved by successive submission of the fine roots to ethanol concentrations ascending by increments of 10% from 50% (v/v) of pure ethanol in ddH_20 to 100% pure ethanol in the last step. The exposure time was limited to 30 min. for each concentration level. This was

followed by an overnight immersion in a 50% (v/v) solution of pure ethanol and previously oven-melted PEG 1500 and, from the next day on, by an infiltration period of at least 72 hours in 100% liquid PEG 1500 in the oven (Figure 10). Both PEG involving infiltration steps need to be carried out in the oven at about 60° C while the dishes need to be covered. Lower oven temperatures my result in accelerated solidification as the product will cool down below the melting point more quickly.

In this context it should be noted, that, corresponding to the respective molecular weight, PEG also has varying melting points; PEG with an average molecular weight of 1500, for example, is present in liquid form at ≥ 45° C, while PEG 8000 requires ≥ 60° C to melt. As for processing, the product temperature should be kept above solidification limits to guarantee purposeful handling (Majumdar et al. 2010, Kitin et al. 2020). Using PEG 1500 here is due to the specific material hardness in the solid state, which provides support on one side, but is easy to cut on the other. In addition, the molecular dimension is suitable for penetrating the tissue, but can also be easily washed out again for further work steps.

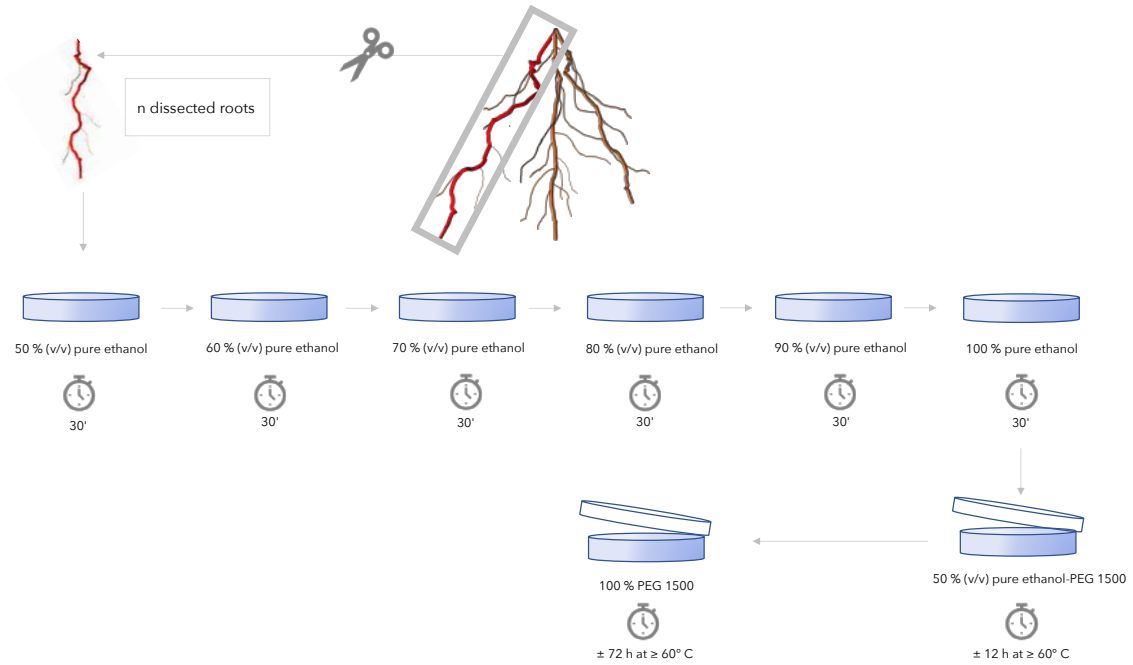

Figure 10 Flowchart providing a schematically overview of the method employed to infiltrate fresh fine roots with PEG 1500 for further processing.

5.4 Sample mounting

While the whole roots are stored in WEG for removal immediately before rinsing and fluorol yellow 088 (FY 088) dyeing for suberin visualization, the PEG infiltrated whole roots need to be set in a PEG embedment on a microscope slide (Figure 11) to become processable for a segment-wise collection of hand-cut cross sections. Accordingly, the roots were cautiously removed from the hot PEG dip by picking the utmost basipetal end with forceps. Especially for shorter root samples it is important to not minimize the sample length by wide pinches.

To facilitate PEG- and sample handling, it is advisable to have all required instruments and commodities (e.g. microscope slides, PEG liquid) preheated as otherwise the roots might break or the PEG will solidify before the embedment is completed. Subsequently, a sufficient portion of liquid PEG was

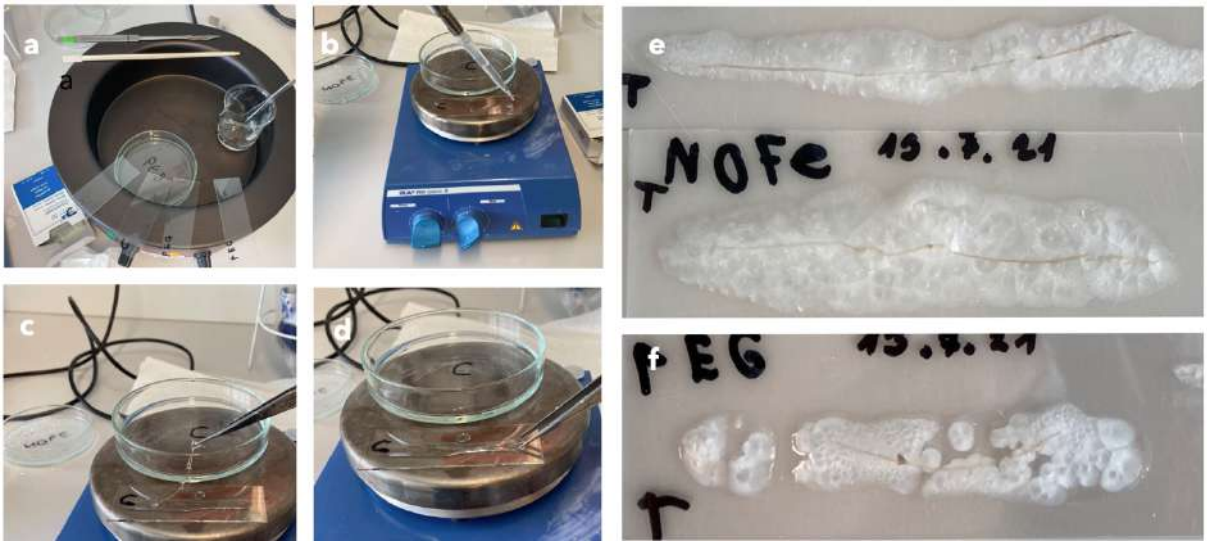

Figure 11 Steps showing the embedment procedure of dissected roots into a PEG strip. In a preparatory step (a) all instruments and commodities are preheated. Subimage (b) displays the start of pipetting a line of PEG onto the microscope slide. The root is then fit into the liquid PEG on the slide (c,d). Once the PEG is solidified, the roots can be further processed or kept in the refrigerator for future use (e). Subimige (f) gives an idea of the hardening process.

pipetted on a microscope slide so that an about pencil wide stripe was forming. Then, a root sample was seized as indicated and fit to the PEG strip. Both tip and bottom of the sample should be displayed on the slide as to later segmentation. The PEG was now allowed to solidify. A small but controllable disadvantage may be the low melting point of the PEG 1500 used here, so that material softening may occur if the slide-mounted samples are handled for a prolonged period.

5.5 Sectioning of root samples for microscopy

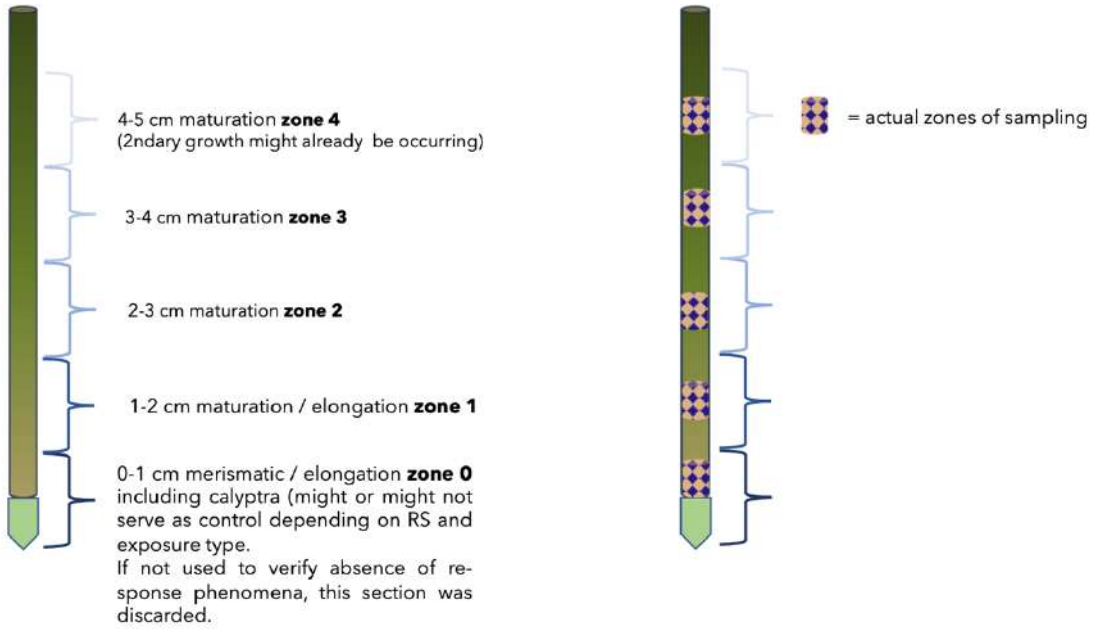

Figure 12 Subdivision into verisimilar developmental units or zones of morpho-histological distinction. The sectioning follows assessments of literature related to relevant fields of research as well as comprehensive pre-trials.

While the WEG-immersed whole roots for FY 088 dying required no pretreatment other than a sufficient rinse (approx. 5 minutes in ddH_20), the samples embedded in PEG for berberine-aniline staining first had to be subdivided into verisimilar developmental units or zones of morpho-histological distinction respectively (Figure 12) so that assignable cross-sections could then be obtained. The sectioning units were chosen after substantial literature consultation (Gambetta et al. 2013, Barberon 2017, Holbein et al. 2019, Namyslov et al. 2020) and appropriate pre-trials with at least 8 samples per treatment. This gradual determination was achieved by a condensed run-through of the actual assessment process, i.e., skipping the PEG infiltration and monitoring fresh hand-cut sections after dyeing as described below (Paragraph 5.7). As a result, zoning was realized in 4 test sections of one centimeter length each and designated as sections 1- 4 in ascending, basipetally directed order. As additional reassurance regarding the correctness of the allocation, control sections were also taken from the first, root distal centimeter in every third sample.

5.6 Fluorol yellow 088 dyeing and mounting for microscopy assessment

For the examination of exodermal suberization gradients, 3 whole roots of each treatment were obtained from the WEG immersion, rinsed thoroughly in ddH_20 and submerged overnight in the fluorol yellow 088 dye (Table 12) in a dark cupboard at room temperature. Petri dishes are a suitable and reusable container for this purpose. Regarding the dye itself, the protocol established by Brundrett et al. (1991) was consulted (Appendix 2). That is, 0,01% (w/v) FY 088 was dissolved in PEG 400 at 90° C for 60 min. Then, a mixture of 90% (v/v) glycerol in ddH_2O is made, after which both preprepared solutions are mixed in a 1:1 ratio.

PEG with an average molecular weight of 400, dissolves dyes excellently and leads to a consistently good and intense staining of lipids after mixing with glycerol and water (Brundrett et al. 1991), it may be re-mentioned here that suberin consists in part of aliphatics such as ω-hydroxy fatty acids, α,ω-dicarboxylic fatty acids, and primary fatty alcohols (Vishwanath et al. 2015, Kreszies et. al 2019).

Once accordingly infiltrated, the whole root samples were rinsed sufficiently in a ddH_20 bath and mounted to microscope slides by using Roti® -Mount FluorCare and elongated cover plates. Again, sample handling is delicate and should be carried out under avoidance of sample damages of any kind.

Being viscose, Roti® -Mount FluorCare has the advantage to stabilize the whole root sample in preference to ddH_2O. With regard to an average maximal root diameter approximated to 0,75 mm, a sample enclosing bonding surface between cover plate and microscope slide needed about 1 to 2 drops depending on sample length and pressure exerted on the dosing vial. Overdosing however, will further complicate clean processing and varnish sealing. According to the supplier (Carl Roth GmbH), Roti® -Mount FluorCare also prevents stained samples from photobleaching, so that they can be stored for re-evaluation over a prolonged period of time. Since all samples were monitored the same day, this initial advantage did not apply.

Although fresh dye has been prepared for each current staining routine during the experimental main phase, pre-trials showed, that readily compounded dye surpluses can be kept in the dark for at least 10 days at room temperature to still yield faultless results.

Table 12 Recipe for the Fluorol yellow 088 dye. Components were chosen and mixed according to Brundrett et al. (1991)

Name		Ingredients and ratios	
Fluorol yellow 088 dye	A	0,01% (w/v)	Fluorol yellow 088 in double distilled water (ddH_20)
		0,005 g : 50 ml	Unit example
	B	90% (v/v)	Glycerol in double distilled water (ddH_20)
		45 ml : 5 ml	Unit example
Solution A and B are mixed in a ratio of 1:1			

5.7 Cross sectioning, berberine-aniline blue dyeing and mounting for microscopy assessment

For the examination of endo- and exodermal Casparian strip formation (lignification gradients), 3 PEG infiltrated whole roots of each treatment have been zoned into the respective target sections. Appropriate markings were made under the stereo microscope (Olympus SZ61) by use of spacer. Subsequently, about 40 – 50 thin freehand cuttings (with a desired section thickness of < 2 cell layers) were made with a halved razor blade while attention was paid to squashing avoidance. For the final assessment ≥ 10 of these cuttings were used for each section, i.e. ≥ 30 per section and treatment. Remembering that PEG 1500 is easily soluble, it seemed strongly advisable not to use any water for wetting the blade or the sample area, as the thin transversal cuttings might be washed off the slide and the stabilizing embedment could possibly become dissolved. However, working waterless, the PEG sheathing on the microscope slides held the root samples in place and the PEG coated single cuts could be carefully transferred block by block to the designated section holders (cell sieves) by using forceps. To prevent dehydration from here on and to allow the PEG elution to start, the cell sieves were placed in Petri dishes filled with ddH_20.

Immediately prior to the staining process, the cell sieves were successively introduced to a serial rinsing in warm ddH_20 (± 30° C) to thoroughly elute excess PEG from the samples.

For berberine (Table 13) and aniline blue dyeing henceforth the protocol established by Brundrett et al. (1988) was consulted (Appendix 3). However, as indicated in the following, several small adjustments and omissions have been made.

For berberine staining, the cell sieves containing the cross sections were submerged in 0,1% (w/v) berberine hemisulfate in ddH_2O for 60 min. in a dark cupboard. The second step required a thorough cleansing of the cell sieves in an appropriate series of Petri dishes filled with ddH_2O, where excess dye or water must have drained off well after each rinsing. Once dye stopped leaching off the samples, the cell sieves were transferred to the aniline blue solution (2,5% in 2% acetic acid; as provided by Sigma Aldrich Chemie GmbH) and counterstained for 30 min. in a dark cupboard. According to Brundrett et al. (1988) the counterstaining procedure efficiently suppresses unwanted background fluorescence and non-specific binding berberine. It also eliminates the need for complex clearing steps. Further, aniline blue reduces over-intense xylem (lignin) foreground fluorescence as well as general suberin fluorescence, rendering the Casparian strips more distinctive.

Table 13 Recipe for the berberine hemisulfate dye. Components were chosen and mixed according to Brundrett et al. (1988)

Name	Ingredients and ratios	
Berberine hemisulfate dye	0,1% (w/v)	berberine hemisulfate in double distilled water (ddH_20)
	0,05 g : 50 ml	Unit example

Although several authors (Haseloff et al. 2003, Lux et al. 2005, Ursache et al. 2018) recommend additional clearing or solvent solutions like chloral hydrate, lactic acid or ClearSee™, both the high throughput approach and the intended avoidance of toxic substances suggested proceeding with a minimum level of intervention. The usability of the results thus obtained having been tested in advance.

Subsequent to staining, again a thorough cleansing of the cell sieves in an appropriate series of Petri dishes filled with ddH_2O was required. As compared to berberine cleansing, excess dye or water needed a more extended series of washing dishes to have been completely rinsed out, what may be considered in accurate preparation.

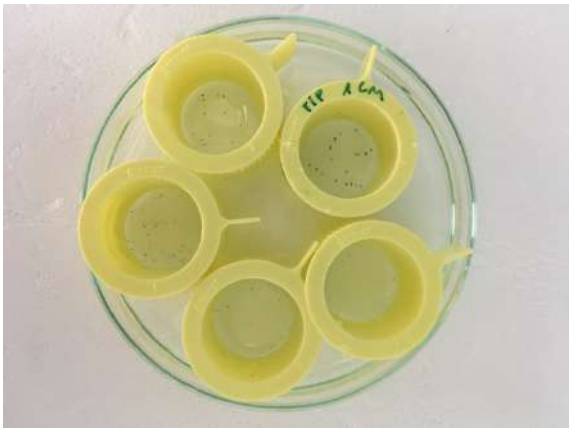

Figure 13 Berberine-aniline stained freehand cross sections of a 3309 C rootstock's fine main root in cell sieves. Starting from the sieve labeled "Tip 1 CM", which contains zone 0, zones 1-4 are found counterclockwise. The descending intensity of cross section colorization was explained unexamined by a possible excess staining of nonspecific tissues in the division or elongation meristem. Under the microscope, this intensity sequence did not occur, which presumably resulted from the specified light excitation.

For mounting purposes, the cell sieves were placed in a ddH_20 filled Petri dish (Figure 13) under the stereo microscope and the single cross sections were picked off the sieves by the tip of a fine paint brush and redistributed to 1 or 2 drops of ddH_20 preliminarily pipetted on a microscope slide. Appropriate cover glasses were then sealed with varnish and stored to dry in the dark.

Again, several authors advised mounting with glycerol at pH 9 or 2,2-thiodiethanol (Donaldson 2013) or iron(III) chloride-glycerol (Brundrett et al. 1988) to enhance definition or inhibit decolorization. However, in view of the microscopy within a few hours after mounting and with respect to the high throughput approach and the intended avoidance of toxic substances, a straightforward mounting with ddH_20 seemed adequate. The usability of the results thus obtained having been tested in advance.

5.8 Microscopy

Exclusive of some pixel-scanned whole root images, where a SP8-STED super-resolution microscope was used, microscopic imaging was carried out with a confocal laser scanning biological microscope (FV 1000) and operated by the Fluoview FV 1000 software. The high throughput imaging has been kept to fluorescence lamp light only and the pictures were retained by a microscope mounted photo camera (Olympus E-620).

6. Methods IV: The rhizobox approach for 3309 Couderc

For additional execution of a rather phene focused experiment in larger scale root environments with more realistic simulation of field conditions (Poorter et al. 2016), the presumably more lime-susceptible of the two genotypes (3309 C) was submitted to three stresses (iron deficiency, iron deficiency and drought as a combined application and drought as single noxa) in rhizoboxes. The experiment was set up in a non-climatized greenhouse on the BOKU location in Tulln, Austria (Figure 14).

Figure 14 For the implementation of the rhizobox experiment, 24 rhizoboxes were filled with substrate and populated with 3309 C cuttings. Two 25 l jerrycans supplied nutrient solutions by pump support. One main hose per jerrycan branched into two irrigation hoses per rhizobox. Inclined positioning of the boxes promotes root growth onto the transparent back panel of the boxes. Each last box in one block was sheeted to prevent excess light exposure.

6.1 Pre-growth and planting of 3309 Couderc to the rhizoboxes

3309 C cuttings have been planted to a 1:1 mixture of perlite and type 1 substrate (Einheitserde, group II) and were pre-grown for 6 – 8 weeks. 24 homogeneous phenotypes were chosen and received a thorough washout for removal of all perlite and substrate residues before being replanted to one rhizobox each. The rhizoboxes having previously been filled up to approx. 5 cm from the rim with type 1 substrate (Einheitserde, group II) sieved through a 4 mm mesh. To achieve a preferably uniform planting ground, the substrate was thoroughly compacted but not over-tightened and pre-soaked with deionized water.

6.2. Gradual exposure of rhizobox planted 3309 Couderc to stress conditions

The experiment (Figure 15) was intended as a pioneering pre-trial for future approaches and as a support for the findings made on laboratory scale. In this purpose, all plants have been initially irrigated with nutrient solution I (modified half strength Hoagland nutrient solution, Table 14) for 5 days. The solution was stored in two 25 l jerrycans and provided by a pump serving two main hoses branching into two irrigation hoses per rhizobox. The diurnal total volume added up to 540 ml and came about through two drippers providing 45 ml per minute and having been timer clock activated at 9:00 am for 2 minutes, at 2:00 pm for 3 minutes and at 6:00 pm for 1 minute.

In order to apply the iron deficiency treatment, one jerrycan was thoroughly rinsed and freshly filled up with nutrient solution II (modified half strength Hoagland nutrient solution, Table 14), that is, for half

of the vines the iron supply was stopped on day five of the experiment. The drought stress was introduced in a third step (removal of one dripper) after 16 days and in a fourth step (removal of the second dripper) with an additional delay of 10 days. This bipartition was due to the assumed possibility, that an

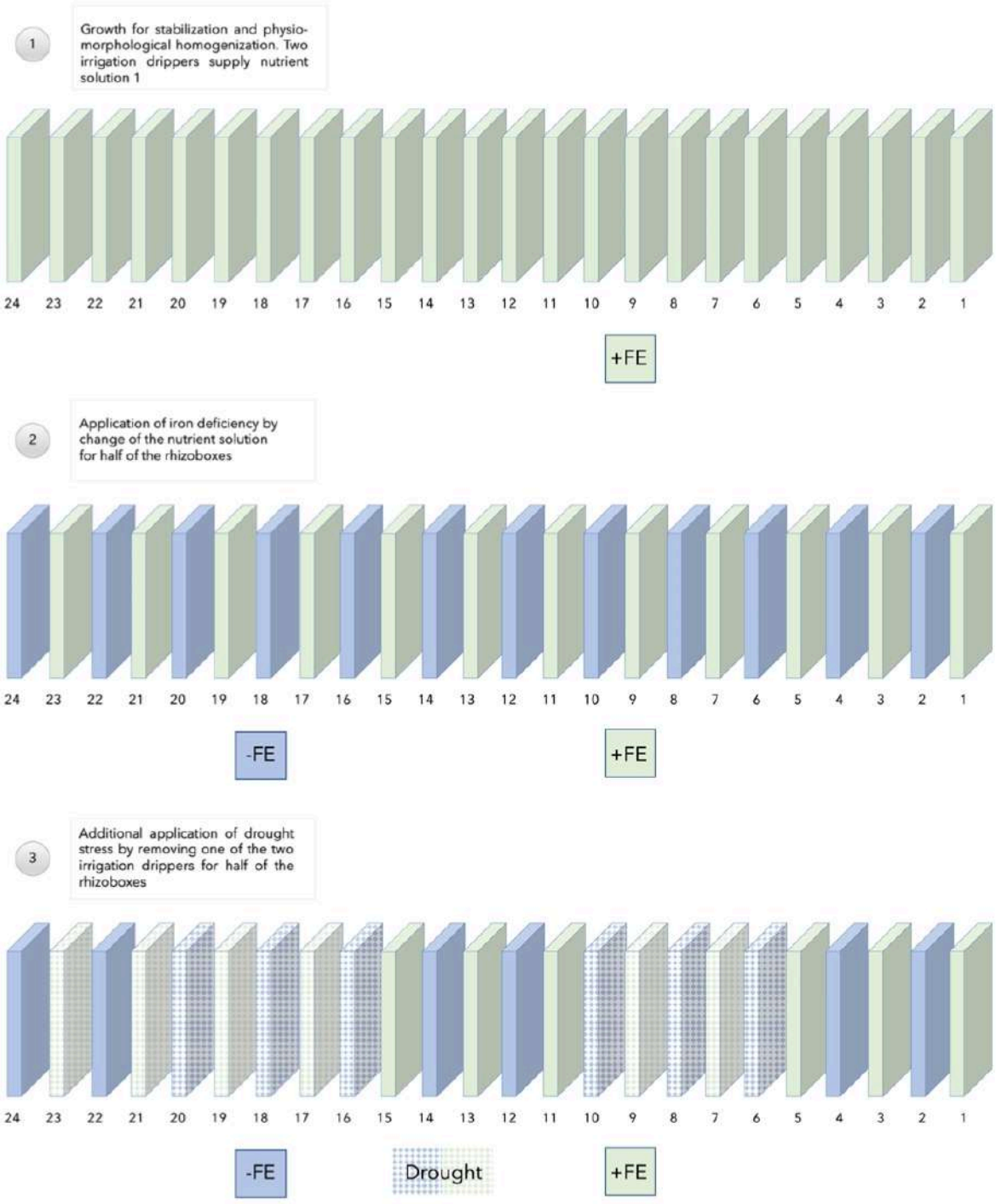

Figure 15 Schematic overview showing setup and chronology of the treatment applications within the scope of the rhizobox approach. The numbering followed the feed direction.

earlier onset of drying would interfere with an iron related symptom expression or physiologically measurable shortcomings in such a way that drought responses would become severe before iron deficiency could be recognized. However, shoot length was measured at several times and root development has

been photographically captured. In addition, stomatal conductance and chlorophyll fluorescence were regularly queried by use of the LI 600 porometer/fluorometer (final results still await evaluation).

6.3 Nutrient solutions for the rhizobox approach

6.3.1 Rhizobox nutrient solution 1 and 2

Since the smallest deviations, especially in the range of micronutrients, can lead to a significant deviation in substance availability, the accuracy of the data was specified with the greatest possible precision. The sequence and a complete solution of the individual components in partial quantities of the total quantity of deionized water (DIW) have proven to be decisive.

The solutions need to be prepared separately in the indicated order. Nutrient solution 1 and 2 are obtained by later adding the individual solutions in the appropriate ratio to the water volume needed. For nutrient solution 1, the addition of solution I, II and III is required. For nutrient solution 2, only solutions I and II are needed.

Table 14 Recipe for the nutrient solutions required to produce nutrient solution 1 and nutrient solution 2

Name	Ingredients and ratios							
	Nutrient	Formula	µM	mM	mW (g mol^{-1})	g l^{-1}	g l^{-1} (1 : 100 stock)	Order
Nutrient solution I	Calcium nitrate tetrahydrate	$Ca(NO_3)_2.4H_2O$	-	2	236,15	0,4723	47,23	I-1
	Ammonium nitrate	NH_4NO_3	-	1	80,04	0,0800	8,00	I-2
Nutrient solution II	Potassium dihydrogen phosphate	KH_2PO_4	-	1	136,09	01361	13,61	II-1
	Potassium sulfate	K_2SO_4	-	0,75	174,26	0,1307	13,07	II-2
	Magnesium sulfate heptahydrate	$MgSO_4 \cdot 7\ H_2O$	-	1	246,48	0,2465	24,65	II-3
	Manganese (II) Chloride Tetrahydrate	$MnCl_2.\ 4H_2O$	4,6	-	197,91	0,00091	0,0910	II-4
	Boric acid	H_3BO_3	23,2	-	61,83	0,00143	0,1434	II-5
	Copper sulfate monohydrate	$CuSO_4.H_2O$	0,31	-	159,6	0,00005	0,0049	II-6
	Sodium molybdate dihydrate	$Na_2MoO_4.\ 2H_2O$	0,06	-	241,95	0,00001	0,0015	II-7
	Zinc sulfate monohydrate	$ZnSO_4.\ H_2O$	0,4	-	179,46	0,00007	0,0072	II-8
Nutrient solution III	Sodium Iron EDTA	FeNaEDTA	50	-	421,1	0,02106	2,1055	III-1
The pH was adjusted 5.9 to 6.2 by NaOH addition after admixing the single solutions to the required water volume								

Used as a stock solution I and II were added each in a 1 : 100 ratio to the water volume needed for the nutrient solutions intended to induce iron deficiency; I, II and III were added each in a 1: 100 ratio to the water volume needed for the nutrient solutions intended to serve as control. The pH was adjusted with NaOH to about 5.9 – 6.2.

7. Statistical analyses

The Kruskal-Wallis test, the one-way Anova, or the two-way Anova (partially including effect sizes), or both the non-parametric and the parametric test variant were used for result differentiations according to the respective requirements estimates and tested post hoc with the Dunn test or the Tukey HSD where possible. The confidence interval was set at $\alpha = 0.05$. When two results were collected but tended to match, the reference result chosen was the one that, after examination and inclusion of the non-adjusted outliers, most closely reflected the conspicuousness of the corresponding graph.

In general, the normal distribution precondition has been interpreted progressively, as Anova appears to be more robust to this formerly strict constraint than previously suspected. This seems to be especially true for independent samples and small data sets ($n < 50$). In such cases normal distribution seems to be difficult to measure anyway (especially if outliers are not eliminated or smoothed, which was not intended here for reasons of completeness and the multifactorial determined individual character of the measured values). In addition, the Anova seems to be more robust to violations of the preconditions as commonly assumed and it generally seems to be increasingly recommended to test statistical results for plausibility with additional cognitive tools; a recommendation which seems to notably apply for bio-data. (Glass et al. 1972, Harwell et al. 1992, Lix et al. 1996, Salkind, 2010, Schmider et al. 2010, Blanca et al. 2017. Amrhein et al. 2019). Except for a few exceptions where Excel was used for plotting, statistical evaluations and plotting were performed by employing R commander or R respectively.

IV. Results and discussion

The main result was the successful method establishment for both the in vitro and the rhizobox treatment of different rootstocks (3309 Couderc, Fercal). The experiments can be carried out with the selected means, i.e. with the employed techniques and their combination; further, the adjustments made as described in the method section were target-oriented in the sense of the research question and it was possible to observe rootstock responses to lime and drought stress or to their interaction (phene realignments, root pattern plasticity, suberization, Casparian strip formation).

However, since the fluorol yellow stained whole roots were observable with laser scan techniques under the microscope, but image fixation using the fluorescent lamp alone did not produce the desired results in the given time frame for this staining approach, only a limited output-overview is provided for this particular subsection. Similarly, the not completely satisfactory photo comparisons of the rhizobox rooting seems to need elaboration, for which reason only a workaround has been imparted. Here, material shortage due to pre-breeding problems and schedule limitations allowed the rhizobox variant of the experiment also only for 3309 C.

The separate one-way Anova evaluation of the individual parameter performances for the respective rootstocks is intended to determine significance for the within-treatment comparison. In addition, the boxplot-charts allow a more conclusive allocation of the variances (in the sense of intra-genotype diversity). To make this variance observable for the individual rootstocks, i.e. without inter-genotype involvement, is a core concern in the sense of the research questions. Due to the complexity of the genotype x environment interaction, corresponding rootstock by rootstock comparisons will also be

made separately hereinafter. This allows a clear visualization of the genotype influence by further displaying the associated interaction effects.

The individual results are presented or contrasted according their segmental acquisition.

1. Results of the in vitro root measurements

The evaluation of the root parameters, that developed from the respective media-type application are oriented primarily to the actual performance of the genotypes under given conditions. As noted (III.7), no smoothing or adjustment was applied and the preconditions for the statistical tools were interpreted liberally with respect to the bio-genetic nature of the trait objects. The Kruskal-Wallis test was used as one-way Anova and two-way Anova with the post hoc exertion Dunn test and Tukey HSD. 0.05 was set for α.

Expectedly, different responses have been observed in accordance to the treatments. Thus, it can be assumed, that the experimental setting and the replicable media impositions were likely to cause adaptive phenetic performance; the latter may be assessed by perusal of the displayed results.

1.1. Treatment-related performance comparison for Fercal

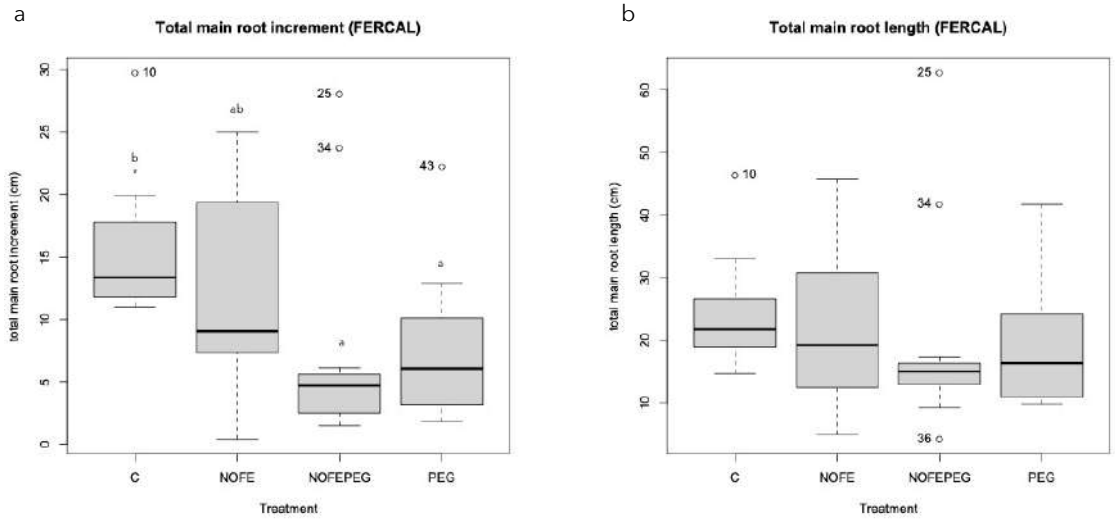

*Figure 16 Boxplot charts displaying the different root parametric ratios. Regarding **a**, the whiskers and the outliers (○ with sample number) indicate variance. According to the p-values being < 0.05 ("*" = 0.05) and comparing the corresponding means, C (15.47 sd ± 5.42), NOFE (12.36 sd ± 7.68), NOFEPEG (7.49 sd ± 8.74) and PEG (7.57 sd ± 5.90) do significantly differ as indicated by different letters. The null hypothesis (H_0) therefore can be rejected and it can be said, that there is difference. A Kruskal-Wallis test performed in addition to the one-way Anova led to the same result; **b**: according to the p-values being > 0.05, C (23.93 sd ± 8.65), NOFE (21.82 sd ± 11.87), NOFEPEG (19.63 sd ± 16.23) and PEG (19.38 sd ± 10.65) do not differ..*

The means of the total main root increment (Figure 16 a), that is the averaged total increase in root length for each treatment group signifies a clear impact of stress exposure on a length determined iron and or water foraging for the Fercal rootstock; with regard to NOFE the whiskers indicate intra-genotypic performance variance. Depending on the result valuation, the displayed responses point out to a balanced approach of Fercal as to C and NOFE. The possibility of the latter two groups being differentiated from the other two might be considered obvious after all. However, the means of the total main root length (Figure 16 b), that is the total length of all main roots added, do not show performance variance

if the p-value is recalled. With the inclusion of the outliers, this could be reinterpretable at least for NOFEPEG.

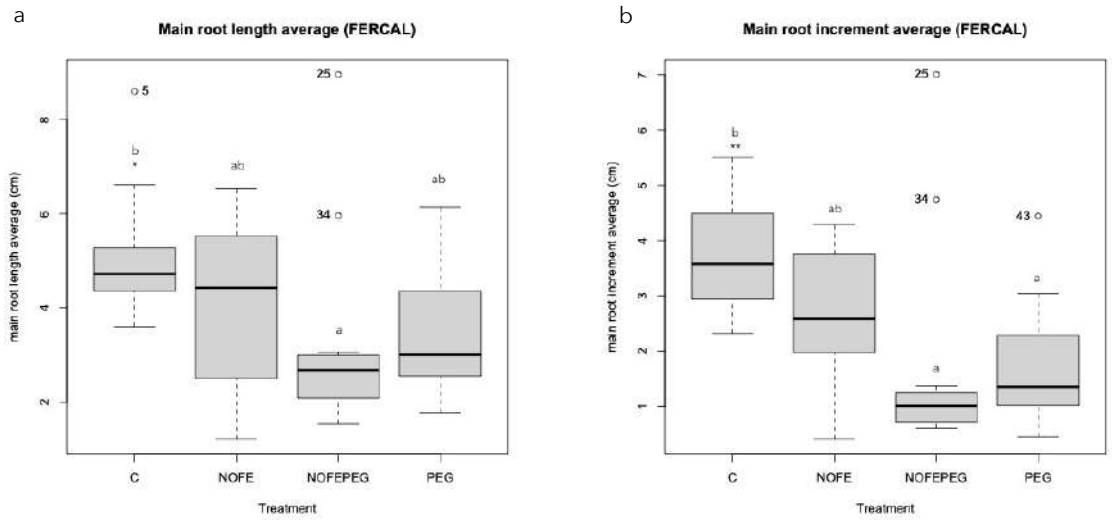

*Figure 17 Boxplot charts displaying the different root parametric ratios. Regarding **a**, the whiskers and the outliers (○ with sample number) indicate variance. According to the p-values being < 0.05 ("*" = 0.05) and comparing the corresponding means, C (5.08 sd ± 1.36), NOFE (4.15 sd ± 1.72), NOFEPEG (3.27 sd ± 2.11) and PEG (3.44 sd ± 1.31) do significantly differ as indicated by different letters. The null hypothesis (H_0) therefore can be rejected and it can be said, that there is difference. A Kruskal-Wallis test performed in addition to the one-way Anova led to the same result. **b**: According to the p-values being < 0.05 ("**" = 0.01) and comparing the corresponding means, C (3.77 sd ± 1.07), NOFE (2.69 sd ± 1.16), NOFEPEG (1.74 sd ± 2.00) and PEG (1.73 sd ± 1.13) do significantly differ as indicated by different letters. The null hypothesis (H_0) therefore can be rejected and it can be said, that there is difference. A Kruskal-Wallis test performed in addition to the one-way Anova led to the same result.*

Regarding the main root length average (Figure 17 a), that is the average length of the assumed single main root, once again a bi-partite pattern is suggested, which could possibly be even more pronounced with the inclusion of the outliers or the intra-genotypic performance variance. Meaning, C, NOFE and PEG appear to not differ only due to a balanced performance behavior towards NOFE and PEG mitigation. The main root increment average (Figure 17 b), that is the average increase of the assumed single main root, is supporting this assumption with minor deviation. Again, an independent chart interpretation seems to be additionally recommended.

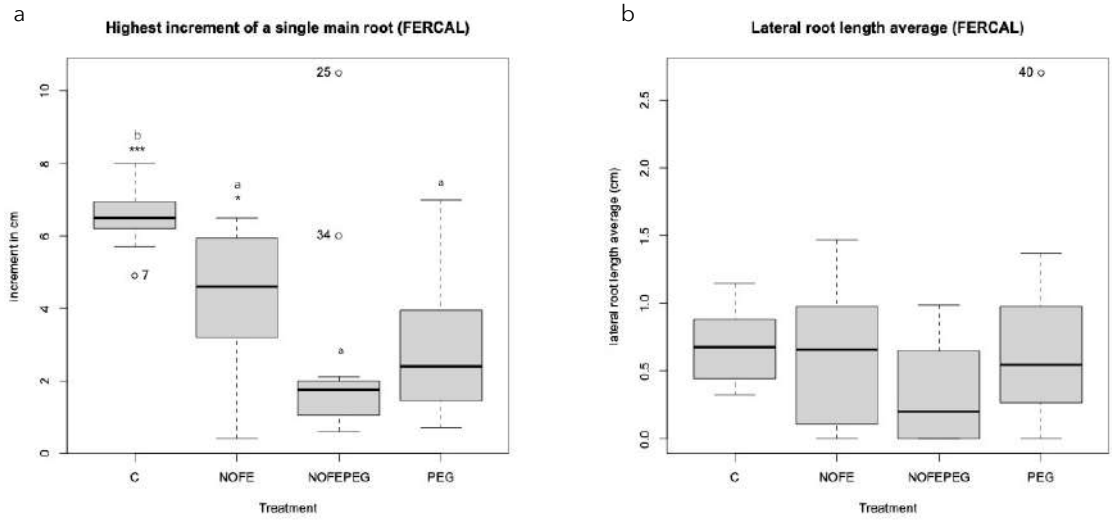

*Figure 18 Boxplot charts displaying the different root parametric ratios. Regarding **a**, the whiskers and the outliers (○ with sample number) indicate variance. According to the p-values being < 0.05 ("**" = 0.01, "*" = 0.05) and comparing the corres-*

*ponding means, C (6.56 sd ± 0.81), NOFE (4.29 sd ± 1.92), NOFEPEG (2.57 sd ± 2.86) and PEG (2.87 sd ± 1.81) do significantly differ as indicated by different letters. The null hypothesis (H_0) therefore can be rejected and it can be said, that there is difference; **b**: according to the p-values being > 0.05, C (0.68 sd ± 0.27), NOFE (0.61 sd ± 0.50), NOFEPEG (0.33 sd ± 0.39) and PEG (0.74 sd ± 0.74) do not differ.*

Basically, the highest measured increment of a single main root (Figure 18 a) draws the same outline, even if the statistical analyses clearly show C in the lead. However, in principle similar adaption strategies can again be assumed for NOFE and PEG, even if they could not be statistically reproduced here. The length distribution of the first order laterals (Figure 18 b), on the other hand, is optically and statistically congruent; which also applied sample-wise during the measurement. This finding further is consistent with the presumably preventive and reactive energy adjustment in main root formation, which, however, seems to be different for the lateral root quantity, where Fercal also exhibits a restrained approach, i.e. a more efficient use of resources (IV.1.3).

1.2 Treatment related performance comparison for 3309 C

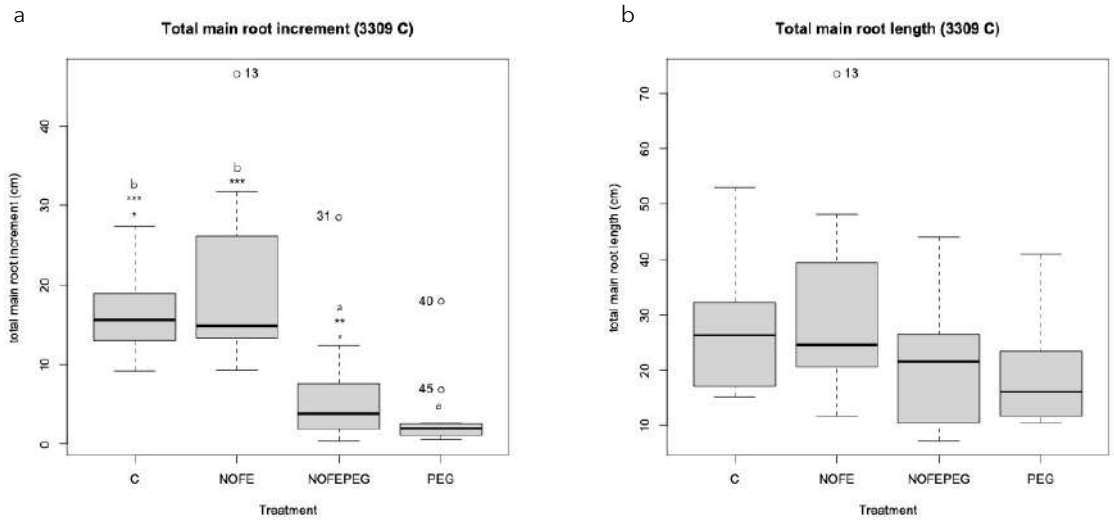

*Figure 19 Boxplot charts displaying the different root parametric ratios. Regarding **a**, the whiskers and the outliers (○ with sample number) indicate variance. According to the p-values being < 0.05 ("***" = 0.001, "**" = 0.01, "*" = 0.05) and comparing the corresponding means, C (16.36 sd ± 5.03), NOFE (19.74 sd ± 11.69), NOFEPEG (6.32 sd ± 7.85) and PEG (3.40 sd ± 4.84) do significantly differ as indicated by different letters. The null hypothesis (H_0) therefore can be rejected and it can be said, that there is difference; **b**: according to the p-values being > 0.05, C (27.85 sd ± 12.80), NOFE (31.96 sd ± 18.32), NOFEPEG (20.59 sd ± 11.41) and PEG (19.25 sd ± 9.57) do not differ.*

For 3309 C, there also seems to be a bi-partition with regard to the main root length average (Figure 19 a), which is reflected in a clear pairwise difference significance of C and NOFE versus NOFEPEG and PEG. The distribution for the total main root length (Figure 19 b) however appears to be largely uniform, as it was for Fercal, suggesting a homogeneous prior distribution of starting conditions. The value diminution for PEG is to be explained by the reduced increment effect.

The main root length average and the main root increment average (Figure 20) initially seem to be more broadly distributed across the spectrum. This may indicate a more explorative and thus energy intensive strategy as compared to an efficiency increase on the micro-spatial level. However, the differentiation of C and NOFE from NOFEPEG and PEG is likewise significant here.

With a view to the highest increment of a single main root (Figure 21 a), where C and NOFE exhibit

significant different performances compared to NOFEPEG and PEG, and the average first order lateral length (Figure 21 b), the impression of a dualistic performance pattern is apparently repeated.

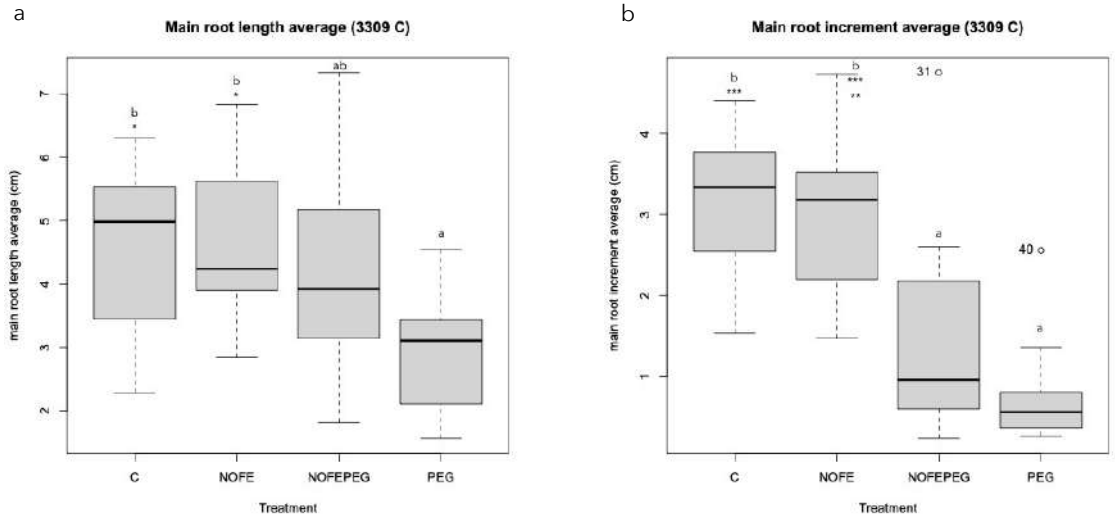

*Figure 20 Boxplot charts displaying the different root parametric ratios. Regarding **a**, the whiskers and the outliers (○ with sample number) indicate variance. According to the p-values being < 0.05 ("*" = 0.05) and comparing the corresponding means, C (4.61 sd ± 1.30), NOFE (4.63 sd ± 1.30), NOFEPEG (4.17 sd ± 1.50) and PEG (2.96 sd ± 0.88) do significantly differ as indicated by different letters. The null hypothesis (H_0) therefore can be rejected and it can be said, that there is difference. A Kruskal-Wallis test performed in addition to the one-way Anova led to the same result. **b**: According to the p-values being < 0.05 ("***" = 0.001, "**" = 0.01) and comparing the corresponding means, C (3.19 sd ± 0.87), NOFE (3.07 sd ± 0.99), NOFEPEG (1.50 sd ± 1.29) and PEG (0.76 sd ± 0.64) do significantly differ as indicated by different letters. The null hypothesis (H_0) therefore can be rejected and it can be said, that there is difference. A Kruskal-Wallis test performed in addition to the one-way Anova led to the same result.*

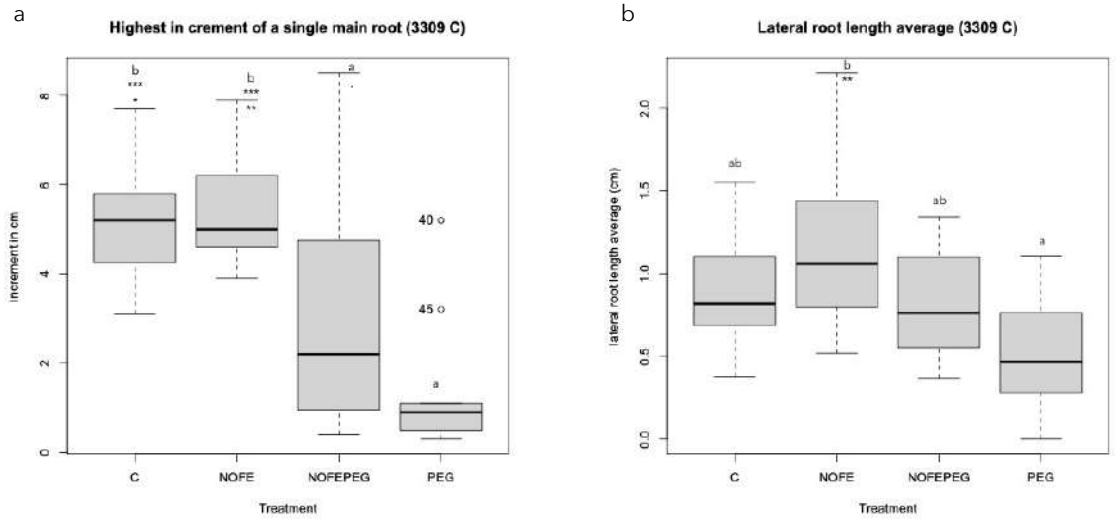

*Figure 21 Boxplot charts displaying the different root parametric ratios. Regarding **a**, the whiskers and the outliers (○ with sample number) indicate variance. According to the p-values being < 0.05 ("***" = 0.001, "**" = 0.01, "*" = 0,05, "." = 0.1) and comparing the corresponding means, C (5.29 sd ± 1.34), NOFE (5.52 sd ± 1.38), NOFEPEG (3.00 sd ± 2.49) and PEG (1.30 sd ± 1.44) do significantly differ as indicated by different letters. The null hypothesis (H_0) therefore can be rejected and it can be said, that there is difference. A Kruskal-Wallis test performed in addition to the one-way Anova; except for the irrelevant 0.1 level significance found for the difference between NOFEPEG and NOFE, it led to the same result. **b**: According to the p-values being < 0.05 ("**" = 0.01) and comparing the corresponding means, C (0.90 sd ± 0.38), NOFE (1.16 sd ± 0.49), NOFEPEG (0.81 sd ± 0.34) and PEG (0.52 sd ± 0.35) do significantly differ as indicated by different letters. The null hypothesis (H_0) therefore can be rejected and it can be said, that there is difference. A Kruskal-Wallis test performed in addition to the one-way Anova led to the same result.*

However, it again seems likely, that attempts are being made to counter NOFE with a more explorative strategy. As an intermediate result and taking into account the outliers' influence on the quantifiable output, a tendency of reduced performance can be observed especially for NOFEPEG and PEG, while NOFE, at least for these parameters and for this observation frame, does not show any actual under-performance.

1.3 Rootstock and treatment related effect comparison (Fercal – 3309 C)

The subsequent comparisons serve to assess the response performance of the two different rootstocks, whereby Fercal with a rather medium drought tolerance and a high resistance to lime induced chlorosis feedbacks is understood to be the superior genotype according the methodological set-up.

The sample size may be somewhat small to make generally reliable statements. However, the statistics suggest that the rootstocks acidify the root environment with varying intensity. In accordance with the Fe acquisition strategies described above, the increased drop for NOFE is also conspicuous and congruent (Figure 22). As further and more specialized rhizosphere examinations were envisaged in case of a successful method establishment, an approximate indication was considered sufficient for pH-change purpose.

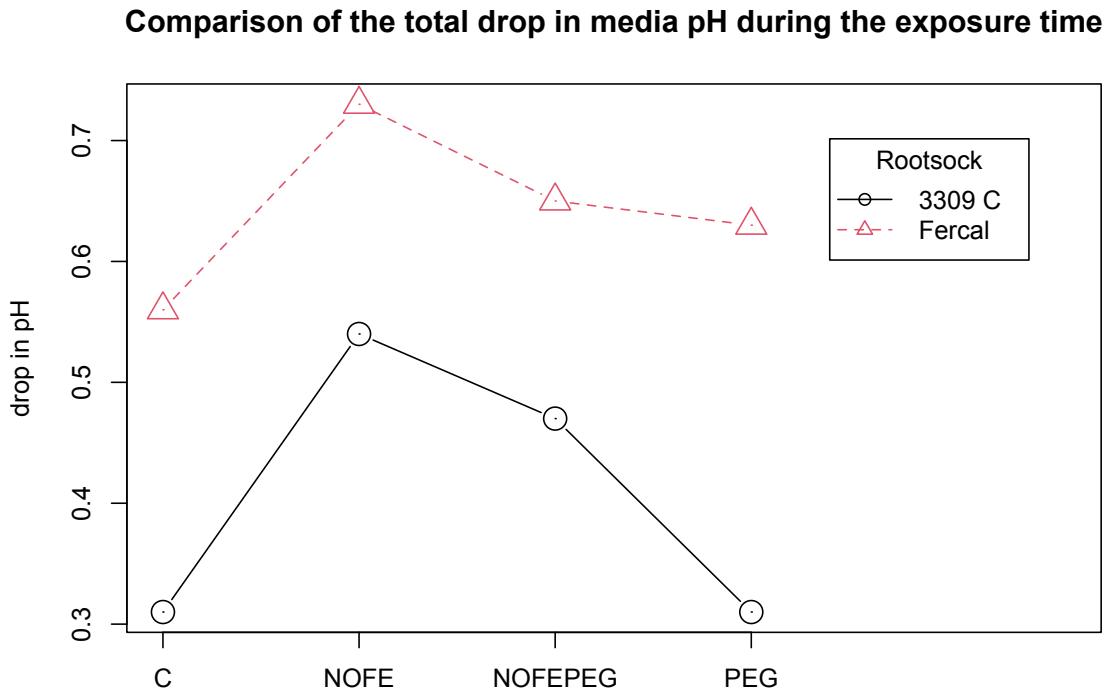

Figure 22 The total drop of pH was measured before and after the treatments by the use of 15 gram of pure media or post-treatment media diluted in 50 ml ddH_2O. The portion to be measured was obtained from a pre-homogenized and averaged total mixture from all dishes of one treatment or from an untreated dish containing the control medium and that was kept under the same conditions. Comparisons were *made by a two-way Anova application, the Pr(>F) for rootstock is 0.0134 which does imply significance at a level of $\alpha = 0.05$, Comparing the corresponding means, C (0.43 sd ± 0.17), NOFE (0.63 sd ± 0.13), NOFEPEG (0.56 sd ± 0.13) and PEG (0.47 sd ± 0.23) and according to the Pr(>F) of 0.6699 no difference can be assumed after a within treatment comparison.*

Nevertheless, in the present context, an interpretation and consideration of H^+ excretion for pH lowering is of additional significant importance, since here too, via interrelationship cascades cell wall reinforcements with lignin or suberin for iron storage purposes are associated (Müller et al. 2015).

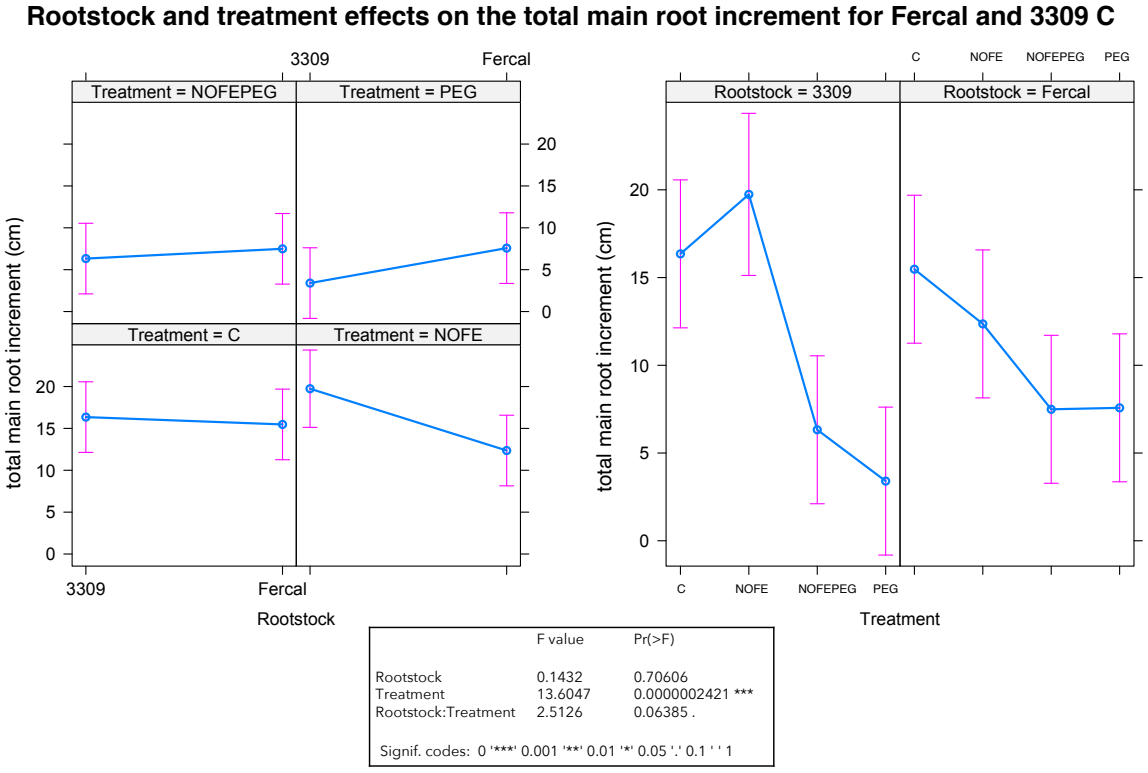

Figure 23 Comparing the total main root increments of Fercal and 3309 C by a two-way Anova application, there is significant difference with regard to the treatments, which confirms earlier results. The detectable interaction indicated by the rootstock:treatment comparison is below the chosen significance level; Regarding effect size (partial eta squares) however, within the frame of the experimental settings, rootstock choice seems not to be without any effect on root increment performance. The values are 0.0011 for 'rootstock' (small), 0.3035 for 'treatment' (big) and 0.0560 for 'rootstock:treatment' (small). As > 0.06 values indicate moderate interaction, the result might be consistent with the significance indicated by the Pr(>F) of 0.1.

While, of course, the intra-treatment differences remain essential, the research question is supposed to be just as much about the inter-rootstock relation. Unsurprisingly, the adaption patterns of the individual rootstocks to the treatments are repeated (monitored in IV.1.1 and IV.1.2), so that letters or asterisks have been omitted in the interest of graph clarity. This also seems appropriate as the direct comparison is more concerned with determining the rootstock effect on performance.

For the given α of 0.05, figure 23 reveals significance for the treatment differences but only indicates an interaction of the fixed factors by trend (Pr(>F) = 0.1 and effect size ranges just below medium strength (>0.06) at 0.0560. Meaning, rootstock choice will nevertheless most probably affect performance. At least for NOFE and PEG the assumption of a direct interdependence would supposably be acceptable. When, again, comparing the rootstocks directly, it seems, that for Fercal main root increment can be better maintained under moderate draught stress. Encountering iron deficiency, the approaches towards length growth seem to diverge in the opposite direction, here 3309 C shows clear increment trends.

As the evaluation approach displayed by figure 24 seem to somewhat primarily smoothen the margins, a significance is neither assumed for the single main effects nor regarding an interaction effect. This is also reflected by the effect sizes of 0.0194 for rootstock (small), 0.0652 for treatment (medium strength) and 0.0233 for rootstock:treatment (small). However, a further look may be appropriate regarding the 3309 C behavior towards NOFE or the rootstock related performance with respect to

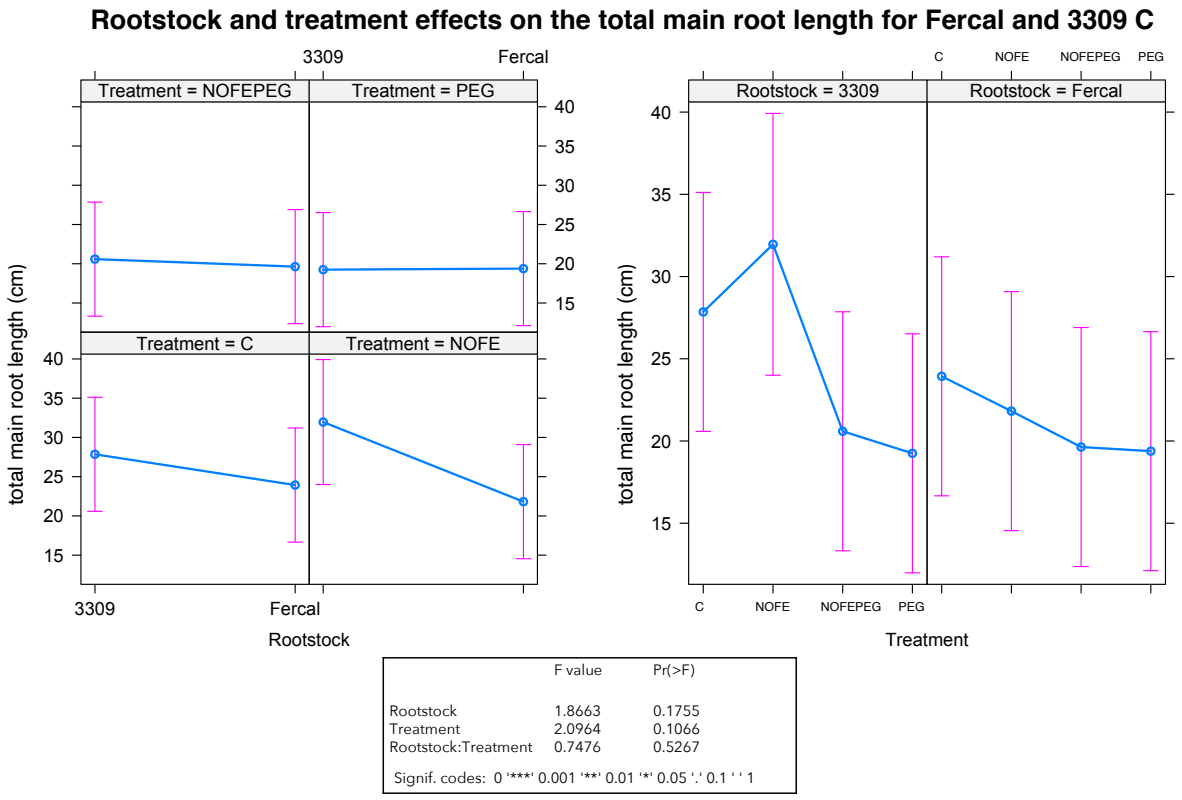

Figure 24 Comparing the total main root lengths of Fercal and 3309 C by a two-way Anova application, there is no significant difference with regard to the treatments, nor there is detectable interaction indicated by the rootstock:treatment comparison. Reflecting the latter results, the computation of the respective effect sizes are 0.0194 for 'rootstock' (small), 0.0652 for 'treatment' (small) and 0.0233 for 'rootstock:treatment' (small).

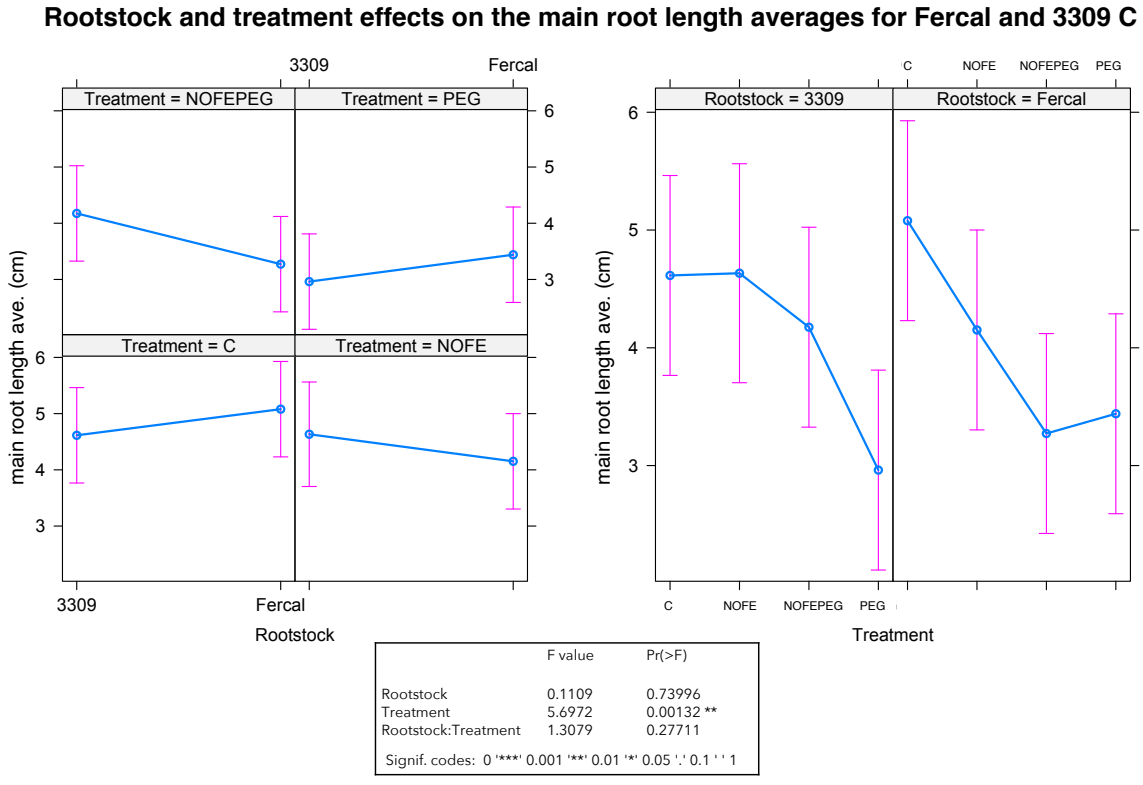

Figure 25 Comparing the total main root length averages of Fercal and 3309 C by a two-way Anova application, there is significant difference with regard to the treatments, which confirms earlier results. There is no detectable interaction between

rootstock and treatment. Effect sizes are 0.0010 for 'rootstock' (small), 0.1595 for 'treatment' (big) and 0.0366 for 'rootstock:treatment' (small). This would indicate, that the stress response represented by the measured performance of this phene feature does not appear to be divergent for the laboratory conditions applied.

iron deficiency in general. Fercal seems not to react with foraging, i.e. explorative length growth.

Applying the effect sizes, main root length averages (Figure 25) again do not reveal a rootstock effect even though the indicated intra-genotypic performance variance should be noted here to the disadvantage of definiteness. However, despite the statistical intangibility, the patterns plotted are, to some extent, striking and seem to make it possible to still estimate behavior trends. Although the effect lines displaying the rootstock influence on performance are not exceptionally unparalleled, they nonetheless do not match.

Again, in direct comparison to 3309, Fercal seems not to increase root length when iron deficiency is involved, but at the same time appears to be capable of foraging intensification when encountering water shortage. Of course, the low effect tendency plotted may be additionally explainable by ay reduced maintenance of root functioning in contrast to simple dieback.

Since the overall increment could be considered precondition parameter, the latter observations do of course also prove to be valid for figure 26. When directly compared with 3309 C, the tendency of Fercal to at least not make significant expenditures for length growth when iron deficiency is endured, seems to be confirmed. However, it also appears necessary to capture, that a noticeably similar pattern repetition continues to exist for C and NOFE in juxtaposition to NOFEPEG and PEG independent of the chosen rootstock.

Rootstock and treatment effects on the main root increment average for Fercal and 3309 C

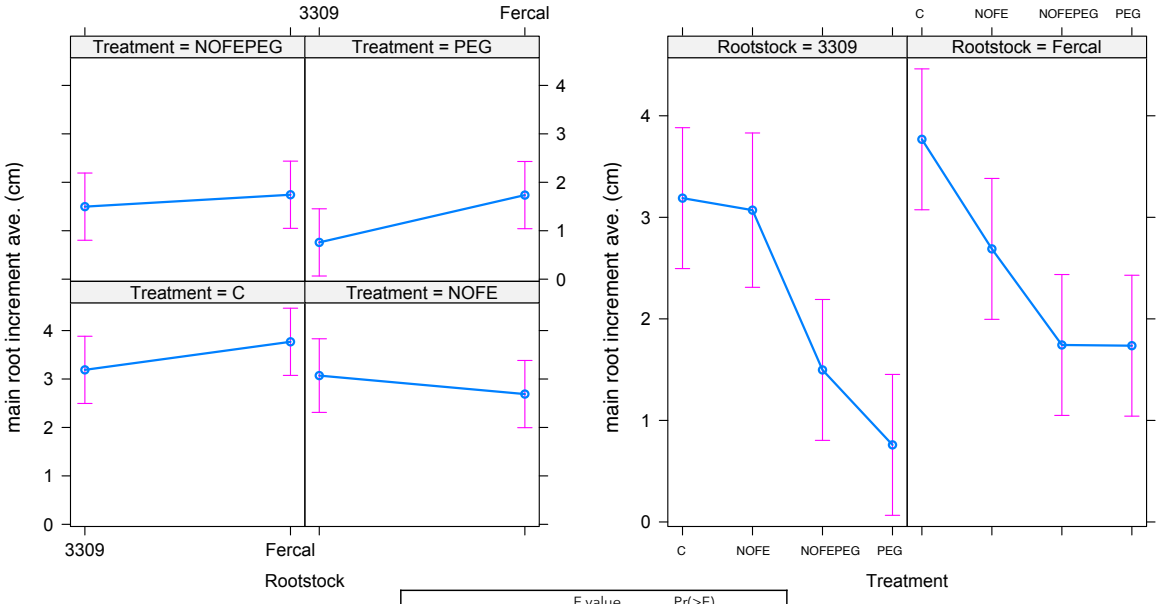

	F value	Pr(>F)
Rootstock	2.2224	0.1397
Treatment	17.6855	4.986e-9 ***
Rootstock:Treatment	1.2873	0.2839

Signif. codes: 0 '***' 0.001 '**' 0.01 '*' 0.05 '.' 0.1 ' ' 1

Figure 26 Comparing the main root increment averages of Fercal and 3309 C by a two-way Anova application, there is significant difference with regard to the treatments, which confirms earlier results. There is no detectable interaction between rootstock and treatment. Effect sizes are 0.0153 for 'rootstock' (small), 0.3656 for 'treatment' (big) and 0.0266 for 'rootstock:treatment' (small). This would indicate, that the stress response represented by the measured performance of this phene feature does not appear to be divergent for the laboratory conditions applied..

Monitored for the purpose of testing a possible formation of a single main explorative root, the values for the highest increment of a single main root (Figure 27) do repeat the current pattern. However, they suggest clear significance respecting the interdependence of factors; meaning, that the deviation strength which determines the performance differentiation of Fercal and 3309 C, could thus be interpreted as an adaptation indicator. Which here noteworthily is supported more by the Pr(>F) of 0.03691 (= 0.05) than by the effect size, which again ranks just below the medium effect strength (>0.06) at 0.0554. Here, a differentiable response pattern possibly indicates varying disposition regarding bio-component use on a function that could be provisionally designated pioneer rooting.

With a view to lateral root length average (Figure 28) a comparison of both rootstocks significantly displays a factor interdependency. With an upward pointing effect size of 0.0939, particularly the responses to iron deficiency both with and without PEG addition seem to support the assumed influence of the genotype on the adjustment strategy. Whereas, with the exception of some PEG-values and the clear discrepancy in the NOFE approaches, the strategies have so far tended to be recognized as trends, the patterns for the lateral roots are clearly distinct. To substantiate this with more statistical power, one the one hand a much larger number of replicants with correction for the outliers would be necessary; one the other hand this would possibly ignore the obvious variance in individual performances with such a small sample size already.

However, the descriptive power of the plot itself is, again, noteworthy, as it provides additional valuable context for the assessment and interpretation of these bio-data.

Rootstock and treatment effects on the highest single main root increment for Fercal and 3309 C

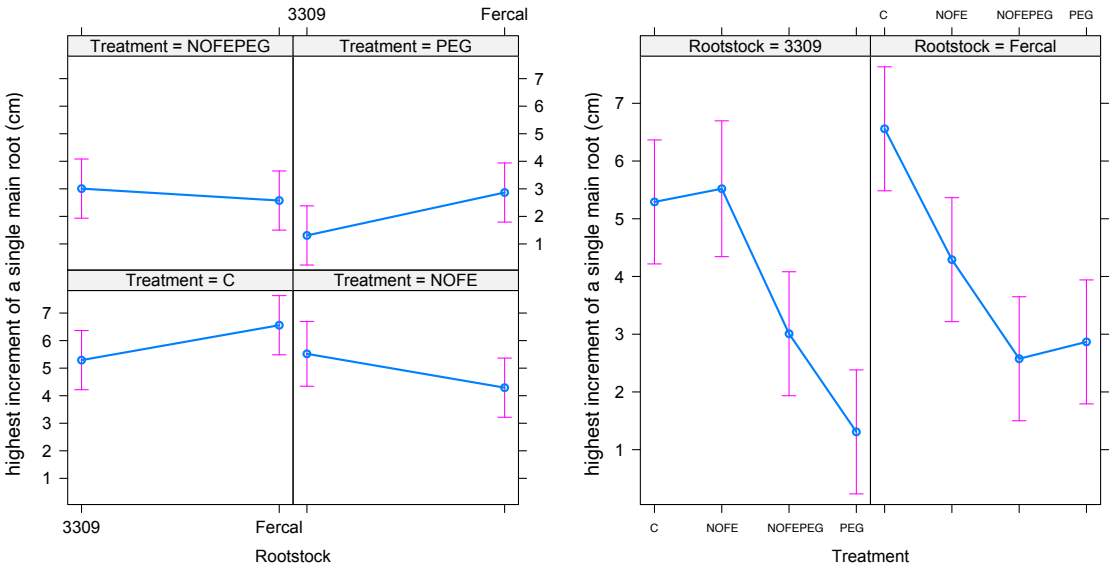

	F value	Pr(>F)
Rootstock	0.7125	0.40096
Treatment	21.5052	1.749e-10 ***
Rootstock:Treatment	2.9563	0.03691 *

Signif. codes: 0 '***' 0.001 '**' 0.01 '*' 0.05 '.' 0.1 ' ' 1

Figure 27 Comparing the highest increments of a single main root of Fercal and 3309 C by a two-way Anova application, there is significant difference with regard to the treatments, which confirms earlier results. The detectable interaction indicated by the rootstock:treatment comparison is significant for the chosen significance level. Effect sizes are more conservative here with the values 0.0045 for 'rootstock' (small), 0.4030 for 'treatment' (big) and only 0.0554 for 'rootstock:treatment' (small). As > 0.06 values indicate moderate interaction, the result might be consistent with the significance indicated by the Pr(>F) of 0.05. This would indicate, that the stress response represented by the measured performance of this phene feature appears to be a rootstock effect trait for the laboratory conditions applied.

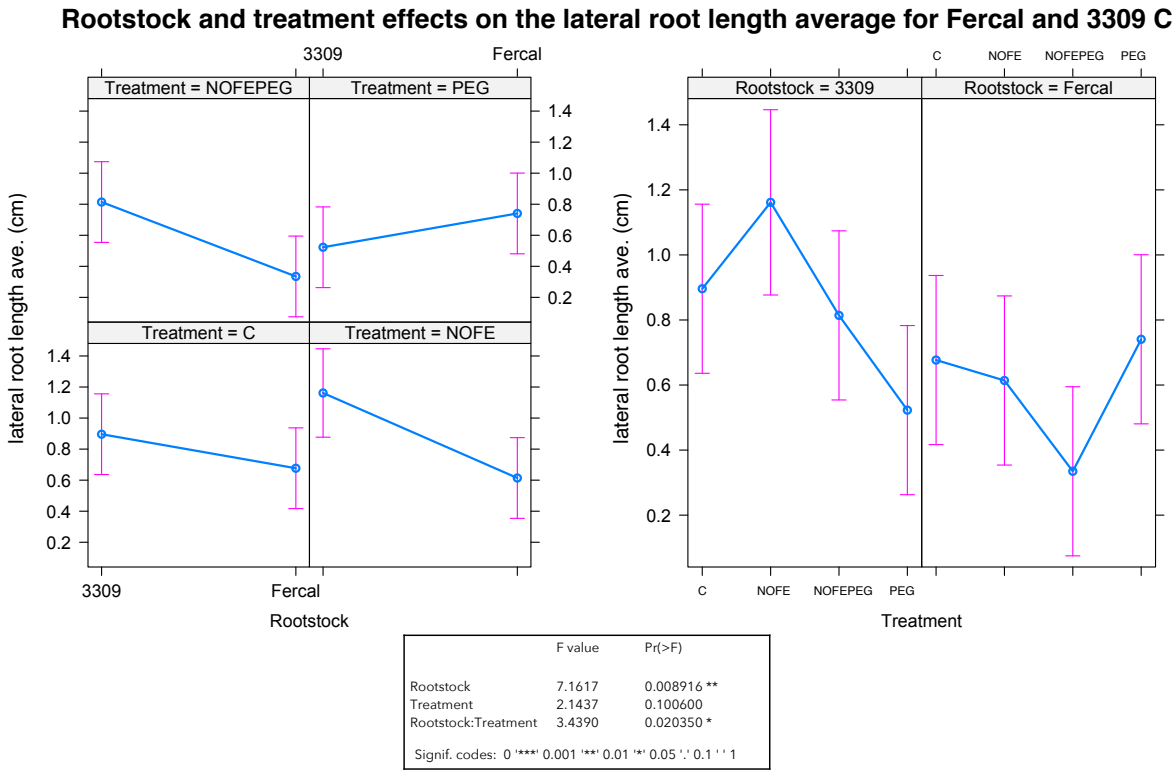

Figure 28 Comparing the lateral root length averages of Fercal and 3309 C by a two-way Anova application, there is significant difference with regard to the rootstock. Further, the detectable interaction indicated by the rootstock:treatment comparison is significant for the chosen significance level. Effect sizes reflect the output with the values 0.0652 for 'rootstock' (medium), 0.0585 for 'treatment' (small) and 0.0939 for 'rootstock:treatment' (medium). This would indicate, that the stress response represented by the measured performance of this phene feature appears to be a rootstock effect trait for the laboratory conditions applied.

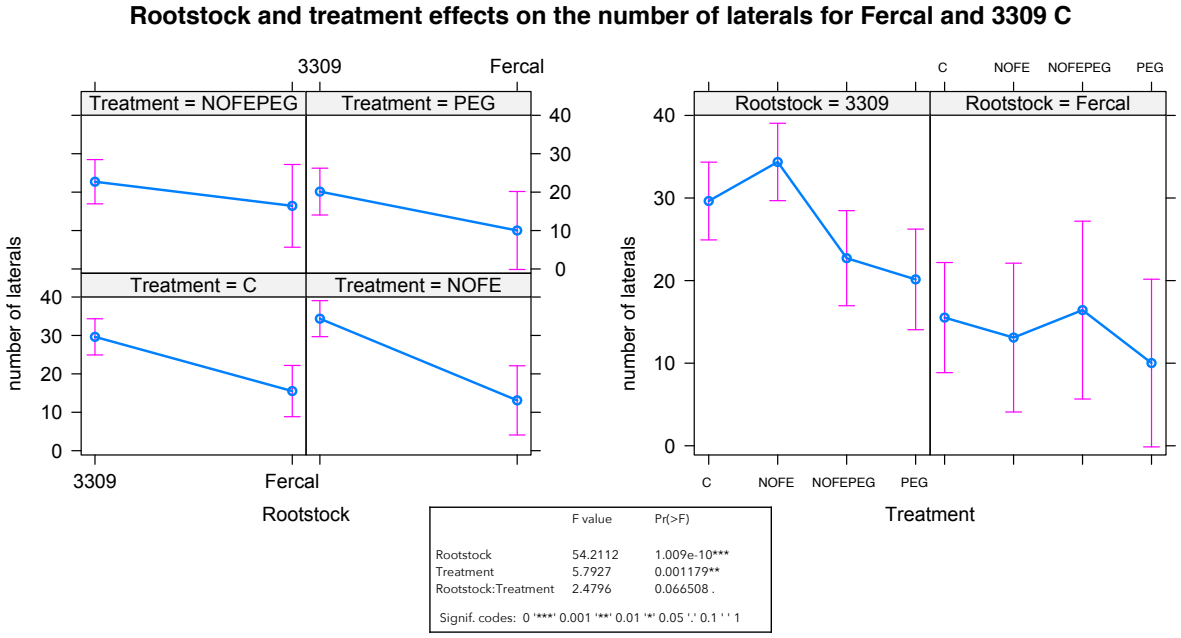

Figure 29 Comparing the number of laterals of Fercal and 3309 C by a two-way Anova application, the Pr(>F) for rootstock is 1.009e-10 which implies a significance at $\alpha = 0.001$, for treatment the Pr(>F) is 0.001179 which implies a significance at $\alpha = 0.01$. The interaction levels at 0.066508 which only does imply a significance at $\alpha = 0.1$. Effect sizes reflect the output with the values 0.3285 for 'rootstock' (high), 0.1053 for 'treatment' (medium) and 0.0451 for 'rootstock:treatment' (small).

Similar to the lateral length, the effects and interdependencies are obvious for the first order lateral true counts (Figure 29). Not only the rootstock effect alone and the indication for rootstock:treatment effects are significant, also the mere count averages, suggest, that Fercal might be supported by a highly efficient lateral regime. Thus, it seems the laterals have a key role to play in homeostasis insurance under the conditions that have become effective here. The rootstock:treatment effect is again most clearly displayed by the rootsock:NOFE effect.

Summing it up with a total performance plot (Figure 30), where all parameters except the unitless lateral true count are computed to give an overall impression of phene dynamics expressed in length measure. Although the outcome reflects some of the previous tendencies, the rootstock:treatment interaction is denied by both the Anova and the effect size. This is comprehensible insofar, as the overall dynamics of the factors are restricted. The significance regarding the treatment effect is expectably definite, which underlines that the adaption strategies measured were of rather defensive, i.e. non-manipulative nature, other than active approaches not taken into account here such as pH lowering or microbiome recruiting.

Nevertheless, looking at NOFE and PEG a rootstock effect seems to not be neglectable, while the effects for C and NOFEPEG are negligible. For NOFEPEG most probably because the combined strain was too intense to be encountered by whatever means over the complete exposure time and for C of course, because no adaption was required. In turn, the most differentiation power seemed to originate from NOFE, which again would be explainable by the initial rootstock choice.

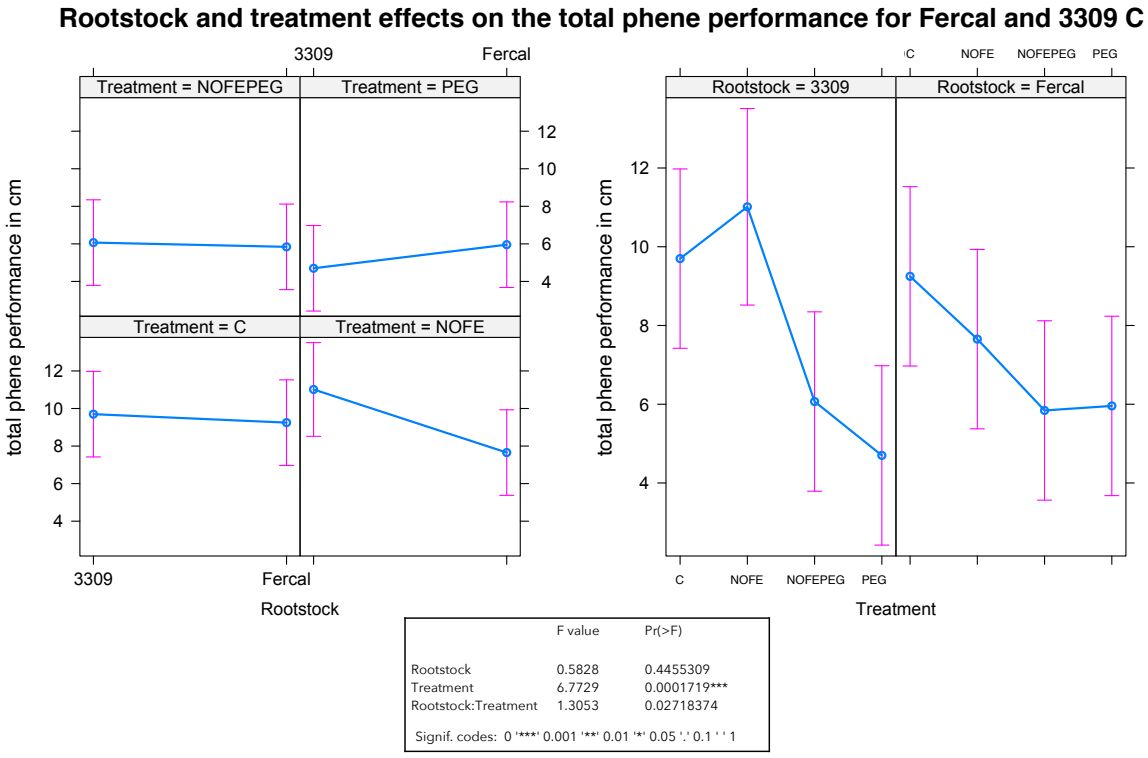

Figure 30 Comparing the overall phene performance of Fercal and 3309 C by a two-way Anova application, the Pr(>F) for rootstock is 0.4455309 which does not imply any significance, for treatment the Pr(>F) is 0.00011719 which implies a significance at $\alpha = 0.001$. The interaction levels at 0.2718374 which does not imply any significance. Effect sizes deviate insofar, as the output with the values are 0.0010 for 'rootstock' (small), 0.0350 for 'treatment' (small) and 0.0067 for 'rootstock:treatment' (small).

Figure 31 (a) once again very conspicuously opposes one of the parameters presumed to have a main effect (the effect size for rootstock on lateral count values 0,3238 > 0.14 = big) and does confirm to have significant influence on the overall performance (Appendix 4).

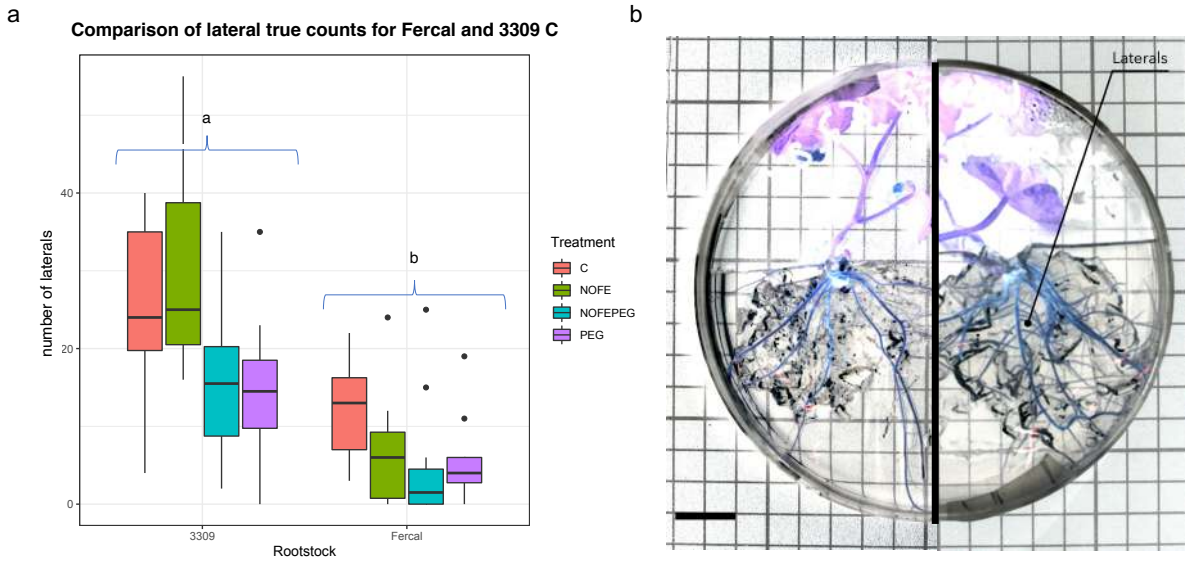

*Figure 31 Comparison of the true count of laterals (**a**). The p-value for rootstock 2.18e-9 < 0.05 ("***" = 0.001) suggests a high significance for the rootstock distinctive distribution of laterals. Subimage (**b**), left: Fercal; right: 3309 C. The scale bar in the lower left corner indicates 2 cm.*

The contrast image (Figure 31 b) tries to give an impression of the lateral distribution. The smaller laterals (< 2 mm) are graphically not taken into account here; in fact, for the 3309 C sample (≥ 40 counts) are about twice the number of laterals is present as compared to the Fercal sample (24 counts). But of course, clearer appearance is limited to sizes > 2mm.

1.4 Visualized endomorphological response phenomena

As defined by the research question, differences and gradients regarding endomorphological, i.e. endodermal and exodermal responses to situations of strain caused by iron deficiency and drought or a combined approach, could be observed. Particularly, the berberine-aniline based imaging approach was

*Figure 32 Micrographs of an unstained freehand cross section of 3309 C (**a**) and a berberine-aniline stained freehand cross section of 3309 C which had been exposed to drought stress (**b**) observed with transmitted light at a 10 x magnitude. The scale bars indicate 100 µm. On the right-hand side the development of root hairs is clearly visible. Both sections are fresh cuttings and have not been infiltrated with PEG prior to their preparation.*

successfully executed. The results are satisfactory to make approximately confirming statements in the sense of the work objective and to establish congruencies with the consulted literature (Chapter 1 and 2). The results are reproducible and based on > 30 cross sections from each zone of interest, which were randomly allocated from ≥ 3 main roots per treatment.

Nevertheless, it should be noted, that the establishment character of the various work steps is likely to have contributed to the fact that the optical results can be considered only approximate assessments in the sense of the intra- and inter-genotypic variance, which is, however, a reassuring result in itself.

A first impression regarding the tissue distribution and the dimensions in general may be given by figure 32. The influence of the stain on the structure visualization of the different tissues becomes already obvious with transmission light alone. Of course, the regions of interest are much more distinct when using fluorescent light microscopy.

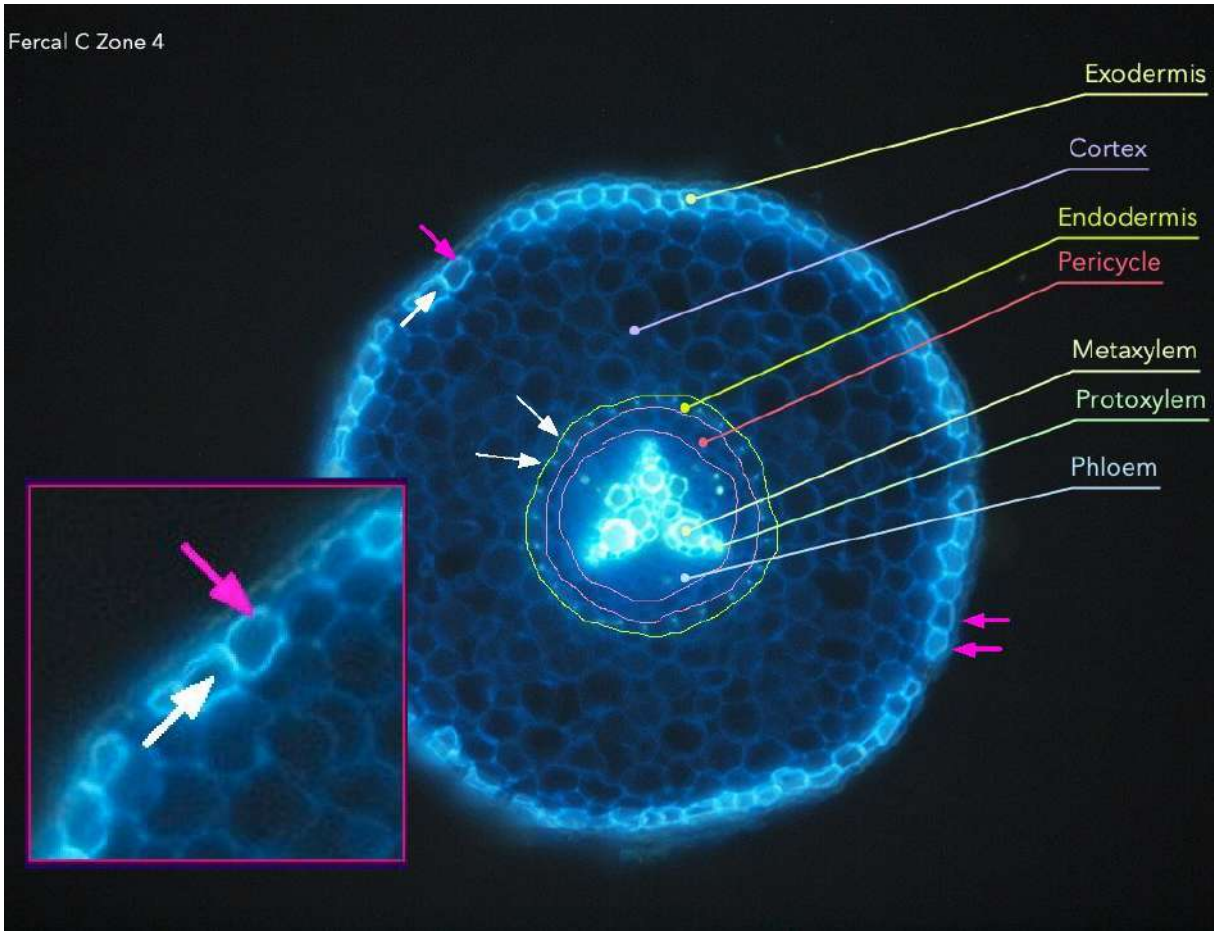

Figure 33 A cross section of a young, unstressed Fercal main root, which had been pre-infiltrated with PEG, stained with berberine hemisulfate and counterstained with aniline blue . Zone 4 refers to a segment of 1 cm width starting at centimeter 4 off the tip. Magnification was set at 20 x. The tissue structures of interest are labeled. White arrows indicate anticlinal cell wall enhancements, i.e. the presence of a lignin-like polymer forming the Casparian strips. Pink arrows indicate cell wall suberization. The subimage is a magnification of the exodermis in the upper left corner and intends to help differentiating between Casparian strips and suberin lamellae.

However, since it was not possible to integrate the microscope software when photographing through the microscope lens, most micrographs were to be reproduced without scale. Nevertheless, it can be asserted that all samples range between approximately 0,4 mm and 1 mm, depending also on the respective root section. Figure 33 gives an overview and should also make the most important

endomorphological target tissues allocatable.

As a general guideline, with reference to e.g. Brundrett et al. (1988, 1991), Gambetta et al. (2013) and considering the experience from the present work on berberine-aniline staining, Casparian strips (lignin-like polymers) are more likely to appear in a bright yellowish to whiteish blue and suberin lamellae in a reduced, light pale blue. However, the lignified parts do always express more radiant white as can be determined from a comparison with the xylem. For this sample, Casparian strip formation (indicated by white arrows) can be observed for all anticlinal cell walls of the endodermis (encircled in yellow). In this stage of maturation (Zone 4), the exodermis is nearly completely supported with both anticlinal Casparian strips and periclinal suberin enhancements, while the endodermis is lacking the suberin support, which represents an exemplary tissue pattern for an unstressed root in this cross-sectional segment.

While the xylem is displayed bright and glaring by reasons of the intense lignin accumulation in this vessel type, the phloem is rather of the same color as the cortex as both cell types are vivid and non-dermal; that is, no barrier function requires flexible or permanent setup.

1.4.1 Synopsis of dermal tissue development – Fercal

For all treatments, a corresponding cross section is assigned to each zoning. Although occasional blurring can be recognized, which is particularly frequent but not exclusive in zone 0, it should remain possible to read off a gradient in lignification and suberization, both in the basipetal direction (from 0 to 4) and between treatments.

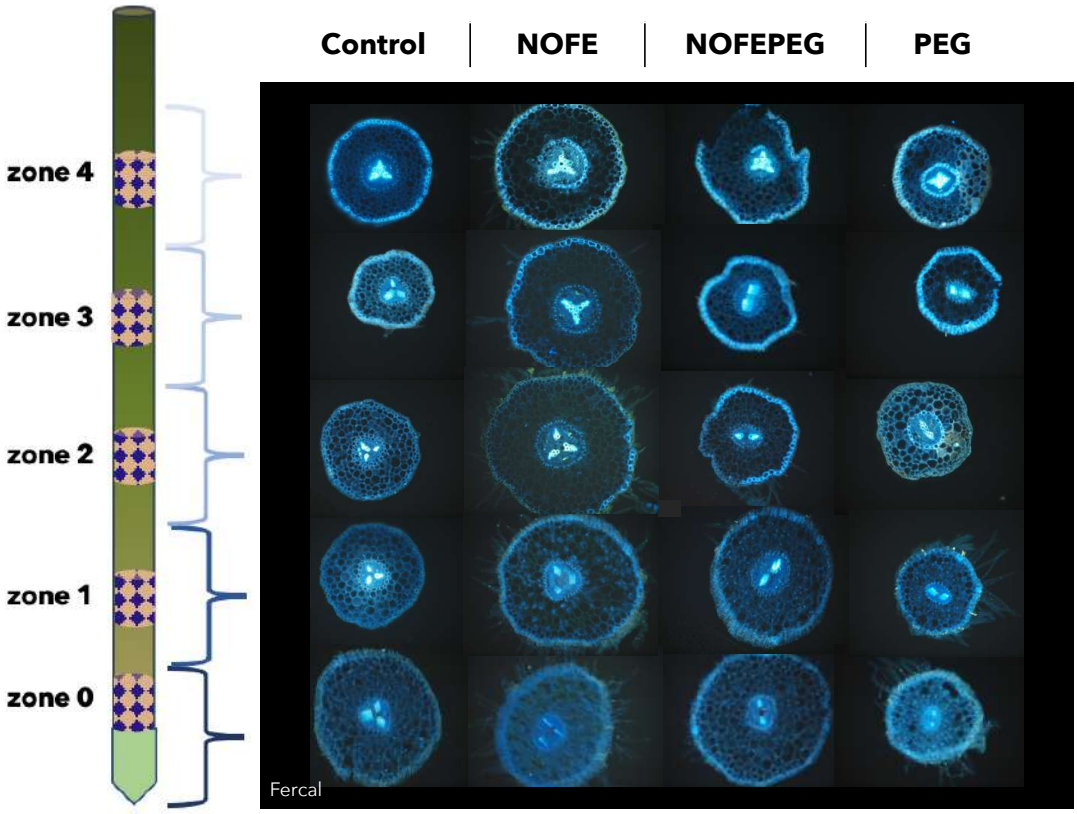

Figure 34 Micrographs of berberine-aniline stained cross sections of Fercal allocated to maturation zones and treatments. The lower sections seem to appear less bright in color, which should be an indicator for less binding sites, thus less lignin or suberin respectively. Magnification was set at 20 x.

Figure 34 should at least tend to show a color-light intensification along the vertical axes and from zone 2 upwards also a color-light increase for NOFEPEG and PEG compared to C and NOFE.

Although, suberin lamellae can generally be determined more accurately and distinctly by the use of fluorol yellow staining, the reduced method employed here is sufficient in terms of the initial research question; in this sense, the exodermis cell walls appear to display distinguishable tendencies to lignification and suberization increase.

1.4.2 Synopsis of dermal tissue development – 3309 C

The comparison of the different treatments for 3309 C (Figure 35) shows similar but not identical gradient pattern formation according to the preliminary visual assessments. A frequent incompleteness of suberin enclosure is conspicuous for the exodermis in NOFE, NOFEPEG and PEG, while the Casparian strip occurrence, other again than the endodermis suberization, seems to be gradient-appropriate and complete.

Considering the respective support functions with regard to stress response flexibility, it becomes obvious, that stress exposure enforces suberin lamination of endo- and exodermis more than the Casparian strip formation in the endodermis only, which is reasonable insofar as anticlinal lignin-polymer coating is used more than suberization as a stress-independent pass control or flow regulation (Ranathunge and Schreiber 2011, Barberon and Geldner 2014, Odgen et al. 2018).

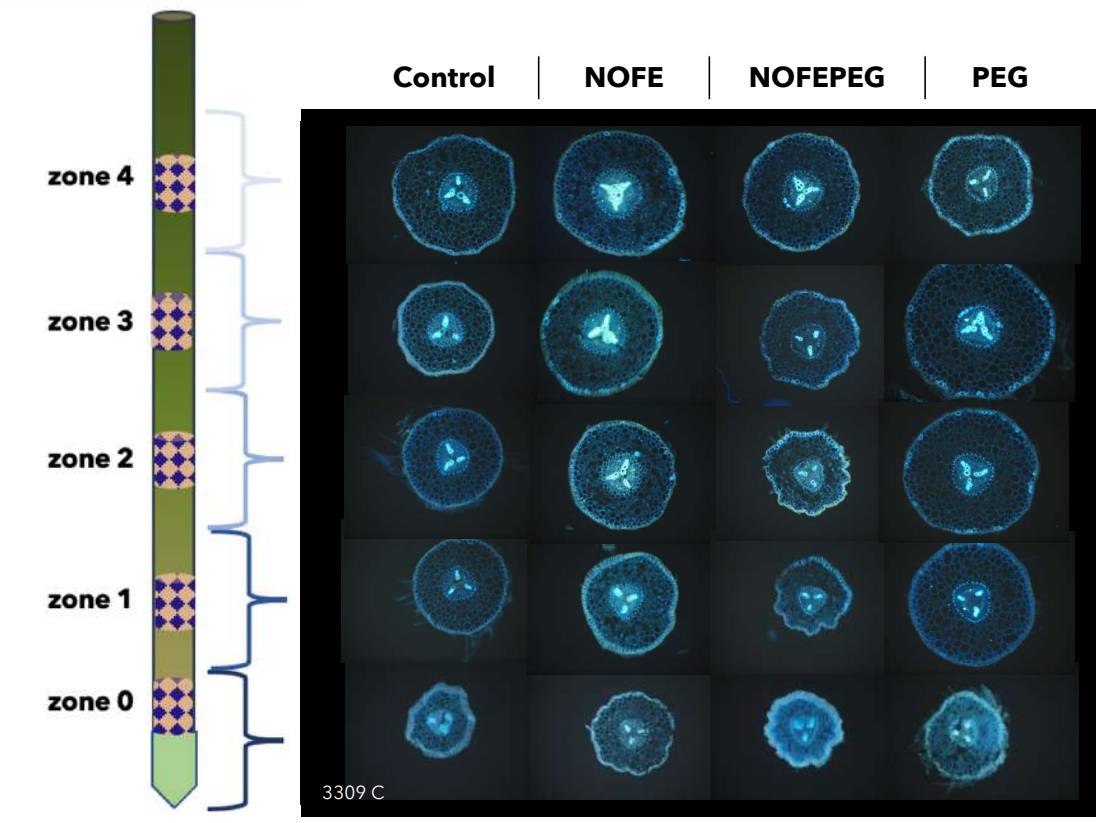

Figure 35 Micrographs of berberine-aniline stained cross sections of 3309 Couderc allocated to maturation zones and treatments. The lower sections seem to appear less bright in color, which should be an indicator for less binding sites, thus less lignin or suberin respectively. A first impression suggests a rather patchy distribution of suberization in the exodermis and punctual enhancements of endodermal tissues. Magnification was set at 20 x.

However, this basic concept is applicable to plant roots in general and therefore in the given context also to both rootstocks examined. The respective fitness in relation to environmental constrains is therefore most probably attributable to the pattern distribution, the intensity of the enforcements in interaction with the individual phene expression and a backup support on the part of proteome and metabolome, which could not be experimentally considered here.

In this regard, suberization needs to be valued as a virtually irreversible senescence phenomenon, which, however, may occur closer to the root apex (earlier) or rather basipetally (later) depending on stress levels and mitigation strategies of the respective rootstocks; thereby, the osmotic gradients may be regulated in favor of water inflow.

Progressive suberization of the exodermis will gradually lead to an interruption of the soil-root continuum, to a decreasing exudation, to a stagnant water uptake and finally to discontinuation of biomass build-up, which would also be unfavorable for subsequent foraging resumption after a possible circumstance re-improvement (Barrios-Masias et al. 2015, Sun et al. 2016). Since for both iron and water uptake at least a certain permeability must remain guaranteed if no other, continuum-independent strategies (such as storage recapture) become effective, there seem to be tendencies towards a balanced suberin distribution, which, according to preliminary impressions, is associated with additional effort for the overall performance of 3309 C; with particularly pronounced effects in the case of NOFEPEG and PEG endurance.

1.4.3 Comparison of dermal tissue development – Fercal and 3309 C

As a basic but still preliminary assumption, an earlier and more intense Casparian strip formation for Fercal in NOFE seems to appear, which could possibly argue for a protein controlled and thus directed transport to begin spatially premature. Further, a more intense and more complete endodermis suberization in NOFE and PEG can be observed for Fercal as compared to 3309 C (Figures 36-39), which again might be suitable to support the latter assumptions.

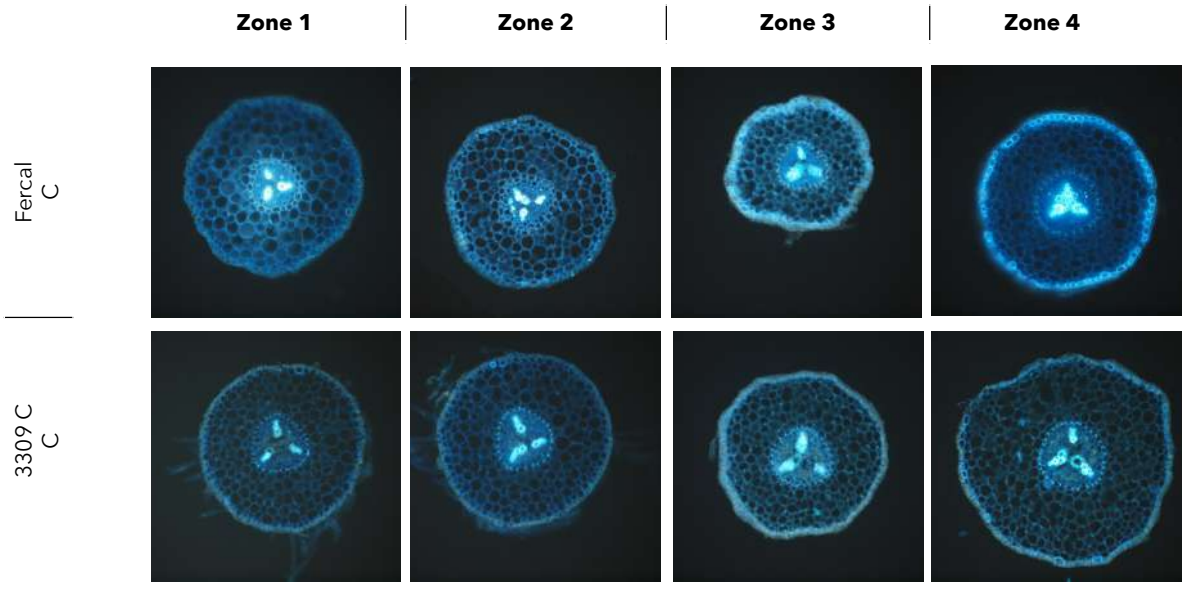

Figure 36 Micrographs of berberine-aniline stained cross sections of Fercal and 3309; a comparison of dermal tissue development for the control group. Magnification was set at 20 x.

Also, an earlier onset of exodermis suberization seems to be observable. Since suberization and lignification of dermal cell walls will decrease L_{Pr} (root hydraulic conductivity) and further increases negativity for $-P_R$, water continues to be circulated even in the event of a gradually threatening water shortage, which basically makes more adaptive in the sense of a continued root or vessel plasticity.

Fercal is not among the inherently drought resistant rootstocks, but seems to be able to use other strategies compared to 3309 C, especially since even unsusceptible breeds like 110 R exhibit these tendencies simultaneously with an increased exudate distribution to the rhizosphere (Barriois-Masias et al. 2015, Gambetta et al. 2017).

In this context, it might be noteworthy, that at the same time root hair development onset seems to appear earlier and more intense for Fercal in NOFE, a coincidence also observed by Tsai and Schmidt (2017) in the context of iron homeostasis. Here, root hair production is linked to a decreased cell length and thus an attenuated main root growth; a tendency, that can be observed for almost all parameters (Figures 23-29) for Fercal in NOFE and mostly also NOFEPEG when compared to 3309 C. This additionally would suggest, that a differing strategy is co-employed for PEG as a single stressor.

Furthermore, targeted and controlled meristematic and or dermal cell wall sealants are a strategy to secure stored iron, which could lead to the ability to afford more efficiency per unit surface area; i.e. less root mass (Bengough et al. 2011, Müller et al. 2015, Lynch 2019).

At the same time, here again, a complete lignification or suberization of endodermal cell walls would be disadvantageous, if stored Fe distribution should remain facilitated.

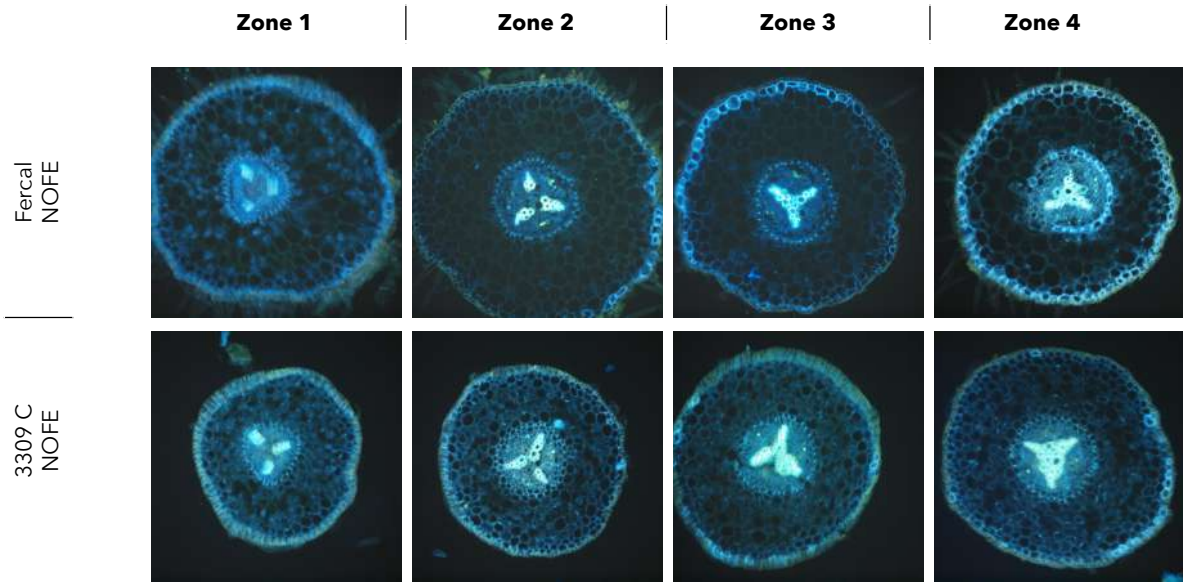

Figure 37 Micrographs of berberine-aniline stained cross sections of Fercal and 3309; a comparison of dermal tissue development for the NOFE treatment. Magnification was set at 20 x.

In general, it is interesting to note, that in NOFEPEG and PEG the overall performance is expectedly poor and that even with the moderate water stress of -0.55 MPa, the adjustment strategies seem to inhibit each other or drought (PEG) is just too impactful as a permanent stress amplifier.

In this context, results provided by Bengough et al. (2011) indicate, that root growth (elongation) is halved at values < -0.50 MPa. Here, too, a strategy that does not rely solely on a large ratio of root surface area (especially of the nutrient-relevant primary growth zones) is advantageous.

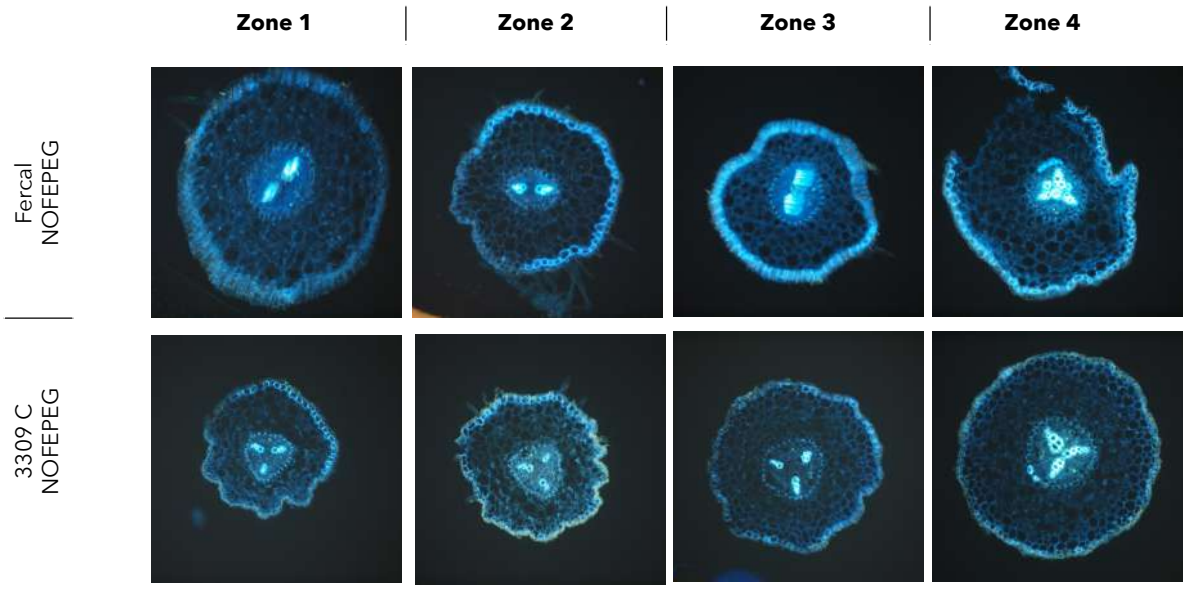

Figure 38 Micrographs of berberine-aniline stained cross sections of Fercal and 3309; a comparison of dermal tissue development for the NOFEPEG treatment. Magnification was set at 20 x.

Of course, it is highly certain, that no simple causality can exist and that manifold other factors (growth angle, diameter, cortex cell size, branching etc.) additionally come into play here (Lynch 2019).

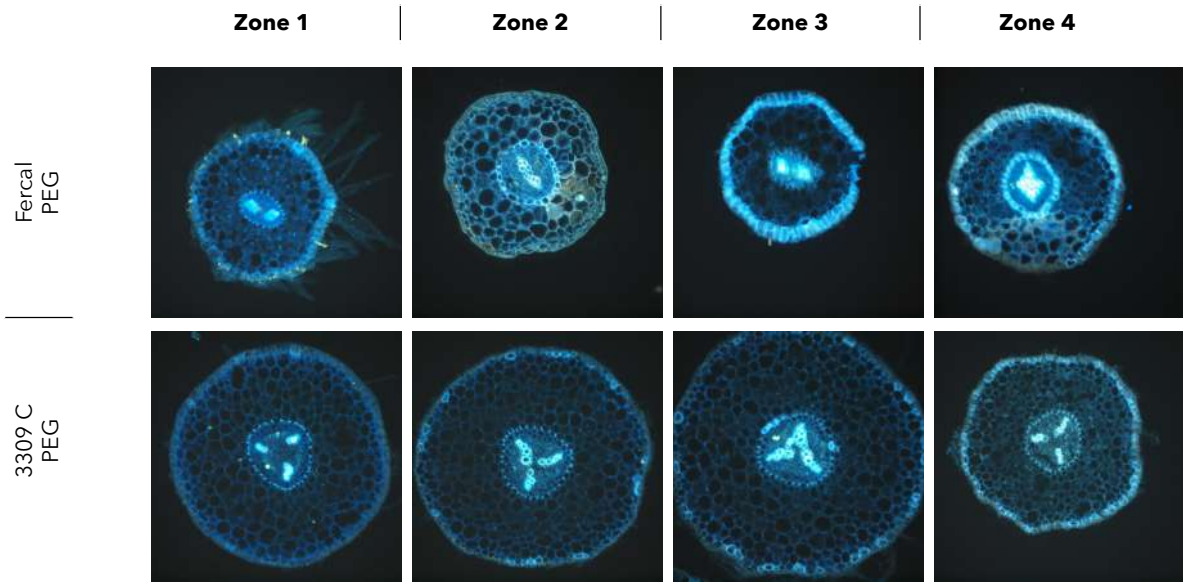

Figure 39 Micrographs of berberine-aniline stained cross sections of Fercal and 3309; a comparison of dermal tissue development for the PEG treatment. Magnification was set at 20 x

1.4.4 Fluorol yellow whole root staining and microscope scanning for Fercal

To improve pattern recognition, it might be advisable to refer to excerpt scans; however, the experiment schedule only allowed one preparation of one whole root each for the Fercal batch (Figure 40), which here is to be understood to be representative and preparatory for intended follow-up imaging approaches.

Nevertheless, a first impression, which admittedly would need multiple repetitions, appears to reveal different gradients of exodermal suberization as indicated by color intensity. While C remains with a clear and typical increase along the maturation axis, NOFE, NOFEPEG and PEG seem to express more bright yellow in earlier stages. The poor colorization for zones 3 and 4 in NOFE and NOFEPEG may be due to sample positioning.

In general, these observations coincide with those made in the berberine-aniline approach, but actually a delayed, i.e. shifted suberization should be observable especially in NOFE (Odgen et al. 2018). To some extent, this may be recognizable if compared with NOFEPEG and PEG, but not with reference to C.

However, the outcomes here are provisional and mainly serve to present possible options to be optimized in consequence experiments.

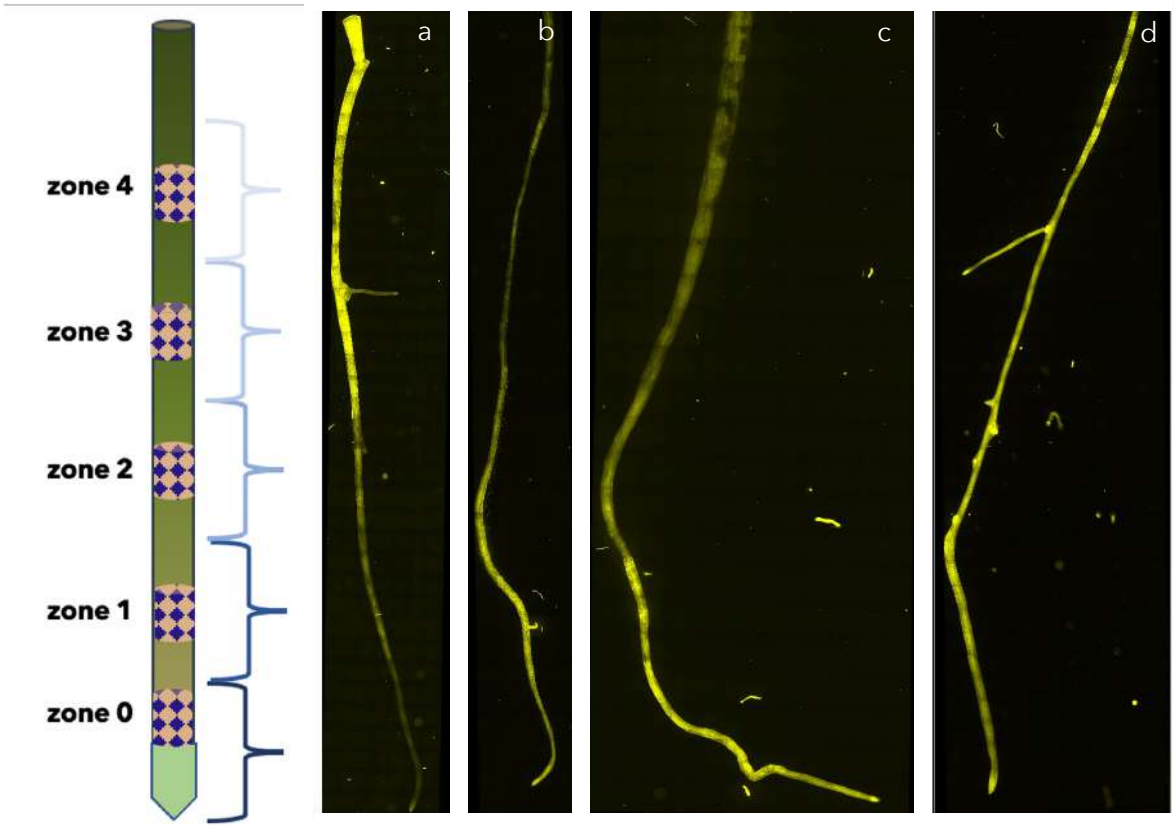

Figure 40 Micrographs of fluorol yellow stained Fercal whole roots ; a = C, b= NOFE, c = NOFEPEG, d = PEG. The intensity of yellow color approximates the respective suberization gradients. The samples appear in an approximate scale of 2,5:1.

1.4.5 Rhizobox approach – first findings: shoot length and shoot weight

As mentioned previously, only 3309 C could be used for the rhizobox approach. Interestingly, for a considerable time, the plants did not show any drought symptoms or non-physiological, i.e. phenotypic evidence of iron deficiency. This may have been due to the applied stress level, but also due to the possible presence of Fe in the organic material of the potting soil declared 0-nutrient by the supplier.

However, 3309 C often appears to be physically unimpressed by various strains for extended time periods to then degenerate instantly (Kahlil 2021, personal communications).

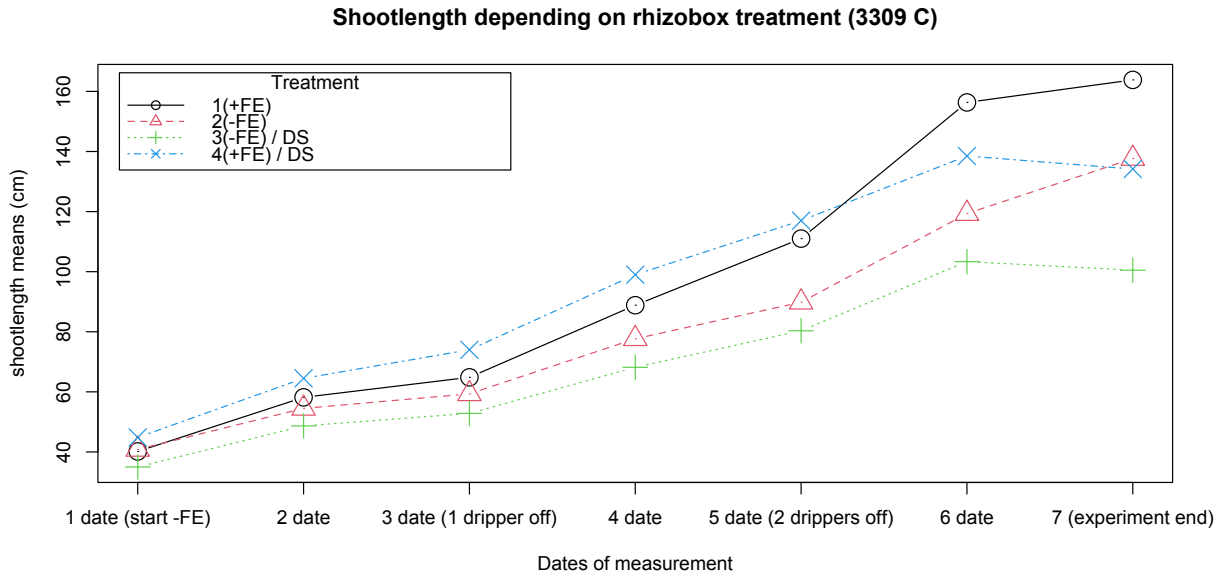

Figure 41 Development of 3309 C shoots in dependence on treatment and measurement dates. The consecutive dates are 12.07, 20.07, 23.07, 30.07, 03.08, 12.08 and 17.08 so that the whole period comprises 36 days.

With regard to the shoot length development, it becomes obvious, that the control is always somewhat ahead of the iron deficient plants and the iron supplied samples are only about to decrease when drought as a second strain is effectuated. The iron lacking samples seem to generally exhibit a restrained growth and appear to differ when one sample group starts to endure drought. In any case, and especially from the fourth date onwards, a pattern is likely to emerge. A first impression of the LiCor date, which had only been pre-assessed so far, would appear to be able to confirm this development, although here the stress trends seemed to emerge from an earlier stage (Kahlil 2021, personal communications).

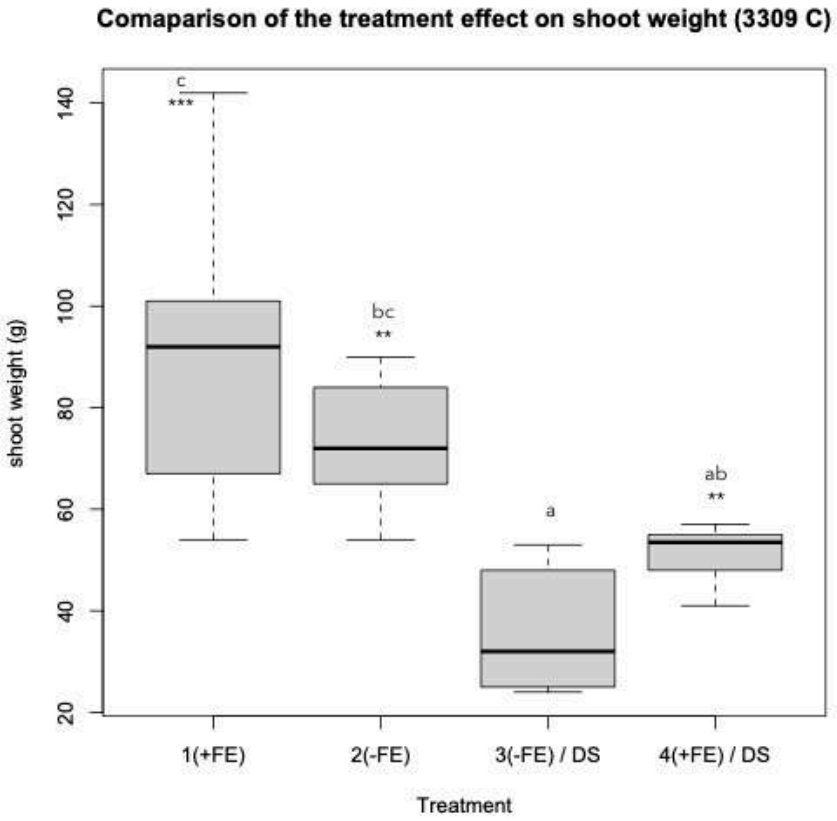

*Figure 42 Boxplot chart displaying the different shoot weight ratios of 3309 C after being treated with either iron abstraction (2) or drought and iron abstraction (3) or only drought (4). The whiskers indicate variance. According to the p-values being < 0.05 ("**" = 0.01, "***" = 0.001) and comparing the corresponding means, 1 (91.33 sd ± 30.51), 2 (72.83 sd ± 13.32), 3 (35.66 sd ± 12.48) and 4 (51.33 sd ± 5.95) do significantly differ as indicated by different letters. The null hypothesis (H_0) therefore can be rejected and it can be said, that there is difference.*

With a view to shoot fresh weights (Figure 42), which were taken on dissection day, the significance of treatment effects on aerial part performance is confirmed. However, previously made observations are re-confirmed here as well.

That is, the most significant decompensations are challenge by drought and by the combined stress, while iron deficiency has been counteracted relatively well for a considerable time. In the present case, however, the altered dimensions as well as the altered substrate, should also be taken into account, since they influence the overall performance.

1.4.6 – Rhizobox approach – first findings: RSA

With regard to homeostasis and an efficiently balanced material input, a high number of roots seem to be beneficial for the acquisition of immobile soil resources like organic nitrogen, phosphorous, copper (unchelated) or iron (unchelated). In contrast, a high number of roots seem not to be supportive to acquire mobile nutrients like nitrate nitrogen or sulfate sulphur and boron. For everything in between (e.g. calcium, potassium, magnesium), as well as for reasonable stress resistance, compromises must be made (Schubert 2018, Lynch 2019, Freschet et al. 2020).

Even if figures 43 and 44 can only serve as an exemplary selection and as substantiation for the concept projection, the approach taken and the results (root pattern images and RSA characteristics), should already be comprehensible. Admittedly, the patterning of the samples my not seem to exactly correspond to the schematic idea of root behavior as previously indicated. Yet this is a desirable result

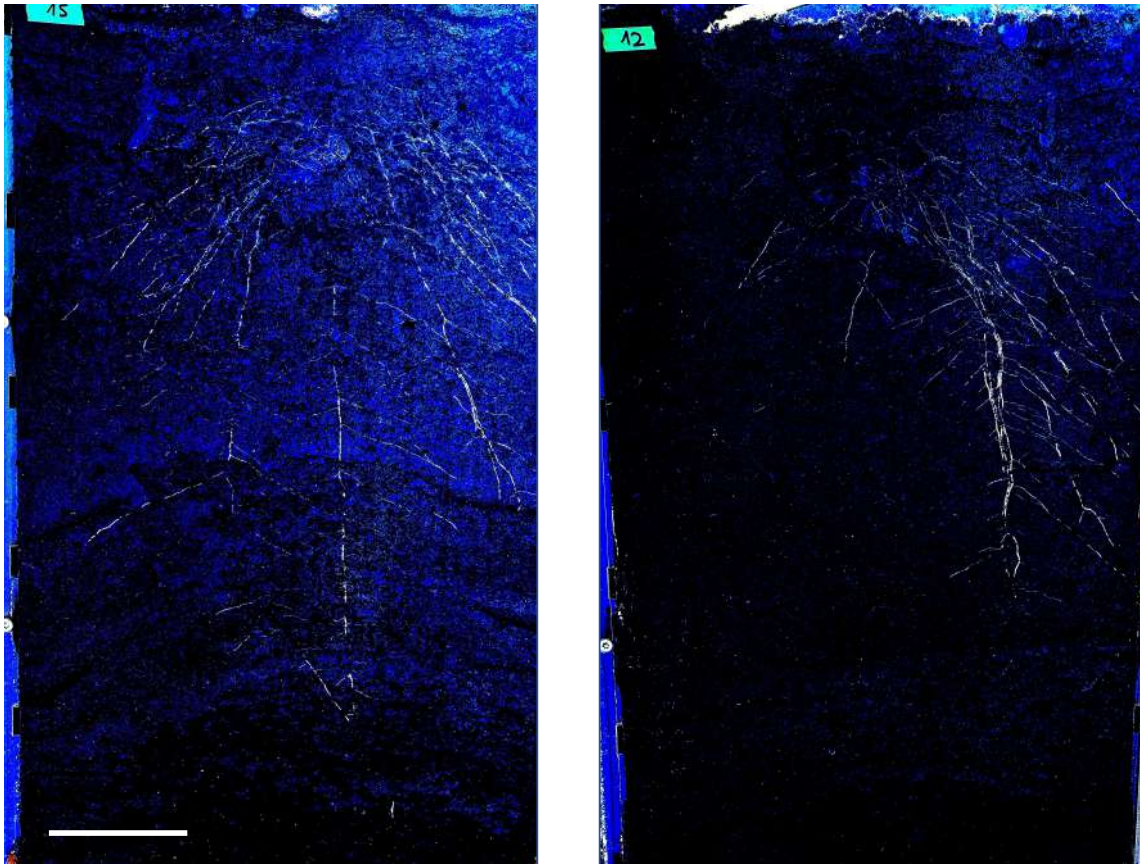

Figure 43 Rhizobox images comparing RSA (root system architecture) +Fe (15) and -Fe (12). Scale bar = 10 cm.

since it is obvious that plants interpret concepts flexibly and according to individual circumstances and intraspecific variance (Freschet et al. 2020).

However, the non-stressed and fully supplied sample 15 (Figure 43), seems to be well and orderly

distributed by following the rootstock specific pattern of numerous and relatively wide angled roots in the top layer, while one to two roots seem to gouge for water resources in deeper soil layers.

Although many roots are supportive in case of iron acquisition, sample 12 (Figure 43) seem to concentrate its root biomass in a specific region, possibly to explore prevailing nutrient patches. So, in this case, this particular RSA would tend to contradict what the in vitro performance seemed to reflect. In fact, however, the glasshouse circumstances are even more multifactorial than that provided by the laboratory conditions.

Sample 17 (Figure 44) again seems to be widely branched and significant material savings are not apparent despite the drought application; the roots of sample 20 (Figure 44) in turn, seem to clearly

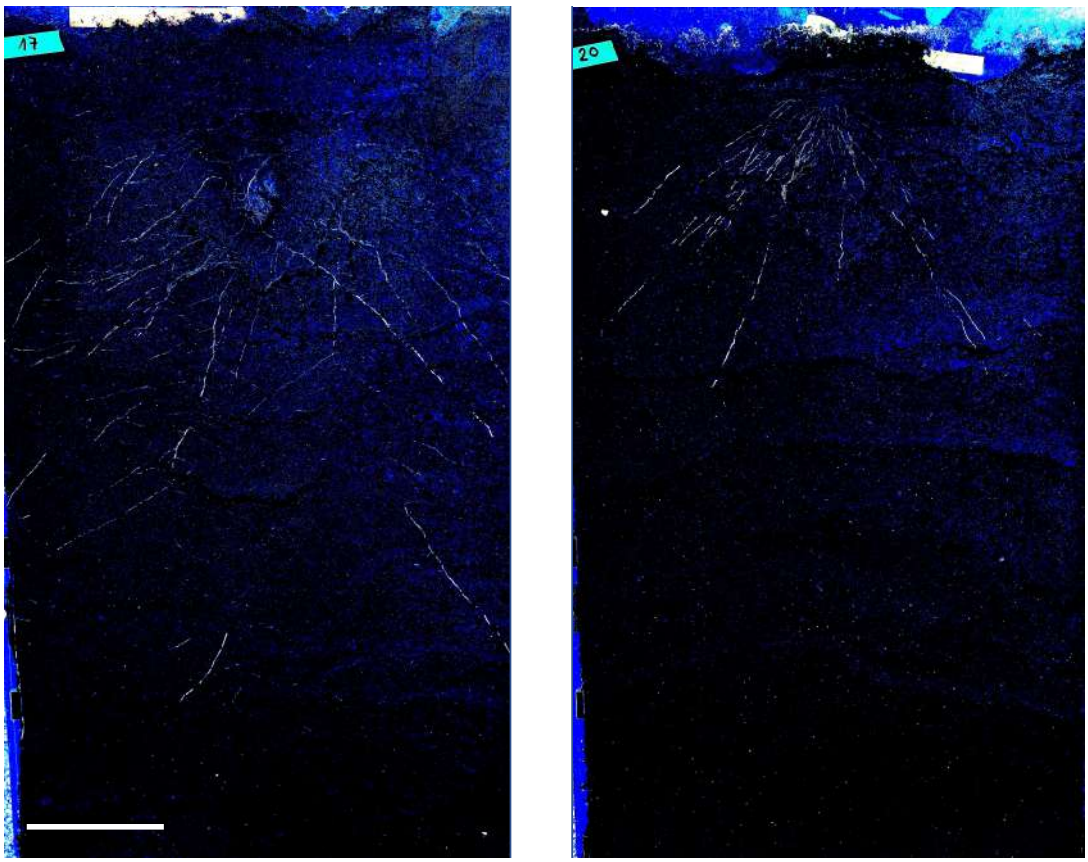

Figure 44 Rhizobox images comparing RSA (root system architecture) +Fe/DS (17) and -Fe/DS (20). Scale bar = 10 cm.

display growth reduction in consequence of the combined stress. Further considering the assumption, that the first drought stress application was too moderate for the rhizobox approach, a preliminary overall finding could therefore be that the stimulus intensity has tremendous influence on the outcome and that between gradual deviation and reliably repeatable significance much room for plant individuality remains.

V. Conclusion

With reference to the bipartite quality of the present work, that is both based on the establishment of methods and on basic research, many findings, especially in the results section, are rather obser-

vations and step-stones and do not claim to be free of doubt. Furthermore, they can only be regarded as results of the given experimental environment and reflect some correlations proven elsewhere only conditionally or as a tendency.

Although some performance markers are found in the in vitro approach, they do not seem to apply consistently in the rhizobox for 3309 C. This is the case, for example, with the intensified growth rates in the NOFE-medium, which seems to be restricted in the potting soil. However, the responses to the combined stress in the soil substrate are again similar to those of the Petri dishes. If this could also be confirmed for Fercal in the future, a kind of accelerated massal selection in the direction of combined stressors would probably become possible. 3309 C, on the other hand, can be expected to remain unsuitable for alkaline and dry soils.

However, the efforts expended on the method establishment were successful and simultaneously offer sufficient potential for future improvements (Figure 45). Firstly, differing root system architecture adjustments could be made observable and assessable for the rootstocks Fercal and 3309 C and secondly, analyzable gradient formations were visualized for endomorphological lignification and suberization tendencies of fine root dermal tissues in response to lime and drought exposure.

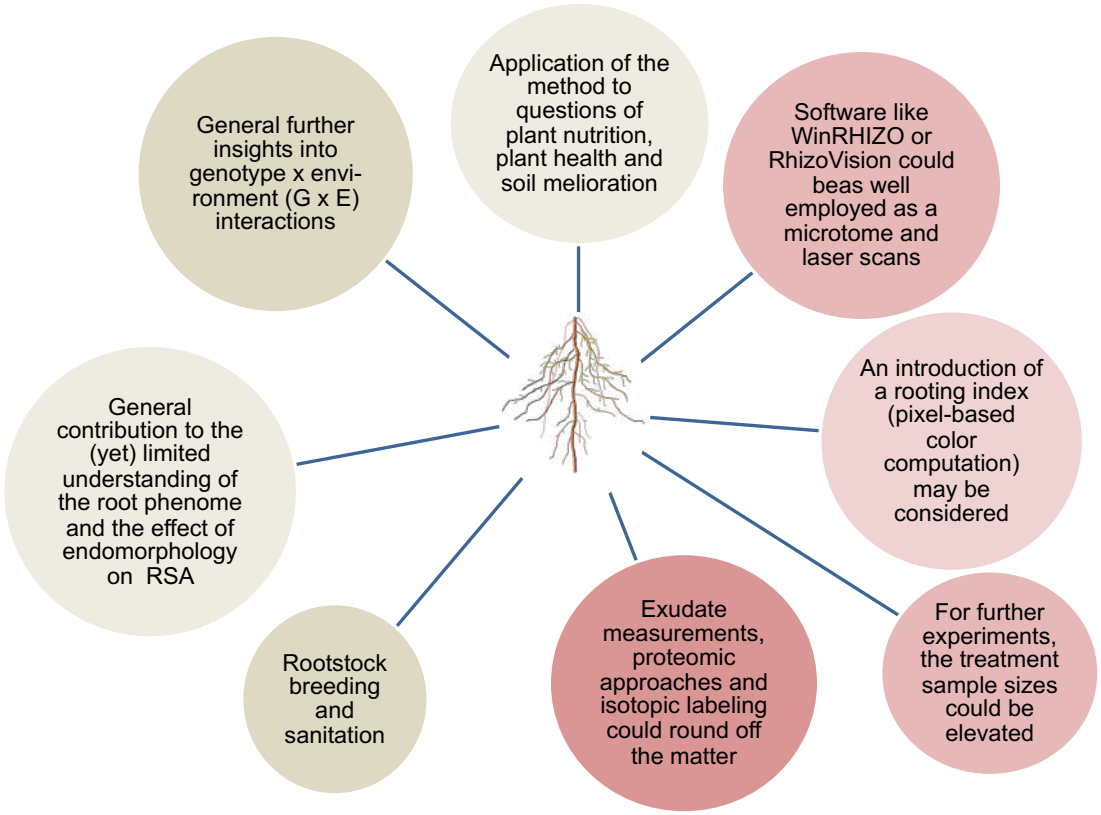

Figure 45 Summary graph illustrating potential benefits (green) of the methods and opportunities for improvement in data collection (red).

For the individual treatments, significant differences in root pattern distribution and length parameters were found. By omitting the true counts of main roots for not being a start variable, the individual rootstocks show a clear tendency towards an overall good NOFE-stress management, although the strategies between Fercal and 3309 C seem to diverge. Fercal is rather efficient in terms of distribution

of growth material and therefore seems to be more efficient per unit root surface. Considering the fact that this rather requires exudation (i.e. pH lowering H^+) which is usually done via the rhizosphere tradespace, i.e. by increasing the area of the root hair zone, this seems to be the problem response, at least for Fercal, since in general less total root mass was formed in NOFE, yet with higher efficiency proportions than for 3309 C. Moreover and despite general root strategies (Tsai and Schmidt 2017), Fercal does not tend to increase lateral density under NOFE, which again may stabilize the assumption of an increased lateral root efficiency in cooperation with elongation zone apoplast and stem-cell storage of Fe in young main roots.

Thus, particularly lateral roots should possibly be assessed more intensively, as it might be likely, that while the main roots may lignify and suberize according to the assumptions, the laterals keep contributing to homeostasis via altered strategy adaptations. This would generally indicate that the laterals have a key role in homeostasis insurance; the more so, as in principle, Fe does not have to be foraged as much as mobilized.

Although complete laminations are obviously disadvantageous for this purpose, especially for the combined stress NOFEPEG and PEG alone, a systematic lignification and suberization can be observed from the elongation upwards and incrementally in the gradation NOFE, NOFEPEG, PEG, which in turn speaks for an interference of the responses to stressors NOFEPEG and PEG, since the strategies counteract each other here.

Obvious is also the basic tendency of both rootstocks to react with almost circular suberin lamellation of both dermal tissues (endodermis and exodermis) on NOFEPEG and PEG rather than with complete lignification of the anticlinal endodermis cell walls. This is appropriate as Casparian strips in the endodermis tend rather to be a partial-adjustment lock of water uptake and a regulative against the wash-in of disadvantageous substances via apoplast, while suberization rather tends to be an undirected stress response. Nevertheless, Fercal performed more stress mitigative than 3309 C in the given experimental setup, probably because less energy was used for biomass production and more energy was used for intrinsic control mechanisms (e.g. aquaporins, upregulation of exudation rates).

As an additional note, it should be remembered that a high lime content is not elevated pH is not iron deficiency, just as draught is not pore or grain size is not an osmotically active polymer; and thus the response patterns will display additional reciprocities and interference cascades as the nature or field similarity of the experimental environment increases.

Summarizing this, the first major outcome would be, that treatment effects are observable and significant. The second major outcome can be considered to be, that rootstock effects are not negligible for total phene performance and significant for lateral root parameters. As a third major outcome, the descriptive statistics suggests, that there are rootstock and treatment specific lignification and suberization dynamics. Finally, this leads to the synoptic outcome, that there are tendency performances, but there are also large inter- and intra-genotypic variances. This variance, however, may also be considered as a finding, which could already be read as a good result in the sense of a performance for reflecting the complexity of the genotype x envirotype dynamics.

In this context and in order to collect more, and more precise bio data for root behavior and to make them reciprocally scalable to both in vitro grown plantlings and rhizobox grown plants, an introduction

of a rooting index may be considered, which would possibly make different experimental approaches better comparable. A such index could take into account the percentages of lignin and suberin, which could be determined for example by a pixel-based color computation of accordingly stained cross sections. In this regard, however, the high-throughput method of direct stained freehand cuts would have to become more routine and the results more definite.

Nevertheless, also the rhizobox approach should be improved to scannable window-sides, so that software like WinRHIZO or RhizoVision could be employed, which would also be valuable for the in vitro approach. Especially in the endeavor to translate smaller scales into larger ones or to match habitat or substrate realities with each other in order to be able to observe and predict statements and trends more flexibly in agricultural science, the intra-genotypic variance and the individual problem-solving strategies of the plants remain challenging and appealing.

In this view, the method established here can be applied to numerous questions in the field of phenotyping, breeding and rhizosphere-organized physiology. The interlocking of the different levels and the interweaving of existing techniques paved the way for a novel approach.

References:

Abisado, R. G., Benomar, S., Klaus, J. R., Dandekar, A. A., & Chandler, J. R. (2018). Bacterial quorum sensing and microbial community interactions. *mBio, 9*(3), pp. 1-14.

Acevedo, M. F., Harvey, D. R., & Palis, F. G. (2018). Food security and the environment: Interdisciplinary research to increase productivity while exercising environmental conservation. *Global Food Security, 16*, pp. 127-132.

Amrhein, V., Greenland, S., & McShane, B. (2019). Scientists rise up against statistical significance. *Nature, 567*, pp. 305-307.

Anderson, M. C., Kustas, W. P., & Norman, J. M. (2003). Upscaling and downscaling - a regional view of the soil-plant-atmosphere continuum. *Agronomy Journal, 95*, pp. 1408-1423.

Annunziata, M. G., Apelt, F., Carillo, P., Krause, U., Feil, R., Mengin, V., . . . Lunn, J. E. (2017). Getting back to nature: a reality check for experiments in controlled environments. *Journal of Experimental Botany, 68*(16), pp. 4463-4477.

Archer, E., & Saayman, D. (2018). *Vine Roots.* Stellenbosch: IGWS, Institute for Grape and Wine Science.

Arnold, C., & Schnitzler, A. (2020). Ecology and genetics of natural populations of North American vitis species used as rootstocks in European grapevine breeding programs. *Frontiers in Plant Science, 11*, pp. 1-14.

Augstein, F., & Carlsbecker, A. (2018). Getting to the roots: a developmental genetic view of root anatomy and function from Arabidopsis to Lycophytes. *Frontiers in Plant Science, 9*, pp. 1-15.

Bünemann, E. K., Bongiorno, G., Bai, Z., Creamer, R., De Deyn, G., de Goede, R., . . . Brussaard, L. (2018). Soil quality - a critical review. *Soil Biology and Biochemistry, 120*, pp. 105-125.

Babaeian, E., Sidike, P., Newcomb, M. S., Maimaitijiang, M., White, S., Demieville, J., . . . Tuller, M. (2019). A new optical remote sensing technique for gigh-resolution mapping of soil moisture. *Frontiers in Big Data, 2*, pp. 1-6.

Baldacci-Cresp, F., Spriet, C., Twyffels, L., Blercacq, A.-S., Neutelings, G., Baucher, M., & Hawkins, S. (2020). A rapid and quantitative safranin-based fluorescent microscopy method to evaluate cell wall lignification. *The Plant Journal, 102*(5), pp. 1074-1089.

Barberon, M., & Geldner, N. (2014). Radial transport of nutrients: the plant root as a polarized epithelium. *Plant Physiology, 166*, pp. 528-537.

Barberon, M., Vermeer, J. E., De Bellis, D., Wang, P., Naseer, S., Anderson, T. G., . . . Geldner, N. (2016). Adaptation of root function by nutrient-induced plasticity of endodermal differentiation. *Cell, 164*, pp. 447–459.

Barrios-Masias, F. H., Knipfer, T., & McElrone, A. J. (2015). Differential responses of grapevine rootstocks to water stress are associated with adjustments in fine root hydraulic physiology and suberization. *Journal of Experimental Botany, 66*(19), pp. 6069-6078.

Baskin, T. I., Preston, S., Zelinsky, E., Yang, X., Elmali, M., Bellos, D., . . . Bennett, M. J. (2020). Positioning the root elongation zone is saltatory and receives input from the shoot. *iScience*, pp. 1-47.

Bast, L., Warncke, D., & Christenson, D. (2011). *Facts about soil acidity and lime. Questions and answers. Extension Bulletin E-1566.* Michigan State University, Department of Crop and Soil Sciences.

Beach, T., Ulmer, A., Cook, D., Brennan, M. L., Luzzader-Beach, S., Doyle, C., . . . Terry, R. (2018). Geoarchaeology and tropical forest soil catenas of northwestern Belize. *Quaternary International, 463*, pp. 198-217.

Beck, C. B. (2010). *An Introduction to Structure and Development, Plant Anatomy for the Twenty-First Century, 2nd ed.* Cambridge, MA: Cambridge University Press.

Beemster, G., Fiorani, F., & Inze, D. (2003). Cell cycle: the key to plant growth control? *Trends in Plant Science, 8*, pp. 154-158.

Bending, G. (2003). Root Development. The Rhizosphere and its Microorganisms. In B. Thomas, *Encyclopedia of Applied Plant Sciences* (pp. 1123-1129). Cambridge, MA: Academic Press.

Benfey, P. N., & Scheres, B. (2000). Root development. *Current Biology, 10*(22), pp. 813-815.

Bengough, G. A., Loades, K., & McKenzie, B. M. (2016). Root hairs aid soil penetration by anchoring the root surface to pore walls. *Journal of Experimental Botany, 67*(5), pp. 1071-1078.

Bengough, G. A., McKenzie, B., Hallet, P., & Valentine, T. (2011). Root elongation, water stress, and mechanical impedance: a review of limiting stresses and beneficial root tip traits. *Journal of Experimental Botany, 62*(1), pp. 59-68.

Berlanas, C., Berbegal, M., Elena, G., Laidani, M., Cibriain, J. F., Sagües, A., & Gramaje, D. (2019). The fungal and bacterial rhizosphere microbiome associated with grapevine rootstock genotypes in mature and young vineyards. *Frontiers in Microbiology, 10*(Article 1142), pp. 1-16.

Bernardo, S., Dinis, L.-T., Machado, N., & Moutinho-Pereira, J. (2018). Grapevine abiotic stress assessment and search for sustainable adaptation strategies in Mediterranean-like climates. A review. *Agronomy for Sustainable Development, 38*(66), pp. 1-20.

Bernards, M. A. (2002). Demystifying suberin. *Canadian Journal of Botany, 80*, pp. 227-240.

Bert, P.-F., Bordenave, L., Donnart, M., Hévin, C., Ollat, N., & Decroocq, S. (2013). Mapping genetic loci for tolerance to lime-induced iron deficiency chlorosis in grapevine rootstocks (Vitis sp.). *Theoretical and Applied Genetics, 126*(2), pp. 451-473.

Blanca, M. J., Alarcón, R., Arnau, J., Bono, R., & Bendayan, R. (2017). Non-normal data: Is ANOVA still a valid option? *Psicothema, 29*(4), pp. 552-557.

Blum, A. (2016). Stress, strain, signaling, and adaptation - not just a matter of definition. *Journal of Experimental Botany, 67*, pp. 115-155.

Blum, J., Fávero, C. E., Ayub, R. A., & Da Fonseca, A. F. (n.d.). Soil chemical attributes and grape yield as affected by gypsum application in southern Brazil. *Communications in Soil Science and Plant Analysis, 42*, pp. 1434-1446.

Bonan, G., Williams, M., Fisher, R., & Oleson, K. (2014). Modeling stomatal conductance in the earth system: linking leaf water-use efficiency and water transport along the soil–plant–atmosphere continuum. *Geoscientific Model Development, 7*, pp. 2193-2222.

Bonfante, A., A., B., Langella, G., Manna, P., & Terribile, F. (2011). A physically oriented approach to analysis and mapping of terroirs. *Geoderma, 167-168*, pp. 103-117.

Boussinesq, J. (1885). *Application des Potentiels à l'Étude de l'Équilibre et du Mouvement des Solides élastiques.* Paris: Gauthier-Villars.

Brevik, E., Cerdà, A., Mataix-Solera, J., Pereg, L., Quinton, J., Six, J., & Van Oost, K. (2015). The interdisciplinary nature of SOIL. *Soil, 1*, pp. 117-129.

Brillante, L., Bois, B., Lévêque, J., & Mathieu, O. (2016). Variations in soil-water use by grapevine according to plant waterstatus and soil physical-chemical characteristics - a 3D spatio-temporal analys. *European Journal of Agronomy, 77*, pp. 122-135.

Brillante, L., Bonfante, A., Bramley, R. G., Tardaguila, J., & Priori, S. (2020). Unbiased scientific approaches to the study of terroir are needed. *Frontiers in Earth science, 8*, pp. 1-4.

Brundrett, M. C., Enstone, D. E., & Peterson, C. A. (1988). A berberine-aniline blue fluorescent staining procedure for suberin, lignin, and callose in plant tissue. *Protoplasma, 146*, pp. 133-142.

Brundrett, M. C., Knedrick, B., & Peterson, C. A. (1991). Efficient lipid staining in plant material with Sudan red 7B or fluorol yellow 088 in polyethylene glycol-glycerol. *Biotechnic and Histochemistry, 66*(3), pp. 111-116.

Brunori, E., Farina, R., & Biasi, R. (2016). Sustainable viticulture: the carbon-sink function of the vineyard agro-ecosystem. *Agriculture, Ecosystems and Environment, 223*, pp. 10-21.

Brussard, L. (2012). Ecosystem services provided by the soil biota. In D. Wall, R. Bardgett, V. Behan-Pelletier, J. Herrick, H. Jones, K. Ritz, . . . W. van der Putten, *Soil Ecology and Ecosystem Services* (pp. 45-58). Oxford, U.K.: Oxford University Press.

Cailloux, M. (1972). Metabolism and the absorption of water by root hairs. *Canadian Journal of Botany, 50*, pp. 557-573.

Calvo, P., Gagliano, M., Souza, G. M., & Trewavas, A. (2020). Plants are intelligent, here's how. *Anals of Botany, 125*(1), pp. 11-28.

Calvo-Garzón, P., & Keijzer, F. (2011). Plants: adaptive behavior, root-brains, and minimal cognition. *Adaptive Behavior, 19*(3), pp. 155-171.

Canarini, A., Kaiser, C., Merchant, A., Richter, A., & Wanek, W. (2019). Root exudation of primary metabolites: mechanisms and their roles in plant responses to environmental stimuli. *Frontiers in Plant Science, 10(157)*, pp. 1-19.

Chaves, M. M., Zarrouk, O., Francisco, R., Costa, J. M., Santos, T., Regalado, A., . . . Lopes, C. (2010). Grapevine under deficit irrigation: hints from physiological and molecular data. *Anals of Botany, 105*(5), pp. 661–676.

Chen, T., Cai, X., Wu, X., Karahara, I., Schreiber, L., & Lin, J. (2011). Casparian strip development and its potential function in salt tolerance. *Plant Signaling & Behavior, 6*(10), pp. 1499-1502.

Chen, Y., & Barak, P. (1982). Iron nutrition of plkanbts in calcarous soils. *Advances in Agronomy, 35*, pp. 217-240.

Chevalier, C., Nafati, M., Mathieu-Rivet, E., Bourdon, M., Frangne, N., Cheniclet, C., . . . Hernould, M. (2011). Elucidating the functional role of endoreduplication in tomato fruit development. *Anals of Botany, 107*, pp. 1159-1169.

Cochetel, N., Ghan, R., Toups, H. S., Degu, A., Tillett, R. L., Schlauch, K. A., & Cramer, G. R. (2020). Drought tolerance of the grapevine, Vitis champinii cv. Ramsey, is associated with higher photosynthesis and greater transcriptomic responsiveness of abscisic acid biosynthesis and signaling. *BMC Plant Biology, 20*(55), pp. 1-25.

Cohen, H., Fedyuk, V., Wang, C., Wu, S., & Aharoni, A. (2020). SUBERMAN regulates developmental suberization of the Arabidopsis root endodermis. *The Plant Journal, 102*, pp. 431-477.

Comas, L. H., Becker, S. R., Cruz, V. M., Byrne, P. F., & Dierig, D. A. (2013). Root traits contributing to plant productivity under drought. *Frontiers in Plant Science, 4*, pp. 1-16.

Connorton, J. M., Balk, J., & Rodriguez-Celma, J. (2017). Iron homeostasis in plants – a brief overview. *Metallomics, 9*, pp. 813-823.

Contin, M. (2020). *Fertilization and legal regulation. 'Salinity of soils'; 'Acid and alkaline soils'. Scripts to lecture*. Montpellier: University of Udine; Montpellier SupAgro.

Cookson, S., Clemente Moreno, M., Hevin, C., Nyamba Mendome, L., Delrot, S., Trossat-Magnin, C., & Ollat, N. (2013). Graft union formationin grapevine induces transcriptional changes related to cell wall modification, wounding, hormone signalling, and secondary metabolism. *Journal of Experimental Botany, 64*(10), pp. 2997-3008.

Correa, J., Postma, J. A., Watt, M., & Wojciechowski, T. (2019). Soil compaction and the architectural plasticity of root systems. *Journal of Experimental Botany, 70*(21), pp. 6019-6034.

Costa, J. M., Oliveira, M., Egipto, R. J., Cid, J. F., Fragoso, R. A., Lopes, C. M., & Duarte, E. N. (2020). Water and wastewater management for sustainable viticulture and oenology in south Portugal - a review. *Ciência e Técnica Vitivinícola, 35*(1), pp. 1-15.

Cousins, P. (2005). A review of the potential climate change impacts and adaptation options for European viticulture. In P. Cousins, & R. Striegler (Ed.), *Grapevine rootstocks: current use, research, and application. Proceedings of the 2005 rootstock symposium; 5 February 2005*, (pp. 1-7). Osage Beach, MO, USA.

Cousins, P. (2011). *Three root-knot nematode resistant rootstocks released by USDA agricultural reserach service*. SDA ARS Grape Genetics Research Unit, Geneva, New York, Geneva, NY.

Cousins, P., & Striegler, K. R. (2005). Grapevine Rootstocks: Current Use, Research, and Application Proceedings of the 2005 Rootstock Symposium. (pp. 1-117). Osage Beach, MO: Mid-America Viticulture and Enology Center Southwest Missouri State University Mountain Grove Campus.

Culman, S. W., Young-Mathews, A., Hollander, A. D., Ferris, H., Sánchez-Moreno, S., O'Geen, A. T., & Jackson, L. E. (2010). Biodiversity is associated with indicators of soil ecosystem functions

over a landscape gradient of agricultural intensification. *Landscape Ecology, 25*, pp. 1333-1348.

Düring, H. (2003). Stomatal and mesophyll conductances control CO2 transfer to chloroplasts in leaves of grapevine (Vitis vinifera L.). *Vitis-Geilweilerhof, 42*, pp. 65-68.

Daldoul, S., Boubakri, H., Gargouri, M., & Mliki, A. (2020). Recent advances in biotechnological studies on wild grapevines as valuable resistance sources for smart viticulture. *Molecular Biology Reports, 47*, pp. 3141-3153.

De Herralde, F., del Mar Alsina, M., Arrandxe, X., Save, R., & Biel, C. (2006). Effects of rootstock and irrigation regime on hydraulic architecture of Vitis vinifera L. cv. Tempranillo. *Journal International des Sciences de la Vigne et du Vin, 40*(3), pp. 133-139.

De Rybel, B., Mähönen, A. P., Helariutta, Y., & Weijers, D. (2016). Plant vascular development: from early specification to differentiation. *Nature Reviews Molecular Cell Biology, 17*, pp. 30-40.

De Smet, I., Vanneste, S., Inzé, D., & Beeckman, T. (2006). Lateral root initiation or the birth of a new meristem. *Plant Molecular Biology, 60*, pp. 871-887.

Degrully, L., & Ravaz, L. (1905). Sur la culture superficielle de la vigne. *Annales de l'Ecole Nationale d'Agriculture de Montpellier, 5*(1), pp. 64-87.

De-Jesús-García, R., Rosas, U., & Dubrovsky, J. G. (2020). The barrier function of plant roots: biological bases for selective uptake and avoidance of soil compounds. *Functional Plant Biology, 47*(5), pp. 383-397.

Deloire, A., & Pellegrino, A. (2020). *Grapevine water relations. Script to lectures.* Montpellier: Montpellier SupAgro.

Deng, Z., Guan, H., Hutson, J., Forster, M. A., Wang, Y., & Simmons, C. T. (2017). A vegetation-focused soil-plant-atmospheric continuum modelto study hydrodynamic soil-plant water relations. *Water Resources Research, 53*, pp. 4965-4983.

Diener, A. C., Gaxiola, R. A., & Fink, G. R. (2001). ArabidopsisALF5,a multidrug efflux transporter gene family member, confers resistanceto toxins. *Plant Cell, 13*, pp. 1625-1637.

Ding, L., Lu, Z., Gao, L., Guo, S., & Shen, Q. (2018). Is nitrogen a key determinant of water transport and photosynthesis in higher plants upon drought stress? *Frontiers in Plant Science, 9*, pp. 1-2.

Donaldson, L. (2020). Autofluorescence in plants. *Molecules, 25*(2393).

Du, Y., & Scheres, B. (2018). Lateral root formation and the multiple roles of auxin. *Journal of Experimental Botany, 69*(2), pp. 155-167.

Dumont, C., Cochetel, N., Lauvergeat, V., Cookson, S. J., Ollat, N., & Vivin, P. (2016). Screening root morphology in grafted grapevine using 2D digital images from rhizotrons. *Acta Horticulturae*, pp. 213-219.

Enstone, D., Peterson, C., & Ma, F. (2003). Root Endodermis and exodermis: structure, function, and responses to the environment. *Journal of Plant Growth Regulation, 21*(4), pp. 335-351.

Ephrath, J. E., Klein, T., Sharp, R. E., & Lazarovitch, N. (2020). Exposing the hidden half: root research at the forefrontof science. *Plant Soil, 447*, pp. 1-5.

Evaristo, J., Jasechko, S., & McDonell, J. J. (2015). Global separation of plant transpiration from groundwater and streamflow. *Nature, 525*, pp. 91-94.

Falk, K. G., Jubery, T. Z., Mirnezami, S. V., Parmley, K. A., Sarkar, S., Singh, A., . . . Singh, A. K. (2020). Computer vision and machine learning enabled soybean root phenotyping pipeline. *Plant Methods, 16*(5), pp. 1-19.

Fang, Y., & Xiong, L. (2015). General mechanisms of drought response and their application in drought resistance improvement in plants. *Cellular and Molecular Life Sciences, 72*(4), pp. 673-689.

FAO. (2017). *The future of food and agriculture. Trends and challenges.* Food and Agriculture Organization of the United Nations, Rome.

Ferguson, R. (2021). Losing ground: farmland consolidation and threats to new farmers, black farmers, and the future of farming. Cambridge, MA: Union of Concerned Scientists.

Ferreira, B. G., & Isaias, R. M. (2014). Efficiency of the polyethylene-gylycol (PEG) embedding medium for plant histochemistry. *Journal of Histochemistry & Cytochemistry, 62*(8), pp. 577-583.

Ferreira, B. G., Falcioni, R., Guedes, L. M., Avritzer, S. C., Antunes, W. C., Souza, L. A., & Isaias, R. M. (2017). Preventing false negatives for histochemical detection of phenolics and lignins in PEG-embedded plant tissues. *Journal of Histochemistry & Cytochemistry, 65*(2), pp. 105-116.

Fort, K., Fraga, J., Grossi, D., & Walker, M. A. (2017). Early measures of drought tolerance in four grape rootstocks. *Journal of the American Society for Horticultural Science, 142*(1), pp. 36-46.

Fraga, H., Malheiro, A., Moutinho-Pereira, J., & Santos, J. (2013). An overview of climate change impacts on European viticulture. *Food and Energy Security*, pp. 1-17.

Fraga, H., Santos, J., Malheiro, A., Oliveira, A., Moutinho-Pereira, J., & Jones, G. (2015). Climatic suitability of portuguese grapevine varieties and climate change adaption. *International Journal of Climatology*, pp. 1-12.

Fraga, H., Santos, J., Moutinho-Pereira, J., Carlos, C., Silvestre, J., Eiras-Dias, J., . . . Malheiro, A. (2016). Statistical modelling of grapevine phenology in Portuguese wineregions: observed trends and climate change projections. *Journal of Agricultural Science, 154*, pp. 795-811.

Freschet, G., Pagès, L., Iversen, C., Comas, L., Rewald, B., Roumet, C., . . . Postma, J. e. (2020). *A starting guide to root ecology: strengthening ecological concepts and standardizing root classification, sampling, processing and trait measurements.* hal-02918834: HAL archives ouvertures.

Freschet, G., Roumet, C., Comas, L., Weemstra, M., Bengough, A., Rewald, B., . . . Stokes, A. (2021). Root traits as drivers of plant and ecosystem functioning: current understanding, pitfalls and future research needs. *New Phytologist*, pp. 1-36.

Freschet, G., Valverde-Barrantes, O., Tucker, C., Craine, J., McCormack, M., Vioelle, C., . . . Kembel, S. (2017). Climate, soil and plant functional types as drivers of global fine-root trait variation. *Journal of Ecology, 105*(5), pp. 1182-1196.

Frioni, T., Biagioni, A., Squeri, C., Tombesi, S., Gatti, M., & Poni, S. (2020). Grafting cv. Grechetto Gentile vines to new M4 rootstock improves leaf gas exchange and water status as compared to commercial 1103P rootstock. *Agronomy, 10*, pp. 1-14.

Fuenzalida, T. I., Callum, B. J., Ovington, L. I., Yoon, H.-J., Oliveira, R. S., Sack, L., & Ball, M. C. (2019). Shoot surface water uptake enables leaf hydraulic recovery in Avicennia marina. *New Pyhtologyst, 224*, pp. 1504-1511.

Galet, P. (1988). *Cépages et vignobles de France.* Montpellier: Dehan.

Galler, J. (2013). *Kalk – Basis für Bodenfruchtbarkeit Einsatz in der Landwirtschaft.* Salzburg: Salzburg, Landwirtschaftskammer.

Gambetta, G. A., Fei, J., Rost, T. L., Knipfer, T., Matthews, M. A., A., S. K., . . . McElrone, A. J. (2013). Water uptake along the length of grapevine fine roots: developmental anatomy, tissue-specific aquaporin expression, and pathways of water transport. *Plant Physiology, 163*, pp. 1254-1265.

Gambetta, G. A., Herrera, J. C., Dayer, S., Feng, Q., Hochberg, U., & Castellarin, S. D. (2020). The physiology of drought stress in grapevine: towards an integrative definition of drought tolerance. *Journal of Experimental Botany, 71*(16), pp. 4658–4676.

Gambetta, G. A., Knipfer, T., Fricke, W., & McElrone, A. J. (2017). Aquaporins and root water uptake. In F. Chaumont, & S. Tyerman, *Plant Aquaporins, Signaling and Communication in Plants* (pp. 133-153). Cham: Springer International Publishing.

Gao, Y., Yu, G., & He, N. (2013). Equilibration of the terrestrial water, nitrogen, and carbon cycles: advocating a health threshold for carbon storage. *Ecological Engeneering, 57*, pp. 366-374.

Gautier, A. T., Cookson, S. J., Lagalle, L., Ollat, N., & Marguerit, E. (2020). Influence of the three main genetic, backgrounds of grapevine rootstocks on petiolar nutrient concentrations of the scion, with a focus on phosphorus. *OenoOne, 1*, pp. 1-13.

Gazengel, K., Aigu, Y., Lariagon, C., Humeau, M., Gravot, A., Manzanares-Dauleux, M. J., & Daval, S. (2021). Nitrogen supply and host-plant genotype modulate the transcriptomic profile of Plasmodiophora brassicae. *Frontiers in Microbiology, 12*, pp. 1-17.

Geng, S., Yan, D., Zhang, T., Weng, B., Zhang, Z., & Qin, T. (2015). Effects of drought stress on agricultural soil. *Natural Hazards*, pp. 1-15.

George, E., Horts, W., & Neumann, E. (2012). Adaption of plants to adverse chemical soil conditions. In P. Marschner, *Marschner's Mineral Nutrition of Higher Plants, 3rd Edition* (pp. 409-472). Academic Press.

Giehl, R. F., & von Wirén, N. (2014). Root nutrient foraging. *Plant Physiology, 166*, pp. 509-517.

Gilinsky Jr., A., K., N. S., & Vega, R. F. (2016). Sustainability in the global wine industry: concepts and cases. *Agriculture and Agricultural Science Procedia, 8*, pp. 37-49.

Ginsburg, S., & Jablonka, E. (2009). Epigenetic learning in non-neural organisms. *Journal of Biosience*, pp. 633-646.

Glass, G. V., Peckham, P. D., & Sanders, J. R. (1972). Consequences of failure to meet assumptions underlying the fixed effects analyses of variance and covariance. *Review of Educational Research, 42*(3), pp. 237-288.

Gorzalek, M. A., Asay, A. K., Pickles, B. J., & Simard, S. W. (2015). Inter-plant communication through mycorrhizal networks mediates complex adaptive behaviour in plant communities. *AoB Plants, 7*, pp. 1-13.

Graça, J. (2015). Suberin: the biopolyester at the frontier of plants. *Frontiers in Chemistry, 3*, pp. 1-11.

Grierson, C., Nielsen, E., Ketelaarc, Tijs, & Schiefelbein, J. (2014). Root hairs. In *Arabidopsis Book*.

Grunwald, S. (2006). What do we really know about the space–time continuum of soil-landscapes? In S. Grundwald, *Environmental Soil-Landscape Modeling. Geographic Information Technologies and Pedometrics* (pp. 4-31). Boca Raton, FL: CRC.

Guerinot, M. L., & Yi, Y. (1994). Iron: nutritious, noxious, and not readily available. *Plant Physiology, 104*, pp. 815-820.

Halpin, C. (2013). Cell biology: up against the wall. *Current Biology, 23*(23), pp. 1048-1050.

Hanson, R. L. (1991). Evapotranspiration and droughts. In R. Paulson, R. Roberts, & D. Moody, *National water summary 1988-89 hydrologic events and floods and droughts: U.S. geological survey water-supply paper 2375*. Washington, D.C.

Harwell, M. R., Rubinstein, E. N., Hayes, W. S., & Olds, C. C. (1992). Summarizing Monte Carlo results in methodological research: the one- and two-factor Ffxed effects ANOVA cases. *Journal of Educational and Behavioral Statistics, 17*(4), pp. 315-339.

Haseloff, J. (2003). Old botanical techniques for new microscopes. *BioTechniques, 34*(6), pp. 1174-1182.

Hatfield, J. L., & Dold, C. (2019). Water-use efficiency: advances and challenges in a changing climate. *Frontiers in Plant Science, 10*, pp. 1-14.

Heberlein, T. A. (1988). Improving interdisciplinary research: integrating the social and natural sciences. *Society and Natural Resources, 1*, pp. 5-16.

Heinitz, C., Fort, K. P., & Walker, A. M. (2015). Developing drougfht and salt resistant grape rootstocks. *Acta Horticulturae, 1082*, pp. 305-312.

Heslop-Harrison, J. (2017). Morphology, adaptation and speciation. *Annals of Botany, 120*(5), pp. 621-624.

Hinsinger, P., Bengough, G. A., Vetterlein, D., & Young, I. M. (2009). Rhizosphere: biophysics, biogeochemistry and ecological relevance. *Plant and Soil, 321*, pp. 117-152.

Hinsinger, P., Plassard, C., Tang, C., & Jaillard, B. (2003). Origins of root-mediated pH changes in the rhizosphere and their responses to environmental constraints: A review. *Plant and Soil, 248*, pp. 43-59.

Holbein, J., Franke, R. B., Marhavý, P., Fujita, S., Górecka, M., Sobczak, M., . . . Siddique, S. (2019). Root endodermal barrier system contributes to defence against plant-parasitic cyst and root-knot nematodes. *The Plant Journal, 100*, pp. 221-236.

Holland, J., Bennett, A. E., Newton, A. C., & White, P. J. (2017). Liming impacts on soils, crops and biodiversity in the UK: a review. *Science of the Total Environment*, pp. 316-332.

Holland, T. C., Reynolds, A. G., Bowen, P. A., Bogdanoff, C. P., Marciniak, M., Brown, R. B., & Hart, M. M. (2013). The response of soil biota to water availability in vineyards. *Pedobiologica, 56*, pp. 9-14.

Hoosbeek, M. R., & Bryant, R. B. (1994). Developing and adapting soil process submodels foruse in the pedodynamic orthod model. In M. R. Hoosbeek, & R. B. Bryant, *Quantitative Modeling of Soil Forming Processes. SSSA Special Publication 39* (pp. 111-128). Madison, WI: SSSA.

Hsieh, E.-J., & Waters, B. M. (2016). Alkaline stress and iron deficiency regulate iron uptake and riboflavin synthesis gene expression differently in root and leaf tissue: implications for iron deficiency chlorosis. *Journal of Experimental Botany, 67*(19), pp. 5671-5685.

Hugget, J. (2006). Geology and wine: a review. *Proceedings of the Geologists Association, 117*, pp. 239–247.

Hyashi, K., Hasegawa, J., & Matsunaga, S. (2013). The boundary of the meristematic andelongation zones in roots:endoreduplication precedes rapid cellexpansion. *Scientific Reports, 3*, pp. 1-8.

IFV. (2007). *Catalogue des variétés et clones de vigne cultivés en France*. Fonds documentaire du Centre de Ressources Biologiques de la Vigne de Vassal-Montpellier, INRAE - Montpellier SupAgro, Marseillan, France. , Le Grau-du-Roi, France.

Imerson, A., & Verstraten, J. (1984). The erodibility of highly calcareous soil material from southern Spain. *Catena, 12*(4), pp. 291-306.

Jackson, D., & Lombard, P. (1993). Environmental and management practices affecting grape composition and wine quaklity - a review. *American Journal of Enology and Viticulture, 44*, pp. 409-430.

Jeudy, C., A, M., Baussard, C., Bernard, C., Bernaud, E., Bourion, V., . . . Salon, C. (2016). RhizoTubes as a new tool for high throughput imaging of plant root development and architecture: test, comparison with pot grown plants and validation. *Plant Methods, 12*(31), pp. 1-18.

Jiménez-Nopala, G., Salgado-Escobar, A. E., Cevallos-Porta, D., Cárdenas, L., Sepúlveda-Jiménez, G., Cassab, G., & Porta, H. (2018). Autophagy mediates hydrotropic response in Arabidopsis thaliana roots. *Plant Science, 272*, p. 272.

Joshi, R., Wani, S. H., Singh, B., Bohra, A., Dar, Z. A., Lone, A. A., . . . Pareek-Singla, S. L. (2016). Transcription factors and plants response to drought stress: current understanding and future directions. *Frontiers in Plant Science, 7*, pp. 1-15.

Kahn, M. M., Akram, M. T., Khan Qadri, R. W., & Al-Yahyai, R. (2020). Role of grapevine rootstocks in mitigating environmental stresses: a review. *Journal of Agricultural and Marine Sciences, 25*(2), pp. 1-12.

Kamiya, T., Borghi, M., Wang, P., Danku, J. M., Kalmbach, L., Hosmani, P. S., . . . Salt, D. E. (2015). The MYB36 transcription factor orchestrates Casparian strip formation. *PNAS, 112*(33), pp. 10533-10538.

Karahara, I., Matsuda, K., & Honma, Y. (2008). Effects of ethylene on the production, elongation, and differentiation of endodermal cells in maize primary root: An integrative analysis of the developmental process of a particular cell type. *Plant Root, 2*, pp. 20-37.

Keller, M. (2015). *The Science of Grapevines. Anatomy and Physiology*. Cambridge: Elsevier - Academic Press.

Kibblewhite, M., Jones, R., Montanrella, L., Baritz, R., Huber, S., Arrouayas, D., . . . Stephens, M. (2008a). *Environmental assesementof soil for monitoring volume VI: soil monitoring system for Europe*. Office for the Official Publications of the European Communities, Luxembourg.

Kibblewhite, M., Ritz, K., & Swift, M. (2008b). Soil health in agricultural systems. *Philosophical Transactions of the Royal Society B, 363*, pp. 685-701.

Kitin, P., Nakaba, S., Hunt, C. G., Lim, S., & Funada, R. (2020). Direct fluorescence imaging of lignocellulosic and suberized cell walls in roots and stems. *AoB Plants, 12*(4), pp. 1-19.

Koch, B., & Oehl, F. (2018). Climate change favors grapevine production in temperate zones. *Agricultural Sciences, 9*(3), pp. 247-263.

Koscis, L., Varga, Z., & Pernesz, G. (2009). Introduction of a lime and drought tolerant rootstock variety. *Acta Horticulturae, 827*, pp. 465-470.

Kozlowski, T. T. (1964). *Water metabolism in plants*. New York: Harper and Row, Biological Monographs.

Kreszies, T., Shellakkutti, N., Osthoff, A., Yu, P., Baldauf, J. A., Zeisler-Diehl, V. V., . . . Schreiber, L. (2019). Osmotic stress enhances suberization of apoplastic barriers in barley seminal roots: analysis of chemical, transcriptomic and physiological responses. *New Phytologist, 221*, pp. 180-194.

Kreszies, V. (2019). *ABA-dependent and -independent regulation of tocopherol (vitamin E) biosynthesis in response to abiotic stress in arabidopsis. Dissertation zur Erlangung des Doktorgrades (Dr. rer. nat.)*. Bonn: Mathematisch-Naturwissenschaftliche Fakultät der Rheinischen Friedrich-Wilhelms-Universität Bonn .

Kroh, G. E., & Pilon, M. (2020). Regulation of iron homeostasis and use in chloroplasts. *Internmational Journal of Molecular Sciences, 21*, pp. 1-30.

Krohling, C. A., Eutrópio, F. J., Bertolazi, A. A., Dobbss, L. B., Campostrini, E., Dias, T., & Ramos, A. C. (2015). Ecophysiology of iron homeostasis in plants. *Soil Science and Plant Nutrition, 62*(1), pp. 39-47.

Kumpf, R. P., & Nowack, M. K. (2015). The root cap: a short story of life and death. *Journal of Experimental Botany, 66*(19), pp. 5651-5662.

Kuzyakov, Y., & Zamanian, K. (2019). Reviews and syntheses: Agropedogenesis – humankind as the sixthsoil-forming factor and attractors of agricultural soil degradation. *Biogeosciences, 16*, pp. 4783-4803.

Läuchli, A., & Grattan, S. (2012). Soil pH extremes. In S. Shabala, *Plant Stress Physiology* (pp. 194-209). Wallingford: CAB International.

Lakso, A. N., & Eissenstat. (2012). *Fifteen years of vine root growth studies in Concords*. Cornell University , Department of Horticulture, NYS Agricultural Experiment Station, Geneva, NY.

Larkins, B. A., Dilkes, B. P., Dante, R. A., Coelho, C. M., Woo, Y.-m., & Liu, Y. (2001). Investigating the hows and whys of DNA endoreduplication. *Journal of Experimental Botany, 52*(355), pp. 183-192.

Lazcano, C., Decock, C., & Wilson, S. G. (2020). Defining and managing for healthy vineyard soils, intersections with the concept of terroir. *Frontiers in Environmental Science, 8*, pp. 1-17.

Le Floch, A., Jourdes, M., & Teissedre, P.-L. (2015). Polysaccharides and lignin from oak wood used in cooperage: composition, interest, assays: a review. *Carbohydrate research, 417*, pp. 94-102.

Lecarpentier, C., Pagès, L. P., & Richard-Molard, C. (2021). Genotypic diversity and plasticity of root system architecture to nitrogen availability in oilseed rape. *PLoS ONE, 16*(5), pp. 1-19.

Lee, M.-H., Jeon, H. S., Kim, S. H., Chung, J. H., Roppolo, D., Lee, H.-J., . . . Park, O. K. (2019). Lignin-based barrier restricts pathogens to the infection site and confers resistance in plants. *The EMBO Journal, 38*(23), pp. 1-17.

Lee, Y., Rubio, M. C., & Alassimone, G. N. (2013). A mechanism for localized lignin deposition in the endodermis. *Cell, 153*(2), pp. 402-412.

Li, S., Gao, J., Zhu, Q., Zeng, L., & Liu, J. (2015). A dynamic root simulation model in response to soil moisture heterogeneity. *Mathematics and Computers in Simulation, 113*, pp. 40-50.

Limm, E., Simonin, K., Bothman, A., & Dawson, T. (2009). Foliar water uptake: a com-mon water acquisition strategy for plants of the redwood fores. *Oecologia, 161*, pp. 449-459.

Líška, D., Martinka, M., Kohanová, & Lux, A. (2016). Asymmetrical development of root endodermis and exodermis in reaction to abiotic stress. *Anals of Botany, 118*, pp. 667-674.

Liu, J.-F., Arend, M., Yang, W.-J., Schaub, M., Ni, Y.-Y., Gessler, A., . . . Li, M.-H. (2016). Effects of drought on leaf carbon source and growth of European beech are modulated by soil type. *Scientific Reports*(7), pp. 1-9.

Liu, Z., Persson, S., & Sánchez-Rodríguez, C. (2015). At the border: the plasma membrane-cell wall continuum. *Journal of Experimen tal Botany, 66*(6), pp. 1553-1563.

Lix, L. M., Keselman, J. C., & Keselman, H. (1996). Consequences of assumption violations revisited: a quantitative review of alternatives to the one-way analysis of variance F test. *Review of Educational Research, 66*(4), pp. 579-619.

Loeppert, R. H., & Suarez, D. L. (1996). Carbonate and Gypsum. In D. Sparks, A. Page, P. Helmke, R. Loeppert, P. Soltanpour, M. Tabatabai, . . . M. Sumner, *Methods of Soil Analysis: Part 3 Chemical Methods, 5.3*. Madison, WI: SSSA Book Series.

Lopes, C. M., Costa, J. M., Egipto, R., Zarrouk, O., & Chaves, M. M. (2018). Can Mediterranean terroirs withstand climate change? Case studies at the Alentejo Portuguese winegrowing region. *E3S Web of Conferences, XII Congreso Internacional Terroir*, *50*.

Loreti, E., & Perata, P. (2020). The many fecets of hypoxia in plants. *Plants, 9*, pp. 1-14.

Lovelock, J. (1987). *Gaia: A New Look at Life on Earth.* New York: Oxford University Press.

Lovelock, J. (2003). The living earth. *Nature, 426*, pp. 769-770.

Lovisolo, C., Perrone, I., Carra, A., Ferrandino, A., Flexas, J., Medrano, H., & Schubert, A. (2010). Drought-induced changes in development and function of grapevine (Vitis spp.) organs and in their hydraulic and non-hydraulic interactions at the whole-plant level: a physiological an molecular update. *Functional Plant Biology, 37*, pp. 98-116.

Lucas, M., Kenobi, K., von Wangenheim, D., Voß, U., Swarup, K., De Smet, I., . . . Bennett, M. J. (2013). Lateral root morphogenesis is dependent on the mechanical properties of the overlaying tissues. *PNAS, 110*(13), pp. 5229-5234.

López-Bucio, J., Guevara-Garcia, A., Ramirez-Rodriguez, V., Nieto, M. F., Fuente, d. l., J.M, & Herrera-Estrella, L. (2000). Agriculture for marginal lands: transgenic plants towards the third millenium. In A. D. Arenvibia, *Plant genteic engeneering: towards the third millenium* (pp. 159-165). Amsterdam: Elsevier.

Lupoi, J., Singh, S., Parthasarathi, R., Simmons, B., & Henry, R. (2015). Recent innovations in analytical methods for the qualitative and quantitative assessment of lignin. *Renewable and Sustainable Energy Reviews, 49*, pp. 871-906.

Lux, A., Morita, S., Abe, J., & Ito, K. (2005). An improves method for clearing and staining free-hand sections and whole-mount samples. *Anals of Botany, 96*, pp. 989-996.

Lynch, J. P. (2019). Root phenotypes for improved nutrient capture: an underexploited opportunity for global agriculture. *New Phytologist, 223*, pp. 548-564.

Müller, J., Toev, T., Heisters, M., Teller, J., Moore, K. L., Hause, G., . . . Abel, S. (2015). Iron-dependent callose deposition adjusts root meristem maintenance to phosphate availability. *Developmental Cell, 33*(2), pp. 216-230.

Majumdar, R., Alexander, S., & Riga, A. T. (2010). Physical characterization of polyethylene glycols by thermal analytical technique and the effect of humidity and molecular weight. *Pharmazie, 65*, pp. 343-347.

Marastoni, L., Lucini, L., Miras-Moreno, B., Trevisan, M., Sega, d., Zamboni, A., & Varanini, Z. (2020). Changes in physiological activities and root exudation profile of two grapevine rootstocks reveal common and specific strategies for Fe acquisition. *Scientific Reports - Nature*, pp. 1-12.

Marguerit, E., Brendel, O., Lebon, E., Van Leeuwen, C., & Ollat, N. (2012). Rootstock control of scion transpiration and its acclimation to water deficit are controlled by different genes. *New Phytologist*(194), pp. 416-429.

Marin, D., Armengol, J., Carbonell-Bejerano, P., Escalona, J., Gramaje, D., Hernández-Montes, E., . . . de Herralde, F. (2021). Challenges of viticulture adaptation to global change: tackling the issue from the roots. *Australian Journal of Grape and Wine Research, 27*, pp. 8-25.

Marschner, P., Crowley, D., & Rengel, Z. (2011). Rhizosphere interactions between microorganisms and plants govern iron and phosphorus acquisition along the root axis-model and research methods. *Soil Biology and Biochemistry, 43*, pp. 883-894.

Marzec, M., Melzer, M., & Szarejko, I. (2014). The evolutionary context of root epidermis cell patterning in grasses (Poaceae). *Plant Signaling and Behavior, 9*, pp. 1-5.

Melnyk, C. W. (2017). Plant grafting: insights into tissue regeneration. *Regeneration, 4*, pp. 3-14.

Miguel, C., & Marum, L. (n.d.). An epigenetic view of plant cells cultured in vitro: somaclonal variation and beyond. *Journal of Experimental Botany, 62*(11), pp. 3713-3725.

Miller, J. O. (2016). *Soil pH affects nutrient availability. Technical report.* University of Maryland, Maryland.

Minasny, B., & McBratney, A. (1999). A rudimentary mechanistic model for soil productionand landscape development. *Geoderma, 90*, pp. 3-21.

Mohanram, S., & Kumar, P. (2019). Rhizosphere microbiome: revisiting the synergyof plant-microbe interactions. *Annals of Microbiology, 69*, pp. 307-320.

Morales-Olmedo, M., Ortiz, M., & Selles, G. (2015). Effects of transient soil waterlogging and its importance for rootstock selection. *Chilean Journal of Agricultural Research, 75*(1), pp. 45-56.

Morrissey, J., & Guerinot, M. L. (2009). Iron uptake and transport in plants: the good, the bad, and the ionome. *Chemical Reviews, 109*(10), pp. 4553–4567.

Moser, D., Zechmeister, H. G., Plutzar, C., Sauberer, N., Wrbka, T., & Grabherr, G. (2002). Landscape patch shape complexity as an effective measure for plant species richness in rural landscapes. *Landscape Ecology, 17*, pp. 657-669.

Namyslov, J., Bauriedelova, Z. J., Soukup, A., & Tylová, E. (2020). Exodermis and endodermis respond to nutrient deficiency in nutrient-specific and localized manner. *Plants, 9*, pp. 1-16.

Naseer, S., Lee, Y., Lapierre, C., Franke, R., Nawrath, C., & Geldner, N. (2012). Casparian strip diffusion barrier in Arabidopsis is made of a lignin polymer without suberin. *PNAS*, pp. 1-6.

Negin, B., & Moshelion, M. (2016). The advantages of functional phenotyping in pre-fieldscreening for drought-tolerant crops. *Functional Plant Biology*, pp. 1-12.

Neina, D. (2019). Thge role of soil pH in plant nutrition and soil remediation. *Applied and Environmental Soil Science*, pp. 1-9.

Neumann, G., & Römheld, V. (2012). Rhizosphere chemistry in relation to plant nutrition. In P. Marschner, *Marschner's Mineral Nutrition of Higher Plant* (pp. 347-368). Cambridge, MA: Academic Press.

Nieder, R. (2008). *Bodenkunde I, Grundlagen der Bodenkunde, 3. Semester Geoökologie, Skript zur Vorlesung 'Bodenkunde - Einführung'.* Braunschweig: Institut für Geoökologie Abteilung für Bodenkunde und Bodenphysik TU Braunschweig.

Nord, E. A., & Lynch, J. P. (2009). Plant phenology: a critical controller of soil resource acquisition. *60*(7), pp. 1927-1937.

Norman, J., & Anderson, M. (2005). Soil-plant-atmosphere continuum. In D. Hillel, *Encyclopedia of Soils in the Environment.* Cambridge, MA: Academic Press.

Oburger, E., & Schmidt, H. (2016). New methods to unravel rhizosphere processes. *Trends in Plant Sciences, 21*(3), pp. 243-255.

Odgen, M., Hoefgen, R., Roessner, U., Perrson, S., & Khan, G. A. (2018). Feeding the walls: how doies nutrient availabilty regulate cell wall composition? *International Journal of Molecular Sciences, 19*, pp. 1-16.

Ollat, N., Bordenave, L., Tandonnet, J., Boursiquot, J., & Marguerit, E. (2016). Grapevine rootstocks: origins and perspectives. *Acta Horticulturae*, pp. 11-22.

Osmolovskaya, N., Shumilina, J., Kim, A., Didio, A., Grishina, T., Bilova, t., . . . Wessjohann, L. A. (2018). Methodology of drought stress research: experimental setup and physiological characterization. *International Jornal of Molecular Sciences, 19*, pp. 1-25.

Ottow, J. C. (2011). *Mikrobiologie von Böden. Biodiversität, Ökophysiologie und Metagenomik.* Berlin Heidelberg: Springer.

Pagay, V., & Kidman, C. M. (2019). Evaluating remotely-sensed grapevine (Vitis vinifera L.) water stress responses across a viticultural region. *Agronomy, 9*, pp. 1-17.

Pavloušek, P. (2010). Lime-induced chlorosis and drought tolerance of grapevine rootstocks. *Acta Universitatis Agriculturae et Silviculturae Mendelianae Brunensis, 58*(5), pp. 431-440.

Pérez-Guzmán, L., Bogner, K. R., & Lower, B. H. (2010). Earth's Ferrous Wheel. *Nature Education Knowledge, 3*(10), p. 32.

Petti, L., Raggi, A., De Camillis, C., Matteucci, P., Balázs, S., & Pagliuca, G. (2006). Life cycle approach in an organic wine-making firm: an italöian case study. *Fifth Australian Conference on Life Cycle.* Melbourne, Australia.

Pierret, A., Maeght, J.-L., Clément, C., Montoroi, J.-P., Hartmann, C., & Gonkhamdee, S. (2016). Understanding deep roots and their functions in ecosystems: an advocacy for more unconventional research. *Annals of Botany, 118*(4), pp. 621-635.

Poimarici, E., & Seccia, A. (2015). Economic and social impacts of climate change on wine production. *Reference Module in Food Sciences*, pp. 1-8.

Poorter, H., Fiorani, F., Pieruschka, R., Wojciechowski, T., Putten, v. d., H., W., . . . Postma, J. (2016). Pampered inside, pestered outside? Differences and similarities between plants growing in controlled conditions and in the field. *New Phytologist, 212*, pp. 838-855.

Prinsi, B., Negri, A. S., Failla, O., Scienza, A., & Espen, L. (2018). Root proteomic and metabolic analyses reveal specific responses to drought stress in differently tolerant grapevine rootstocks. *BMC Plant Biology, 18*(126), pp. 1-28.

Prinsi, B., Simeoni, F., Galbiati, M., Meggio, F., Tonelli, C., Scienza, A., & Espen, L. (2021). Grapevine rootstocks differently affect physiological and molecular responses of the scion under water deficit condition. *Agronomy, 11*(289), pp. 1-15.

Proffitt, T., & Campbell-Clause, J. (2012). *Managing grapevine nutrition and vineyard soils.* The Grape Wine Research Development Corporation (GWRDC).

Radville, L., McCormack, M. L., Post, E., & Eissenstat, D. M. (2016). Root phenology in a changing climate. *Journal of Experimental Botany, 67*(12), pp. 3617-3628.

Ramos, A. C., Martins, M. A., Okorokova-Façanha, A. L., Olivares, F. L., Okorokov, L. A., Sepúlveda, N., . . . Façanha, A. (2009). Arbuscular mycorrhizal fungi induce differential activation of the plasma membrane and vacuolar H+ pumps in maize roots. *Mycorrhiza, 19*, pp. 69-80.

Ranathunge, K., & Schreiber, L. (2011). Water and solute permeabilities of Arabidopsis roots in relation to the amount and composition of aliphatic suberin. *Journal of Experimental Botany, 62*(6), pp. 1961-1974.

Razmkhah, H. (2017). Comparing threshold level methods in development od stream flow drought severity-duration-frequency curves. *Water Resources Management, 31*, pp. 4045–4061.

Regierungspräsidium Darmstadt. (2018). *Ökologischer Weinbau 2018.* Abteilung V - Landwirtschaft, Weinbau, Forsten, Natur- und Verbraucherschutz, Dezernat Weinbau Eltville.

Richards, L. (1954). *Diagnosis and improvement of saline and alkali soils. Agricultural Handbook N0. 60.* United States department of Agriculture.

Richards, L., & Weaver, L. (1944). Moisture retention by some irrigated soils as related to soil moisture tension. *Journal of Agricultural Research, 69*(6), pp. 215-235.

Robbins II, N. E., Trontin, C., Duan, L., & Dinneny, J. R. (2014). Beyond the barrier: communication in the root through the endodermis. *Plant Physiology, 166*, pp. 551-559.

Roppolo, D., & Geldner, N. (2012). Membrane and walls: who is master, who is servant? *Current Opinion in Plant Biology, 15*, pp. 608-617.

Roppolo, D., Boeckmann, B., Pfister, A., Boutet, E., Rubio, M. C., Dénervaud-Tendon, V., . . . Geldner, N. (2014). Functional and evolutionary analysis of the Casparian strip membrane domaine protein family. *Plant Physiology, 165*, pp. 1709-1722.

Salkind, N. (2010). *Encyclopedia of Research Design (Vol. 2).* Los Angeles: Sage.

Salomé, C., Coll, Patrice, Lardo, E., Metay, A., Villenave, C., . . . Le Cadre, E. (2016). The soil quality concept as a framework to assess management practices in vulnerable agroecosystems: a case study in Mediterranean vineyards. *Ecological Indicators, 61*, pp. 456-465.

Sanchez, W. C., García-Ponce, B., de la Paz Sánchez, M., Álvarez-Buylla, E. R., & Garay-Arroyo, A. (2018). Identifying the transition to the maturation zonein three ecotypes of Arabidopsis thaliana roots. *Communicative and Integrative Biology*, pp. 1-7.

Santos, J., Fraga, H., Malheiro, A., Moutinho-Pereira, J., Dinis, L.-T., Correia, C., . . . Schultz, H. (2020). A review of the potential climate change impacts and adaptation options for European viticulture. *Applied Sciences, 10*(9), pp. 1-28.

Scheffer, F. W., Schachtschnabel, P., Blume, H.-P., Brümmer, G. W., Horn, R., Kandeler, E., . . . Wilke, B.-M. (2016). *Scheffer Schachtschnabel: Lehrbuch der Bodenkunde*. Berlin, Heidelberg: Springer.

Schmid, J. (2018). *Ampelografie. Die Unterlagen. Script to Lectures*. Geisenheim: Hocchschule Geisenheim University.

Schmider, E., Ziegler, M., Danay, E., Beyer, L., & Bühner, M. (2010). Is it really robust? *Methodology, 6*(4), pp. 147-151.

Schneijderberg, M., Cheng, X., Franken, C., de Hollander, M., van Welzen, R., Schmitz, L., . . . Bisseling, T. (2020). Quantitative comparison between the rhizosphere effect of Arabidopsis thaliana and co-occurring plant species with a longer life history. *The ISME Journal, 14*, pp. 2433-2448.

Schnepf, A., Leitner, D., Landl, M., Lobet, G., Mai, T. H., Morandage, S., . . . Vereecken, H. (2018). CRootBox: a structural–functional modelling framework for root systems. *Annals of Botany, 121*, pp. 1033-1053.

Scholz, F. G., Phillips, N. G., Bucci, S. J., Meinzer, F. C., & Goldstein, G. (2011). Hydraulic capitance: biophysics and functional significance of internal water sources in relation to tree size. In F. C. Meinzer, B. Lachenbruch, & T. E. Dawson, *Size- and age related changes in tree structure and function*. Dordrecht: Springer.

Schreiber, L., Franke, R., Hartmann, K. D., Ranathunge, K., & Steudle, E. (2005). The chemical composition of suberin in apoplastic barriers affects radial hydraulic conductivity differently in the roots of rice (Oryza sativa L. cv. IR64) and corn (Zea mays L. cv. Helix). *Journal of Experimental Botany*(56), pp. 1427-1436.

Schubert, S. (2018). *Pflanzenernährung*. Stuttgart: Eugen Ulmer Verlag.

Schultz, H. R., & Stoll, M. (2010). Some critical issues in environmentalphysiology of grapevines : future challenges and current limitations. *Australian Journal of Grape and Wine Research, 4*, pp. 4-24.

Seethepalli, A., Dhkal, K., Griffiths, M., Guo, H., Freschet, G. T., & York, L. M. (2021). RhizoVision Explorer: open-source software for root image analysis and measurement standardization. *bioRxiv (Preprint)*, pp. 1-27.

Sheth, B. P., & Thaker, V. S. (2014). Plant systems biology: insights, advances and challenges. *Planta, 240*, pp. 33-54.

Shibata, M., & Sugimoto, K. (2019). A gene regulatory network for root hair development. *Journal of Plant Research, 132*, pp. 301-309.

Shkolnik, D., & Fromm, H. (2016). The Cholodny-Went theory does not explain hydrotropism. *Plant Science, 252*, pp. 400-403.

Shu, Z., Row, S., & Deng, W.-M. (2018). Endoreplication: the good, the bad and the ugly. *Trends in Cell Biology, 28*(6), pp. 465-474.

Silva, L. C., & Lambers, H. (2018). Soil-plant-atmosphere interactions: ecologicaland biogeographical considerations for climate-change research. In W. R. Horwarth, & Y. Kuzyakov, *Climate Change Impacts on Soil Processes and Ecosystem Properties* (Vol. 35, pp. 29-60). Amsterdam: Elsevier.

Simmoneau, T., Lebon, E., Coupel-Ledru, A., Marguerit, E., Rossdeutsch, L., & Ollat, N. (2017). Adapting plant material to face water stress in vineyards: which physiological targets for an optimal control of plant water stastus? *OENO One, 51*(2), pp. 167-179.

Simpson, M. (2018). *Plant Systematics*. Amsterdam: Academic Press.

Slattery, R. A., & Ort, D. A. (2015). Photosynthetic energy conversion efficieny: setting a baseline for gauging future improvements in important food and biofuel crops. *Plant Physiology, 168*(2), pp. 383-392.

Smart, D. R., Schwass, E., Lakso, A., & Morano, L. (2006). Grapevine rooting patterns: a comprehensive analysis and a review. *American Journal of Enology amnd Vioticulture, 57*, pp. 89-104.

Spelt, E., Biemans, H. J., Luning, P. A., Tobi, H., & Mulder, M. (2010). Interdisciplinary thinking in agricultural and life sciences higher education. *Cummunications in Agricultural and Appl,ied Biological Sciences, 75*(1), pp. 1-10.

Spring, J.-L., Ryser, J.-P., Schwarz, J.-J., Basler, P., Bertschinger, L., & Häseli, A. (2003). *Grundlage für die Düngung der Reben*. Eidg. Forschungsanstalt für Pflanzenbau Changins & Eidg. Forschungsanstalt für Obst-, Wein- und Gartenbau Wädenswil.

Stahl, Y., & Simon, R. (2005). Plant stem cell niches. *The International Journal of Developmental Biology, 49*, pp. 479-489.

Stahr, K., Kandeler, E., Hermann, L., & Streck, T. (2016). *Bodenkunde und Standortlehre*. Stuttgart: Eugen Ulmer.

Steudle, E., & Peterson, C. A. (1998). How does water get through roots? *Journal of Experimental Botany, 49*(322), pp. 775-788.

Strock, C. F., & Lynch, J. P. (2020). Root secondary growth: an unexplored component of soil resource acquisition. pp. 1-15.

Suarez, D. L., Celis, N., Anderson, R. G., & Sandhu, D. (2019). Grape rootstock response to salinity, water and combined salinity and water stresses. *Agronomy, 9*(6), pp. 321-338.

Sublett Jr., D. M., Gonzalez, M. M., Rimstidt, D. J., & Bodnar, R. J. (2018). Synthetic fluid inclusions XXI. Partitioning of Na and K between liquid and 1 vapor in the H2O-NaCl-KCl system at 600-800°C and 500-1000 bars. *Geochimica et Cosmochimica Acta, 235*, pp. 173-188.

Sun, K., McCormack, L., Li, L., Ma, Z., & Guo, D. (2016). Fast-cycling unit of root turnover in perennial herbaceous plants in a cold temperate ecosystem. *Scientific Reports*, pp. 1-11.

Tagliavini, M., & Rombolà, A. D. (2001). Iron deficiency and chlorosis in orchard and vineyard ecosystems. *European Journal of Agronomy, 15*, pp. 71-92.

Talbot, M. J., & White, R. G. (2013). Methanol fixation of plant tissue for scanning electron microscopy improves preservation of tissue morphology and dimensions. *Plant methods, 9*.

Tracy, S. R., Nagel, K. A., Postma, J. A., Fassbender, H., Wasson, A., & Watt, M. (2020). Crop improvement from phenotyping roots: highlights reveal expanding opportunities. *Trends in Plant science, 25*(1), pp. 105-118.

Tsai, H.-H., & Schmidt, W. (2017). One way. Or another? Iron uptake in plants. *New Phytologist, 2014*, pp. 500-505.

Tyerman, S. D. (2010). *Root physiology and vine performance*. University of Adelaide, School of Agriculture, Food and Wine. Plant Research Centre, Adelaide.

Ursache, R., Andersen, T. G., Marhavy, P., & Geldner, N. (2018). A protocol for combining fluorescent proteins with histological stains for diverse cell wall components. *The Plant Journal, 93*, pp. 399-412.

Us-Camas, R., Rivera-Solís, G., Duarte-Aké, F., & De-la-Peña, C. (2014). In vitro culture: an epigenetic challenge for plants. *Plant Cell Tissue and Organ Culture*(118), pp. 187-201.

Van Leeuwen, C. (2010). Terroir: the effect of the physical environment on vine growth, grape ripening and wine sensory attributes. In A. G. Reynolds, *Managing wine quality: viticulture and wine quality* (pp. 273-315). Oxford Cambridge New Delhi: Woodhead Publishing Limited.

Van Leeuwen, C., Roby, J.-P., & de Rességuier, L. (2018). Soil-related terroir factors: a review. *OenoOne, 52*(2), pp. 173-188.

Van Leeuwen, J. P., Creamer, R. E., Cluzeau, D., Debeljak, M., Gatti, F., Henriksen, C. B., . . . Rutgers, M. (2019). Modeling of soil functions for assessing soil quality: soil biodiversity and habitat provisioning. *Frontiers in Environmental Science, 7*, pp. 1-13.

Van Loon, L. C. (2016). The intelligent behavior of plants. *Trends in Plant Science, 21*(4), pp. 286-294.

Vandeleur, R. K., Mayo, G., Shelden, M. C., Gilliham, M., Kaiser, B. N., & Tyerman, S. D. (2009). The role of plasma membrane intrinsic protein aquaporins in water transport through roots: diurnal and drought stress responses reveal different strategies between isohydric and anisohydric cultivars of grapevine. *Plant Physiology, 149*, pp. 445-460.

Varsheny, R. K., Thudi, M., Pandey, M. K., Tardieu, F., Ojiewo, C., Vadez, V., . . . Bergvinson, d. (2018). Accelerating genetic gains in legumes for the development of prosperous smallholder agriculture: integrating genomics, phenotyping, systems modelling and agronomy. *Journal of Experimental Botany, 69*(13), pp. 3293-3312.

Venios, X., Korkas, E., Nisiotou, A., & Banilas, G. (2020). Grapevine response to heat stress and global warming. *Plants, 9*(1754), pp. 1-15.

Vermeer, J. E., von Wangenheim, D., Barberon, M., Lee, Y., Stelzer, E. H., Maizel, A., & Geldner, N. (2014). A spatial accomodation by neighboring cells is required for organ initiation in Arabidopsis. *Science, 343*(6167), pp. 178-183.

Vigani, G., Donnini, S., & Zocchi, G. (2012). Metabolic adjustment under Fe deficiency in roots of dicotyledonous plants. In Y. Dincer. New York: Nova Science Publishers.

Vilches-Barro, A., & Maizel, A. (2015). Talking through walls: mechanisms of lateral root emergence in Arabidopsis thaliana. *Current Opinion in Plant Biology, 23*, pp. 31-38.

Violle, C., Navas, M.-L., Vile, D., Kazakou, E., Fortunel, C., Hummel, I., & Garnier, E. (2007). Let the concept of trait be functional! *Oikos*, pp. 1-11.

Vishwanath, S. J., Delude, C., Domergue, F., & Rowland, O. (2015). Suberin: biosynthesis, regulation, and polymer assembly of a protective extracellular barrier. *Plant Cell Reports, 34*, pp. 573-586.

Waite, H., Whitelaw-Weckert, M., & Torley, P. (2015). Grapevine propagation: principles and methodsfor the production of high-quality grapevineplanting material. *New Zealand Journal of Crop and Horticultural Science, 43*(2), pp. 144-161.

Wang, P., Calvo-Polanco, M., Reyt, G., Barberon, M., Champeyroux, C., Santoni, V., . . . Salt, D. E. (2019). Surveillance of cell wall diffusion barrier integrity modulates water and solute transport in plants. *Scientific Reports, 9*, pp. 1-11.

Wangenheim von, D., Banda, J., Schmitz, A., Boland, J., Bishopp, A., Maizel, A., . . . Bennett, M. (2020). Early developmental plasticity of lateral roots in response to asymmetric water availability. *Nature Plants, 6*, pp. 73-77.

Wangenheim von, D., Goh, T., Dietrich, D., & Benett, M. J. (2017). Plant biology: building barriers...in roots. *Current Biology, 27*, pp. 1-3.

Warschefsky, E. J., Klein, L. L., Frank, M. H., Chitwood, D. H., Londo, J. L., von Wettberg, E. J., & Miller, A. J. (2016). Rootstocks: diversity, domestication, and impacts on shoot phenotypes. *Trends in Plant Science, 21*(5), pp. 418-437.

Welker, C. M., Balasubramanian, V. K., Petti, C., Rai, K. M., DeBolt, S., & Mendu, V. (2015). Engineering plant biomass lignin content and composition for biofuels and bioproducts. *Energies, 8*, pp. 7654-7676.

Weston, L. A., Ryan, P. R., & Watt, M. (2012). Mechanisms for cellular transport and release ofallelochemicals from plant roots into the rhizosphere. *Journal of Experimental Botany*, pp. 1-10.

Wheaton, A., McKenzie, B. M., & Tisdall, J. (2008). Management to increase the depth of soft soil improves soil conditions and grapevine performance in an irrigated vineyard. *Soil and Tillage Research, 98*(1), pp. 68-80.

White, R. E., Balachandra, L., Edis, R., & Chen, D. (2007). The soil component of terroir. *Journal International des Sciences de la Vigne et du Vin, 41*(1), pp. 9-18.

Wilson, E. O. (1998). *Consilience. The unity of knowledge.* New York: Vintage Books.

Winkler, A. (1962). *General Viticulture.* Berkeley, Los Angeles: University of California Press.

Winter, S., Bauer, T., Strauss, P., Kratschmer, S., Paredes, D., Popescu, D., . . . Batáry, P. (2018). Effects of vegetation management intensity on biodiversity and ecosystem services in vineyards: A meta-analysis. *Journal of Applied Ecology, 55*, pp. 2484-2495.

Witzany, G. (2006). Plant communication from biosemantic perspective. *Plant Signals and Behavior, 1*(4), pp. 169-178.

Woese, C., Kandler, O., & Wheelis, M. (1990). Towards a natural system of organisms: proposal for the domains Archaea, Bacteria, and Eucarya. *Proceedings of the National Academy of Sciences of the United States of America., 87*(12), pp. 4576-4579.

Woods, J., Williams, A., Hughes, J. K., Black, M., & Murphy, R. (2010). Energy and the food system. *Philosophical Transactions of the Royal Society B, 365*, pp. 2991-3006.

Wu, J. (2013). Landscape ecology. In R. Leemans, *Ecological Systems. Selected Entries from the Encyclopedia of Sustainability Ccience and Technology* (pp. 179-200). Berlin Heidelberg: Springer.

Xu, Y. (2016). Envirotyping for deciphering environmental impacts on crop plants. *Theoretical and Applied Genetics, 129*, pp. 653-673.

Yıldırım, K., & Kaya, Z. (2017). Gene regulation network behind drought escape, avoidance and tolerance strategies in black poplar (Populus nigra L.). *Plant Physiology and Biochemistry, 115*, pp. 183-199.

Yıldırım, K., Yağci, A., Sucu, S., & Tunç, S. (2018). Responses of grapevine rootstocks to drought through altered root system architecture and root transcriptomic regulations. *Plant Physiology and Biochemistry, 127*, pp. 256-268.

Yan, J., Bogie, N. A., Ghezzehei, & A, T. (2020). Root uptake under mismatched distributions of water and nutrients in the root zone. *Biogeosciences, 17*, pp. 6377-6392.

Yeung, E. C., Stasolla, C., Sumner, M. J., & Huang, B. Q. (2015). *Plant microtechniques and protocols.* Cham: Springer International Publishing.

Yu, R., Brillante, L., Martínez-Lüscher, J., & Kurtural, S. K. (2020). Spatial variability of soil and plant water status and their cascading effects on grapevine physiology are linked to berry and wine chemistry. *Frontiers in Plant Science, 11*, pp. 1-18.

Zarebanadkouki, M., Trtik, P., Hyat, F., Carminati, A., & Kaestner, A. (2019). Root water uptake and its pathways across the root: quantification at the cellular scale. *Scientific Reports, 9*, pp. 1-11.

Zhang, L., Merlin, I., Pascal, S., Bert, P.-F., Domergue, F., & Gambetta, G. A. (2020). Drought activates MYB41 orthologs and induces suberization of grapevine fine roots. *Plant Direct*, pp. 1-17.

Zhang, X., Zhang, D., Sun, W., & Wang, T. (2019). The adaptive mechanism of plants to iron deficiency via iron uptake, transport, and homeostasis. *International Journal of Molecular Sciences*(20), pp. 1-14.

Zhou, Y., Minio, A., Massonnet, M., Solares, E., Lv, Y., Beridze, T., . . . Gaut, B. S. (2019). The population genetics of structural variants in grapevine domestication. *Nature Plants, 5*, pp. 965-979.

Zhu, S., Huang, C., Su, Y., & Sato, M. (n.d.). 3D ground penetrating radar to detect tree roots and estimate root biomass in the field. *Remote Sensing, 6*, pp. 5754-5773.

Zobel, R. W., & Waisel, Y. (2010). A plant root system architectural taxonomy: a framework for root nomenclature. *Plant Biosystems, 144*, pp. 507-512.

Appendix

1.

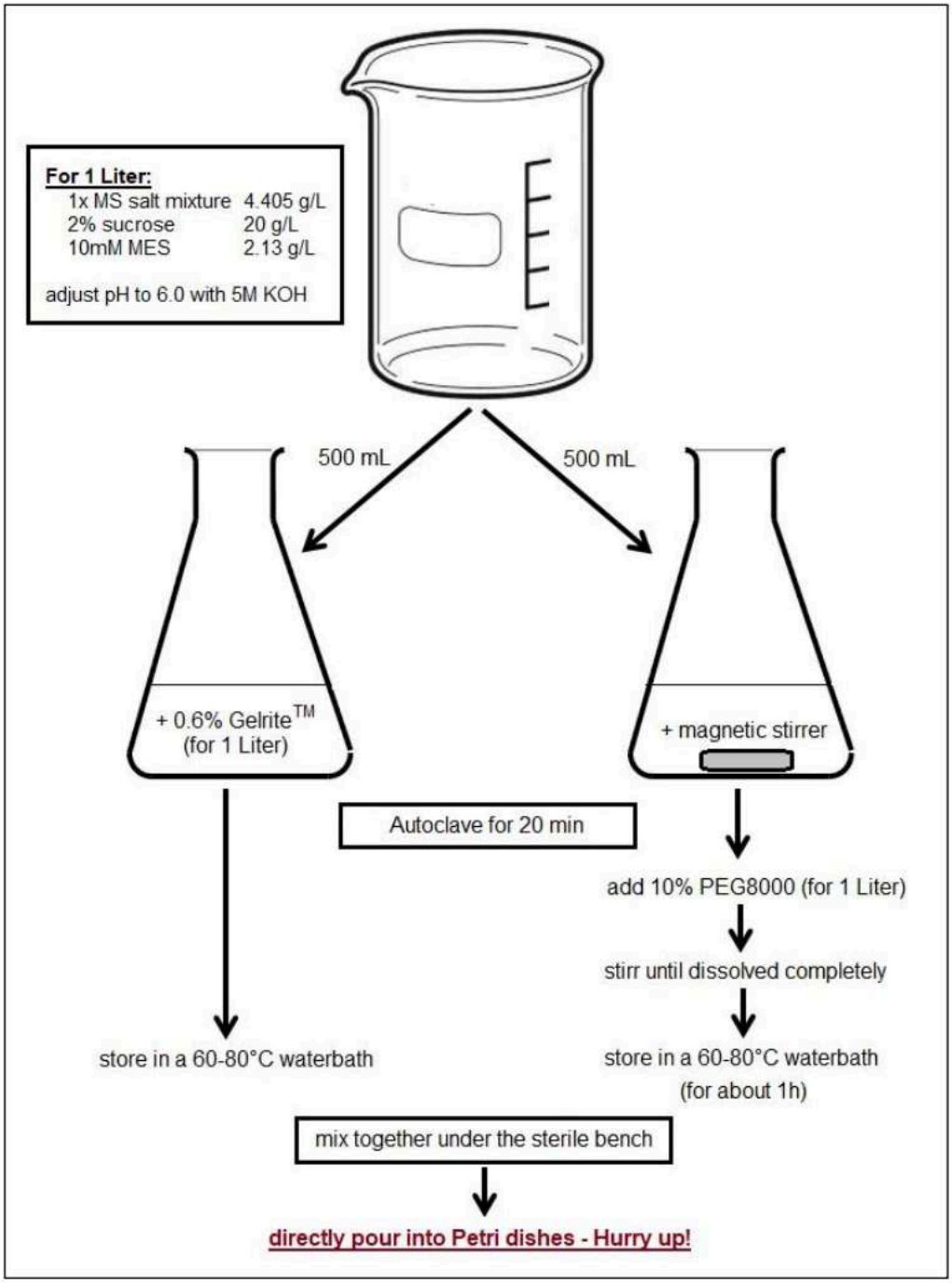

Figure 6: Scheme of the protocol for the preparation of PEG8000-containing solidified medium

Flow chart outlining the key steps of the protocol to prepare MS medium containing PEG8000. Concentrations for Gelrite™ and PEG8000 are exemplified here for preparing medium with 10% PEG (w/v). For a detailed description of the protocol see chapters 2.3.4 and 3.2.

1a).

Excerpts from the doctoral dissertation by **Victoria Kreszies**

ABA-Dependent and -Independent Regulation of Tocopherol (Vitamin E) Biosynthesis in

Response to Abiotic Stress in Arabidopsis

3.2Establishment of a Protocol for PEG8000-Containing Medium

Due to concerns about equal distribution of the PEG polymers in the medium following the PEG-infused protocol by van der Weele et al. (2000) an alternative protocol to introduce a high-molecular-weight PEG (PEG8000) into plant culture mediumwas established, as described in detail in section2.3.4.This protocol describes the preparation of solidifiedmedium plates with different concentrations of PEG8000 (no PEG, 10% and 20%). This protocol can also be used for other concentrations ofPEG resulting in various different water potentials(Table 2). Since the commonly used phyto agar does not solidify in the presence of PEG, GelriteTM (i.e.GelriteTM, Duchefa, Haarlem, Netherlands) was used instead. GelriteTMhas different characteristics compared with phyto agar. It is a gelling polymer solidifyingvery fast when getting cool. Once solidified it cannot be reheated again. Additionally GelriteTMstill solidifiesvery fast in the presence of PEG. This can be controlled with split-up prepared medium, and keeping the medium at higher temperatures before mixing. Also it should be notedthat the addition of PEG increases the volume of the medium, therefore larger flasks should be used with higher concentrations of PEG. Different concentrations of GelriteTMwere tried with five different concentrations of PEG8000 and the water potential was measured using the WP4C Water Potential Meter (METER Group, USA) (Table 2).

Table 2: Combinations for PEG8000-containing media

Amount of Gelrite™ and PEG8000 to obtain different PEG-containing media, with corresponding water potentials. Values of water potential are given as means ± SD of at least five independent replicates (n=5). Different letters indicate significant differences between means at a significance level of 0.05 in One-Way-ANOVA (Fisher LSD). Please note that the absolute value for the water potential of PEG-free medium is ~-0.40 MPa, due to the presence of MS salts and agar (ddH_2O has a water potential of 0 MPa). The value of -0.4 MPa for PEG-containing medium presented in Fujii et al. (2011) presumably refers to the difference of water potential between PEG-containing and PEG-free medium.

	Gelrite	PEG8000	Water Potential (MPa)
No PEG	3 g/L	-	- 0.40 ± 0.05 a
5% PEG8000	4.5 g/L	50 g/L	- 0.43 ± 0.03 a
10% PEG8000	6 g/L	100 g/L	- 0.55 ± 0.07 b
15% PEG8000	7 g/L	150 g/L	- 0.64 ± 0.03 c
20% PEG8000	8 g/L	200 g/L	- 0.95 ± 0.06 d
25% PEG8000	9 g/L	250 g/L	- 1.21 ± 0.07 e

For plates containing no PEG, 0.3% GelriteTM(Duchefa, Haarlem, Netherlands) was added directly to the liquid MS medium before autoclaving. The MS medium was composed of 1xMS basalt salts, 2% sucrose and 10mM MES (pH 6.0, adjusted with 1M KOH). After autoclaving,the medium was poured into 145 x 20 mm petri dishes.Preparation of medium containing either 10% or 20% PEG8000(w/v)required a split-up of the medium. Therefore, 1Lof liquid MS medium, composed exactly as described above, was divided equally to two flasks. Into one flask the required amount of GelriteTMwas added (6g/L for 10% PEG and 8g/L for 20% PEG, respectively).After autoclaving, the flask containing the Gelrite was stored at 60-80°C in a water bath until further use. The other flask containing amagnetic stirrer was filled under asterile bench with the required amount of PEG8000 (Roth, Karlsruhe, Germany). The medium was stirred until the PEG8000was completely dissolved. Then, the PEG-containing solution was also stored in a water bath at 60-80°C for at least 30 minutes. When both solutions reached the same temperature,the PEG solution was mixed with the Gelrite- containing medium under the sterile bench. Medium was directly poured into 145 x 20 mm petri dishes.

2.

Excerpts from the original paper **Efficient Lipid Staining in Plant Material with Sudan Red 7B or Fluoral Yellow 088 in Polyethylene Glycol-*G*lycerol** by Brundrett et al. 1991

MATERIALS AND METHODS

Preparation of *staining solutions.* (1) A sufficient amount of dye to make a 0.1% (w/v) or 0.01% (in the case of fluorescent stains) final solution was dissolved in pol- yethylene glycol (average mw 400 Daltons) by heating at 90 C for 1 hr. (2) An equal volume of 90% (v/v) glycerol (containing 10%distilled water) was added to the pol- yethylene glycol plus stain. Synonyms and sources of the solvent dyes used are pro- vided in Table 1.

Staining procedure. Folded Parafilm was used to immobilize plant material dur- ing sectioning with a razor blade (Frohlich 1984). The numerous sections generated in this way were examined under a dis- secting microscope, and thin sections were selected for staining. Sections of fresh or 50%alcohol- preserved plant ma- terial werk stained for 1 hr at room tem- perature, rinsed briefly in water and mounted on slides in 75% (v/v) glycerol. To process many sections simultaneously, specially designed section holders were used (Brundrett et al. 1988). In this case, excess stain was blotted off, then the hold- ers were rinsed several times in water.

Stain comparisons. The lipid-staining properties of each of the solvent dyes listed in Table 1 were compared. Suberin lamel- lae in cross-sections of potato tuber peri- derm and onion root were examined after sectioning and staining as described above. Staining intensity, color contrast, and the stability of staining solutions (in- versely related to their degree of precipitation) were noted for each dye.

3.

Excerpt from the original paper

A Berberine-Aniline Blue Fluorescent Staining Procedure for Suberin, Lignin, and Callose in Plant Tissue by Brundrett et al. 1988

2. Materials and Methods

2.1. Preparationand Handling of Sections

The following system facilitates the production and handling of numerous freehand sections. Fresh or alcohol-preserved roots were hand-sectioned using a modification of Frohlich's Parafilm section- ing technique (Fröhlich 1984). One coarse or many fine roots were immobilized within folded Parafilm on a plastic surface, then sec- tioned by drawing the corner of a sharp double-edged razor blade across them repeatedly. The sections produced in this way were transferred through various staining solutions in holders constructed for this purpose, as follows.

Mesh-bottomed, multi-chambered section holders (see Fig. 1) were assembled from 10-mm-long sections of a transfer pipette (or other polyethylene tubing) and nylon screen (50 gm mesh). A number of thin (1-2 mm) rings of tubing were first arranged in a regular pattern on a glass slide, then heated on a hotplate until they began to melt. At this time, a piece of nylon screen just large enough to cover all the rings was placed over them, followed by the tubing segments which were lined up vertically with the melting rings so that they bonded together through the screen (see Fig. 1). We have formed 1-, 4-, and 7-chambered section holders with handles attached to the screen in the same fashion; other configurations are possible. These section holders permit many separate samples to be stained simul- taneously and eliminates repeated handling of sections. The holders can be used with solutions contained in shallow vessels, such as Petri dishes, to carry sections through a variety of staining procedures.

2.2. Staining Procedure

I. Transfer freehand sections into holder chambers and stain sections in 0.1% (w/v) berberine hemi-sulphate (Sigma, C.I. no. 75160) in distilled water for 1 hour.

II. Rinse by passing holders through several changes of distilled water; blot excess water from holders after each transfer.

IlL Transfer holders to 0.5% (w/v) aniline blue WS (Polysciences, C.I. no. 42755) in distilled water for 30 minutes, then rinse as above. IV. Transfer holders into 0.1% (w/v) FeC13 in 50% (v/v) glycerine (prepared by adding glycerine to filtered aqueous FeCI3). After sev- ern minutes in this solution, transfer sections to slides and mount in the same solution.

2.3. Alkaloid Comparisonand Controls"

Chelidonium majus extract,prepared as described by Werdenburg and Peterson (1983), and 0.1% (w/v) ethanol solutions of the al- kaloids berberine (Sigma), chelerythrine (Accurate Chemical and Scientific Corp.), sanguinarine (Research Plus Inc.), and chelidonine (ICN Biomedicals Inc.) were used in step I of the procedure given in 2.2 above. The resultant fluorescent staining of suberin in onion root exodermal Casparian bands was compared microscopically un- der UV excitation. Emission colours of stained Casparian bands were categorized by comparison with ISCC-NBS Centroid Color Charts, standard sample no. 2106 (KzLLy 1965). Staining intensities and rates of fading under UV illumination were also compared under standardized conditions.

Hand-sections of onion roots were used to compare combinations of stains. The fluorescence of either C. majus extract-stained, ber- berine-stained or unstained tissues of the endodermis and stele were examined alone or with aniline blue counterstaining. Differences in fluorescence intensity were documented by recording the duration of automatic photographic exposures.

2.5. Microscopy and Photography

Sections were observed using a Zeiss Photomicroscope III and a Zeiss Axiophot microscope, with UV illumination using excitation filter G 365 (365 nm peak emission), chromatic beam splitter FT 395 (395 nm) and barrier filter LP 420 (allowing wavelengths>420 nm to pass). Most photographs were taken with 100 ASA colour slide film exposed at 50 ASA. These slides were used to make direct colour prints (colour plate) or black and white prints from internegatives. Control micrographs (Figs. 2-7) were taken with 32 ASA black and white negative film and printed at equal contrast. The FeC13moun- tant prevented destaining of sections for up to 1 day, but best results were obtained when photographs were taken within a few hours of staining.

4.

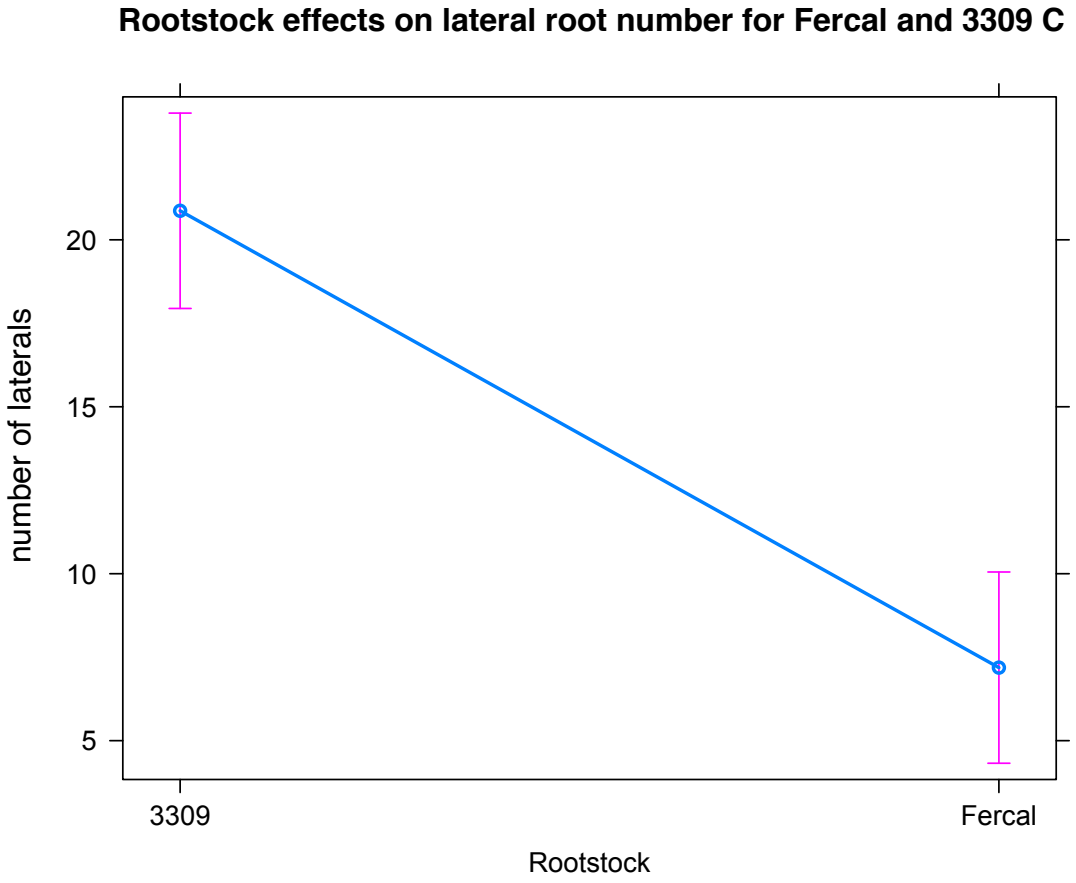
Rootstock effects on lateral root number for Fercal and 3309 C
number of laterals
20
15
10
5
3309
Fercal
Rootstock